STUDY OF SILT EROSION ON PELTON TURBINE FOR A SMALL HYDRO POWER PLANT

A THESIS

Submitted in partial fulfilment of the requirements for the award of the degree of

DOCTOR OF PHILOSOPHY

by

MAMATA KUMARI PADHY

ALTERNATE HYDRO ENERGY CENTRE
INDIAN INSTITUTE OF TECHNOLOGY ROORKEE
ROORKEE - 247 667 (INDIA)

SEPTEMBER, 2009

INDIAN INSTITUTE OF TECHNOLOGY ROORKEE
ROORKEE

CANDIDATE'S DECLARATION

I hereby certify that the work which is being presented in the thesis entitled "**STUDY OF SILT EROSION ON PELTON TURBINE FOR A SMALL HYDRO POWER PLANT**" in partial fulfillment of the requirements for the award of the Degree of DOCTOR OF PHILOSOPHY and submitted in **Alternate Hydro Energy Centre** of the Indian Institute of Technology Roorkee, Roorkee, India is an authentic record of my own work carried out during the period from January 2006 to September 2009 under the supervision of **Dr. R.P.Saini**, Associate Professor, Alternate Hydro Energy Centre, Indian Institute of Technology Roorkee, Roorkee, India.

The matter presented in this thesis has not been submitted by me for the award of any other degree of this or any other institute/university.

Mamata Kumari Padhy

(MAMATA KUMARI PADHY)

This is to certify that the above statement made by the candidate is correct to the best of our knowledge.

R P Saini

(R.P. Saini)
Supervisor

Date: 23.9.2009

The Ph.D. Viva-Voce examination of **Ms. Mamata Kumari Padhy**, Research Scholar, has been held on_____

Signature of Supervisor

Signature of External Examiner

ABSTRACT

Energy is a critical factor in developing countries for economic growth as well as for social development and human welfare. Hydropower is a renewable source of energy, which is economical, non-polluting and environmentally benign among all renewable sources of energy. For efficient operation of hydropower plants, in order to meet the electricity demand, the hydro energy is stored either in reservoirs for dam based schemes or settling basins for run-of-river schemes. These reservoirs or settling basins are filled with sediments over a period of time. This problem must be taken care of by sediment settling systems in power plants. However, lot of unsettled sediment pass through the turbines every year and turbine parts are exposed to severe erosion. The erosion of hydro turbine components is a major problem for the efficient operation of hydropower plants. These problems are more prominent in power stations which are of run-of-river types. The problem is aggravated if the silt contains higher percentage of quartz, which is extremely hard.

Silt erosion is a result of mechanical wear of components due to dynamic action of silt flowing along with water. However the mechanism of erosion is complex due to interaction of several factors viz. particles size, shape, hardness, concentration, velocity, impingement angle and properties of material. The silt laden water passing through the turbine is the root cause of silt erosion of turbine components which consequently leads to a loss in efficiency thereby output, abetting of cavitation , pressure pulsations , vibrations , mechanical failures and frequent shut downs. Since silt erosion damage is on account of dynamic action of silt with the component, properties of silt, mechanical properties of the component in contact with the flow and conditions of flow are therefore, jointly responsible for the intensity and quantum of silt erosion. The hydraulic machines, working under medium and high heads are normally exposed to erosion. High head Francis and impulse turbines are highly affected by sand erosion. Even low head Kaplan turbine and propeller turbines

are also found eroded in rivers with high sediment contents. The erosion damages are to some extent different for Francis and impulse turbines. The most common type of impulse turbine is Pelton turbine, which operates under high head. The available potential energy of water is converted to kinetic energy at the nozzle, which furthermore depend on the mass of water and available head. The energy available in the water is converted into mechanical energy in the form of turbine rotation at the cost of reaction to the turbine components. During this process, the sediment present in the water exerts force on the turbine components; as a result the turbine components get deformed. The dimensional change of the components leads to efficiency loss and eventually the system failure. In case of Pelton turbines needle, seal rings in the nozzles and runner buckets, splitter are most exposed to sand erosion.

It is generally considered that erosive wear is the gradual removal of material caused by repeated deformation and cutting actions. Most common expression for the erosive wear was based on experimental experiences quantified by means of erosive wear rate and generally expressed as a function of properties of eroding particles, properties of substrates and operating conditions.

Theoretical studies were made to discuss the main causes of damage of water turbines viz. cavitation problems, sand erosion, material defects and fatigue. Based on the available studies it was found that the best efficiency point of turbine decreased in direct proportion to the increase in silt concentration. Many investigators reported their experimental results on erosive wear conducted with different base materials and different types of erodent. Based on the case studies it was reported that in run-of-river power plants in steep sediment loaded rivers caused damages to runners due to severe erosion.

Further, it is revealed from the literature survey that a number of investigators have studied the process of silt erosion in Pelton turbines, the effect of different

parameters and the remedial measures to be undertaken. Based on their studies correlations were developed. These correlations are mostly based on experiments on small specimens, which do not match actual turbine components. The flow conditions created in the test rigs used in such experiments did not represent the real flow conditions in turbines. The models based test results obtained during such experimental studies in laboratories may not be able to predict the silt erosion of turbines actually in practice. It is therefore, more theoretical and experimental studies are required to incorporate the actual flow conditions inside the turbines. It becomes necessary to investigate the effect of different parameters, i.e., silt concentration, size of silt and jet velocity under different operating conditions on erosion of turbine components in order to predict silt erosion more accurately.

Silt erosion has impact on both performance and reliability of a Pelton runner. Bucket is the most affected part of the Pelton runner. The change of bucket profile alters the flow pattern causing loss of efficiency. Similarly loss of material weakens highly stressed parts increasing probability of fracture. The maintenance of buckets after erosion is costly in comparison of other components as the maintenance of the eroded turbine mainly depends upon dismantling time of the runner. The present investigation was carried out for erosive wear on Pelton turbine buckets.

Keeping this in view, the present study is carried out with respect to the following objectives;

(i) To design and fabricate the experimental setup for the actual flow condition in the Pelton turbine.

(ii) To predict the pattern of erosive wear and the wear mechanism in the different locations of the Pelton turbine buckets.

(iii) To investigate the effect of various silt parameters (concentration and size of silt particles) and operating parameters (jet velocity and operating hour) on erosive wear of Pelton turbines.

(iv) To develop correlations for erosive wear as a function of silt related parameters.

(v) To investigate the Pelton turbine performance and develop correlations for turbine efficiency parameters as a function of silt related parameters.

An experimental set up was designed and fabricated to investigate the effect of the silt and operating parameters on erosive wear. It consisted of a Pelton turbine with spear valve, water tank, service pump-motor, connecting pipes, stirrer, pressure transducer, open channel, weir, generator, control valves and other accessories.

An extensive experimental study has been carried out to collect the experimental data in order to discuss the wear mechanism and to develop the correlation for normalized erosive wear as a function of particle size, concentration, jet velocity and time of operation of Pelton turbine. Experimental data have been generated taking into account all the parameters contributing their effect on erosion of Pelton turbine bucket. The silt samples were collected from the river Bhagirathi basin (India), where a severely silt affected powerhouse is situated. The range of parameters considered under the present experimental study is as given in Table1.

Table 1 Range of parameters

No.	Parameter	Range
1.	Concentration	5000 to 10000 ppm
2.	Silt size	Upto 355 micron
3.	Jet velocity	26.62 to 29.75m/s
4.	Operating time	8 hrs run for each set

The experimental investigation was carried out in two stages viz. i) Identification of hot spots and analyzing the wear mechanism - Pelton turbine buckets were coated with easily erodible material and wear hot spots were identified after operating the turbine over a short period of time and ii) Determination of quantum of erosive wear and analyzing the efficiency loss of Pelton turbine due to erosive wear.

In order to study the mechanism of erosive wear, small pieces of soft material were glued at the hot spots, identified under the first part of the experimental study. The pattern of erosive wear has been examined by taking photographs of buckets. Scanning Electron Microscope (SEM) micrographs placed at wear hot spot were obtained.

Based on the observations it is predicted that coarser particles travelling at higher velocity relative to the velocity of water jet created pits and craters along the depth of the bucket at higher value of impact angle. However, the particles traveling at higher velocity in the vicinity of the splitter cause the erosion. This may be due to the shearing action of the surface of the silt particles. Smaller particles flow along the water jet causing abrasive type of erosion along the depth and at the outlet of the bucket. These particles seem to be embedded into the surface at inlet of the bucket due to lower kinetic energy and are flown out from the surface by the incoming jet.

The micrographs of splitter tip and along the depth of the Pelton bucket after erosive wear were obtained. The splitter tip has been found to be eroded by plastic deformation and indentation, overlapping craters are found on the splitter tip while along the depth of the bucket erosion takes place by plastic deformation as well as plowing.

The quantum of erosive wear was determined by measuring the mass of individual bucket before and after the experimentation at proposed time intervals. Silt concentration is found to be the strong parameter for mass loss of the Pelton bucket.

The normalized wear varies with silt concentration. Mass loss increases linearly with operating hour and other parameters viz. silt size, silt concentration and jet velocity. On the basis of experimental investigation, it has been found that the normalized erosive wear increases with an increase in the value of silt concentration for all the value of silt size. However, for a given value of silt concentration, the erosive wear rate has been found to be higher for larger size particles as larger particles have higher impact energy.

The bucket erosion has been found to be varied with the jet velocity and it implies that the jet velocity is the strongest parameter in bucket erosion. As jet velocity is the function of head, the high head turbines are more vulnerable to silt erosion. It has been observed that the power output of the turbine decreased in a rapid rate at initial stage and after some time period of operation, the power out put decrease rate achieved asymptote. The inlet or splitter, depth of the bucket and the outlet edges are found to be the prominent parts of bucket erosion. Based on the qualitative study it was found that the sharp edge of the splitter became blunt and the depth of the bucket increased due to silt erosion.

Based on the experimental data collected, a correlation has been developed for normalized erosive wear of Pelton turbine bucket as a function of the silt parameters and operating conditions. Correlation for percentage of efficiency loss has also been developed as a function of silt parameters and operating condition. Based on the experimental data obtained under different conditions following correlation were developed;

(i) Correlation for normalize mass loss

$$W = 7.91\times10^{-13}(t)^{0.99}(S)^{0.13}(C)^{1.23}(V)^{3.79} \qquad (1)$$

(ii) Correlation for percentage efficiency loss

$$\eta_{\%} = 2.43\times10^{-10}\,(t)^{0.75}\,(S)^{0.099}\,(C)^{0.93}\,(V)^{3.40} \qquad (2)$$

A comparison between actual value of mass loss and the value predicted from the correlations are made and the results are found to be in good agreement.

Summarizing, on the basis of experimental investigation it has been concluded that the normalized erosive wear increases with an increase in the silt concentration, silt size and jet velocity. The developed correlations may be useful for turbine manufacturing industries in order to predict the quantum of erosion in Pelton turbine bucket at manufacturing stage.

ACKNOWLEDGEMENT

The author wishes to offer her profound and sincere gratitude to Dr. R. P. Saini, Associate Professor, Alternate Hydro Energy Centre, Indian Institute of Technology Roorkee, for his inspiring guidance, valuable suggestions and substantial encouragement throughout the course of this research work. Words would fail to record the invaluable help which the author was privileged to receive from him on numerous occasions.

The author owes her sincere gratitude to Dr. Arun Kumar, Head, Alternate Hydro Energy Centre, the staff members of his office and the faculty members of the Alternate Hydro Energy Centre for the facilities and the cooperation received whenever needed.

The author wishes to express her sincere thanks to Prof. J. D. Sharma, Chairman, Student Research Committee, and Dr. M. P. Sharma, Associate Professor, Alternate Hydro Energy Centre for being members of her student research committee, reviewing the work and providing valuable suggestions from time to time.

The author is grateful to Dr. S.K. Singal, Senior Scientific Officer, Alternate Hydro Energy Centre, Dr. D. K. Dwivedi, Assistant Professor, Department of Mechanical Engineering, Dr. D. B. Goel, Professor, Emeritus, Department of Metallurgical and Materials Engineering and Dr. S. K. Nath, Professor, Department of Metallurgical and Materials Engineering for their generous support and useful suggestions during the course of this work.

Thanks are due to Sri Khub Chand, Sri Avtar Singh Addi, Sri Ram Baran Chauhan and other staff members of Alternate Hydro Energy Centre for the help rendered by them during the experimental investigations and typing the manuscript of this study.

The financial support received from Ministry of Human Resources Development, Government of India, New Delhi is gratefully acknowledged.

The author would like to place on record her sincere thanks to the authorities of the Orissa Engineering College, Bhubaneswar for allowing her to carry out the research work at IIT Roorkee.

The author wishes to express her heartfelt thanks to her friends Shweta Aterkar and Mr. Sandesh Aterkar, Mr. Nishikant Aterkar (Kaka), for their constant moral support during the entire period of this work.

The author wishes to record her sincere thanks and indebtedness to her colleague research scholars, Mr. Amarsingh Kanase-Patil, Mr.Vishavjeet Singh Hans, Mr. Harmeet Singh Panwar, Mr. Siddharth Jain and others, all of whom have rendered selfless help and support in numerous ways during the course of this study.

The author recognizes with warm appreciation the moral support and ever-growing blessings of her parents, brothers and sisters. The author sincerely and gratefully acknowledges the moral support and blessing of her parents-in-law, brothers-in-law and sisters-in-law. Also the author wishes to record her appreciation for her mother-in-law Smt. Basanti Devi, who has taken care of her daughters at home during the last part of this work. The author is thankful to her brother Mr. P. K. Mohapatra and sister-in-law Mrs. Geeta Mohapatra for their moral encouragement and supporting her family during her absence.

The author wishes to record her appreciation for her husband, Dr. Trilochan Sahu and daughters, Soumyamitra and Saranya, for their constant encouragement and whole hearted support throughout this work in spite of all sorts of inconvenience and hardships during her involvement in this work.

Last, but not the least, the author wishes to thank numerous well wishers and friends who have contributed, directly or indirectly in making this work a success.

(MAMATA KUMARI PADHY)

CONTENTS

LIST OF FIGURES

LIST OF TABLES

NOMENCLATURES

Symbol	Description
$A_1 = antilog\ C_1$	Coefficient as a function of operating hour
$A_2 = antilog\ C_2$	Coefficient as a function of silt concentration
$A_3 = antilog\ C_3$	Coefficient as a function of jet velocity parameter
a	Crack-length
b	Notch width (m)
b_e	Effective width (m)
C	Silt concentration (ppm)
C_0, C_1, C_2, C_3, C_4	Coefficients
C_e	Coefficient of discharge
d	Diameter of particle
D	Characteristic dimension of the machine
$f(\alpha)$	Function of impingement angle α.
g	Acceleration due to gravity in m/s^2 (9.81 m/s^2)
H	Head measured at the entrance of the turbine(m)
h	Measured upstream head over the weir(m)
h_e	Effective head (m)
h_f	Total loss of head between head race and entrance of the turbine(m)
h_m	Mean of n readings of the head
H_g	Gross head(m)
K_{mat}	Material constant and
K_{env}	Constant depending on environment
K_I and K_{II}	Expression constants
K_u	Speed ratio and it varies from 0.43 to 0.48
k_h	Head correction factor

Symbol	Description
k_b	Width correction factor
k_v	Velocity coefficient (0.96 to 0.99)
M_{bf}	Bucket mass after measurement (gm)
M_{bi}	Bucket mass before measurement (gm)
M_{bl}	Bucket mass loss (gm)
N	Runner Speed (rpm)
N_f	Number of spherical projectiles distributed at random over the surface
N_S	Specific speed
n	Exponent of velocity
P_o	Electrical power out put (W)
P	Pressure(kPa)
Pi	Power input to the turbine (W)
Q	Discharge(m^3/s)
R_f	Particle roundness factor
S	Silt size(μm)
S_1-S_2	Particular size range
t	Operating hours of the turbine(h)
t_i	Experiment starting time
t_f	Experiment finishing time
V	Water jet velocity (m/s)
W	Normalized wear per unit discharge($\frac{g/g}{m^3/s}$)
w	Weight of silt (kg)
W_C	Cutting wear
Wc_1	Horizontal velocity component are still present when particle leaves the body surface
Wc_2	Particle horizontal velocity component vanished during the collision

Symbol	Description
W_D	Deformation wear
W_t	Total wear
W_w	Weight of water (l)
δb_e	Uncertainty in the effective width for a rectangular weir
δC_e	Uncertainty in the coefficient of discharge
δh_e	Uncertainty in the effective head
δh_o	Head-gauge zero
δk_b	Width correction
δk_h	Head correction
α	Impingement angle
α_o	Angle of attack at which v_p is zero
ε	Deformation wear factor
$\Delta\, \varepsilon_p$	Plastic strain increment.
η_o	Overall efficiency of the turbine
η_g	Efficiency of the generator (= 0.98 for the considered generator)
$\eta\,\%$	Percentage overall efficiency loss of Pelton turbine
β , γ , φ	Constants
ρ	Density of water (1000 kg/m^3) at 4° C
ρ_p	Density of particle
σ	Mean stress which cause the crack to propagate
ς	Cutting wear factor

ABBREVIATION

Symbol	Description
B	Billion
EDAX	Energy-dispersive X-ray spectroscopy
GWH	Gigawatt Hour
HDPE	High Density Polyethylene
HVOF	High Velocity Oxygen Fuel
MTOE	Million Tons of Oil Equivalent
MW	Mega Watt
ppm	Parts per million
PU	Polyurethane
SHP	Small Hydro Power
SEM	Scanning Electron Microscopy
TWh	Trillion watt hours
UHMWPE	Ultra high molecular weight polyethylene
μm	Micron

CHAPTER-1

INTRODUCTION

1.1 GENERAL

Energy is a critical factor in developing countries for economic growth as well as for social development and human welfare. It has a vital contribution in all developmental activity. The economic development of many countries is hindered due to paucity of energy. Over two billion people in the world are still deprived of electrical energy. The conventional sources of energy are not enough to provide energy to developing world, as energy usage has doubled owing to rising populations, expanding economies, energy intensive industries, urbanization, a quest for modernization and improved quality of life. At the same time the world energy scenario depicts a grim picture. The adverse effects on environment caused by the production and consumption of energy have also resulted in severe environmental impacts across the globe. The green house gases have exacerbated global warming. According to data collected by, Frances Moore of Earth Policy Institute, emissions of green house gases grew 3.1% from 2000 to 2006 [1]. The five largest emitter of energy related CO_2 are China, United States, European Union, India and Russia, and they together account for almost two thirds of global CO_2 emissions. Without clean energy solutions to reduce the world's carbon footprint, carbon dioxide emissions could increase two-fold between 2000 and 2030. At this rate, it would be impossible to avoid an increase in temperature of 3 degrees Celsius above pre-industrial era. Less than 2-degree Celsius increase of temperature would cause dangerous climate change [2].

The major sources of energy in the world are oil, coal, natural gas, hydro energy, nuclear energy, renewable combustible wastes and other energy sources. Combustible wastes include animal products, biomass and industrial wastes. In 1999,

the total supply of primary energy in the world was 9,744.48 Million Tonnes of Oil Equivalent (MTOE). According to estimates of 1999, the total consumption of energy in the world in 2010 is projected to be 11,500 MTOE and that in 2020 it is expected to be 13,700 MTOE. Table 1.1 shows the world energy consumption using fuel [3].

Table 1.1 World energy consumption by fuel [3]

Region	Million Tonnes of Oil Equivalent					
	Oil	Natural Gas	Coal	Nuclear Energy	Hydro-electricity	Total
North America	1132.6	697.1	613.9	209.2	148.6	2801.3
South & Central America	223.3	111.7	21.1	3.7	131.7	501.4
Europe & Eurasia	963.3	1009.7	537.5	286.3	187.2	2984.0
Middle East	271.3	225.9	9.0	-	3.9	510.2
Africa	129.3	64.1	100.3	2.9	19.9	316.5
Asia Pacific	1116.9	366.2	1648.1	125.0	167.4	3423.7
Total	3836.8	2474.7	2929.8	627.2	668.7	10537.1

India is the 7th largest country in the world and the second most populated, with 1.08B (July 2005 estimation) people living in the area of 3.3 million km^2 [4]. Nearly 73% of India's population lives in more than 550 thousand villages. Only one third of electric supply is consumed in the rural areas despite three fourths of Indian population living in rural areas.

Indian per capita consumption of electricity continues to be extremely low around 350 kWh per annum. While 86% of the villages have access to electricity only, about 30% of the rural households are able to use electric power. Severe power shortage is one of the greatest obstacles in India's development. Table 1.2 shows the India's total electricity generation capacity.

Table 1.2 Total electricity generation capacity in India[5]

Source	Capacity (MW)
Total Installed Capacity	132110
Thermal Power Plants	
i) Coal Based	70682
ii) Gas Based	13691
iii) Oil Based	1320
Hydro Power Plants	34654
Nuclear Power Plants	4120
Renewable Power	6761

In rural areas energy for cooking, lighting, water pumping, agro and rural industry and other productive activities can be effectively provided through locally available renewable energy sources. In remote areas, where transmission of grid power is totally uneconomical, off grid electrification can be undertaken through renewable energy systems viz. small and medium hydro schemes. The other sources of renewable energy are: biomass, wind, solar and geothermal.

Hydropower is recognized as a renewable source of energy, which is economical, non-polluting and environmentally benign among all renewable sources of energy. Hydropower represents use of water resources towards inflation free energy, due to absence of fuel cost. It has further become possible due to mature technology characterized by highest prime moving efficiency and remarkable operational flexibility. Hydropower produces essentially no carbon dioxide or other harmful emissions, unlike fossil fuels. Therefore, it is not a significant contributor to global warming through CO_2.

Niagara Fall, was the first of the American hydroelectric power project and is still a source of electric power. Hydroelectric plant design became fairly well

standardized after World War I. Worldwide hydropower potential of different countries are given in Table 1.3

Table 1.3 Worldwide hydropower potential [6]

Continent	Gross Theoretical	Technically or Economically Feasible	
	1000 GWh	1000 GWh	GW
Africa	2936	1522	261
Latin America	9306	3938	643
North America	1406	1161	310
Asia	19902	4225	875
Common Wealth of Independent States	3942	603	150
Europe	3125	760	190
Oceania	592	78	18
World	41305	11754	2447

In India out of the total power generation installed capacity of 134,942 MW, hydro power contributes about 25% i.e. 33,711 MW. India's gross theoretical hydropower potential (2 638 TWh/yr) and technically feasible potential (660 TWh/yr) are amongst the highest in the world [7].

Large hydro projects are having certain disadvantages and it earned so much social opposition due to requirement of huge land posing demographic issues. Tehri and Sardar Sarovar in India are the example of non-acceptability of large hydro amongst common people, though these plants have been commissioned. Following are some other drawbacks and reasons that go against consideration of large hydro as renewable energy source.

i) Large hydro does not have the poverty reduction benefits as realized with decentralized renewable energy usage.

ii) Large hydro in renewable initiatives would large out of the availability of funds for new renewable.

iii) Promoters of large hydro regularly underestimate costs and exaggerate benefits.

iv) Large hydro will increase vulnerability to climate change due to deforestation involved.

v) Large hydro projects have major social and ecological impacts.

vi) Efforts to mitigate the impacts of large hydro are generally short of expectation.

vii) Large hydro is slow, lumpy, and inflexible and gets more expensive ones the project gestation period.

viii) Large hydro reservoirs are often rendered non-renewable due to sedimentation.

On the other hand Small Hydro Power (SHP) contributes numerous economic benefits. It has served to enhance economic development and living standards especially in remote areas with limited or no electricity. In addition the obvious benefits can also be listed as follows:

i) It is the only clean and renewable source of energy available round the clock.

ii) It is reliable, ecofriendly, mature and proven technology.

iii) It is more suitable for the sensitive mountain ecology.

iv) It can be exploited wherever sufficient water flows, along small streams and medium to small rivers.

v) It does not involve setting up of large dams or problems of deforestation, submergence or rehabilitation.

vi) It requires small capital investment, short gestation period and low payback period.

vii) It is having the minimal transmission losses.

viii) It offers the benefits of electrification to isolated or rural communities, with very low load densities.

Among all renewable energy resources small hydro power is considered the most promising source. It is an increasingly important means of generating primary electricity using the water resources of small rivers and canals. SHP technology was introduced in India shortly after the commissioning of the world's first hydroelectric installation at Appleton, USA in 1882. The first hydropower station in India was a SHP station of 130 kW commissioned in 1897 at Sidrapong near Darjeeling in West Bengal. Subsequently, many small hydro power stations were set up.

The globally accepted classification for small hydro power plants is in terms of power output, but the norms vary from country to country. Different countries are following different norms keeping the upper limit of small hydro power ranging from 5 to 50 MW. In India hydro power projects up to 25 MW capacities have been categorized as small hydro power projects. Worldwide definitions for small hydro power are given in Table 1.4.

Table 1.4 Worldwide definitions for small hydropower [4]

Country	**Capacity**
UK	≤5MW
UNIDO	≤10MW
India	**≤25MW**
Sweden	≤15MW
Australia	≤20MW
China	≤25MW
New Zealand	≤50MW

1.2 SCENARIO OF SMALL HYDROPOWER IN INDIA

India has one of the world's largest irrigation canal networks with thousands of dams and barrages. It has monsoon fed, double monsoon fed as well as snow fed rivers and streams with perennial flows. Still about 80,000 villages remain yet to be electrified in spite of the highest priority given to rural electrification in India. Most of these villages are located in remote areas, with very low load densities requiring heavy investment in electrifying these villages. In these remote areas, transmission of grid power is totally uneconomical. In these conditions small hydro power is emerging as appropriate answer of energy need. In India, the Central Electricity Authority further classifies small hydro schemes based on the capacity as given in Table 1.5 [8].

Table 1.5 Classification of SHP scheme based on capacity [8]

Size	Unit size	Installation
Micro	up to 100 kW	100 kW
Mini	101–1,000 kW	2,000 kW
Small	1001–5,000 kW	25, 000 kW

Presently in India total identified potential is around 14294,24 MW, out of which 2045,61 MW at 611 sites have been harnessed, so far. Further, 225 projects are under construction having capacity of 668.86 MW. Target capacity addition by 2012 is 1400MW as given in Table1.6 [4].

Table 1.6 Status of SHP in India [4]

Identified potential	14294.24 MW (5403 sites)
Installed capacity (as on 31/06/2007)	2045.61 MW (611 projects)
Under construction (as on 31/06/2007)	668.86 MW (225 projects)
Target capacity addition – 11^{th} Plan (2007-2012)	1400 MW

1.3 TYPE OF SHP SCHEME IN INDIA

Based on the topographical conditions, small hydropower projects in India can be broadly categorized in two categories as;

i) Small hydropower projects in the hills, where small streams are available and are mostly of medium/high head utilizing small discharges. These projects may be categorized further as run-of-river schemes and dam based schemes.

ii) Small hydropower projects in the plains, which utilize water regulated in canals and small dams constructed for other purposes like irrigation/drinking water. These projects are usually of low head utilizing large discharges and may be categorized, further, as canal based schemes and dam- toe scheme.

1.3.1 Run-of-River Scheme

Run-of-river schemes are those, in which water is diverted from a stream without creating any storage in the river. Water is taken from the main flowing river and with the available head and discharge the power is extracted. The output of a run-of-river plant is subject to the instantaneous flow of the stream. Fig.1.1 shows schematic of a run-of- river scheme.

1.3.2 Canal Based Scheme

The existing canal network has many fall structures; though the head available is very low, the discharge is more. Canal based small hydro power schemes are planned to generate power by utilizing the fall and flow in the canal. These schemes may be planned in the canal itself or in the bypass channel. With slight change in the existing structure, power can be extracted. A schematic of canal based scheme is shown in Fig.1.2.

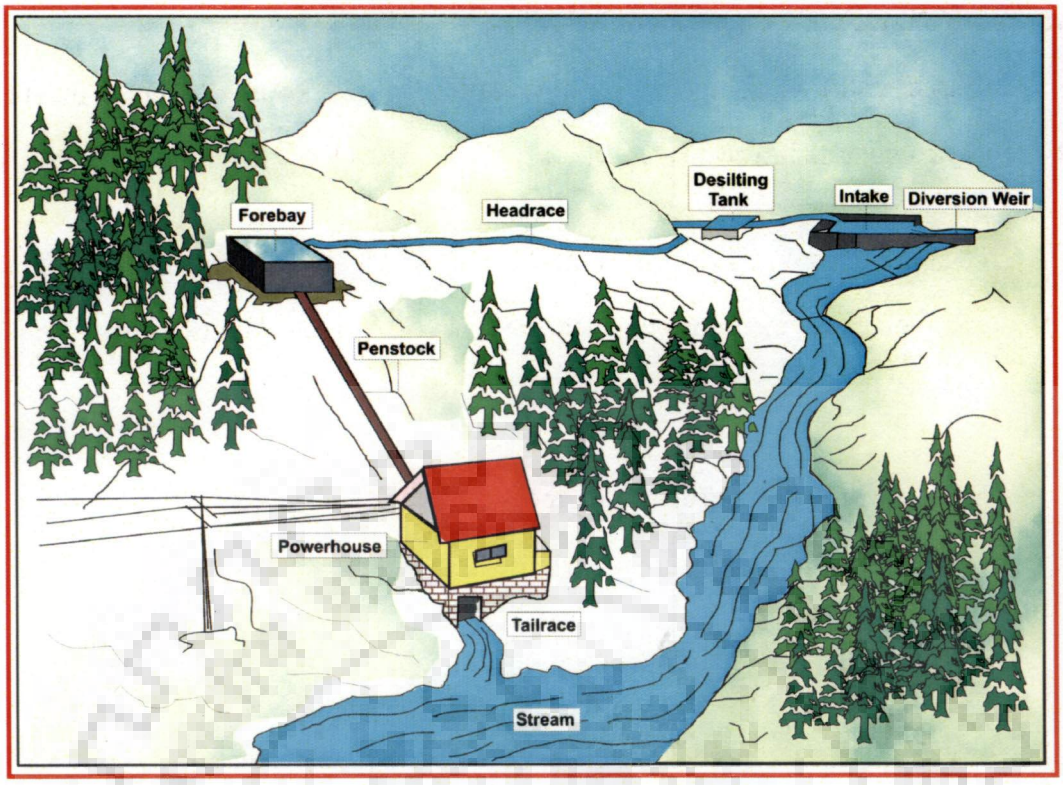

Fig.1.1 Run-of-river small hydro power scheme

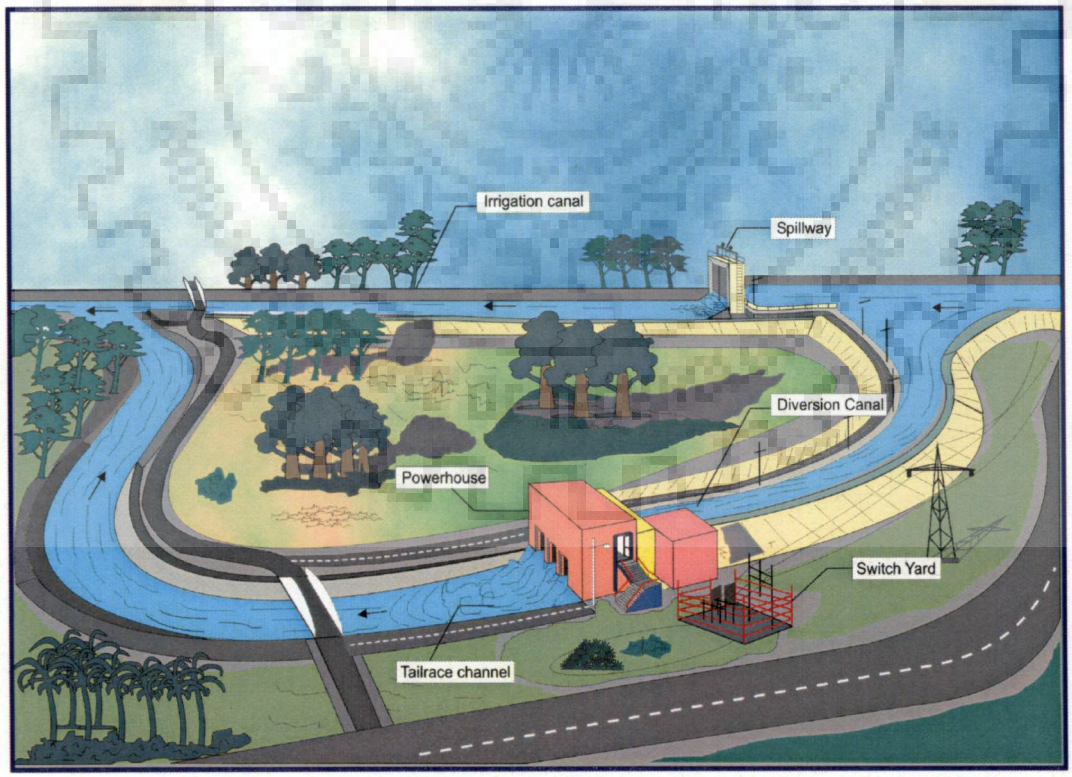

Fig.1.2 Canal based small hydro power scheme

1.3.3 Dam Toe Scheme

Dam toe based schemes are those, in which water is stored in the reservoir by constructing a dam across the river for the purpose of irrigation and supply of drinking water whenever water is required. Fig.1.3 shows a schematic of a dam toe SHP scheme.

1.4 BASIC COMPONENTS OF SMALL HYDRO POWER PLANT

The various components of a typical SHP scheme are shown in Fig.1.4, which are categorized into two main categories as follows:

i) Civil works

ii) Electro-mechanical equipment

1.4.1 Civil Works

The purpose of components under civil works is to divert the water from stream and convey towards powerhouse. In selecting the layout and types of civil components, due consideration should be given to the requirement for the reliability.

1.4.1.1 Diversion weir

It is a structure built across a natural stream to divert the water towards the power house for power generation. It may be in the form of barrage or weir, may be gated or non-gated, and may be temporary or permanent. The design should be based on the following considerations:

i) It should have a narrow and well defined structure.

ii) Location should be such that discharge intensity is high.

iii) The desired amount of water should be diverted most of the time.

iv) The sediment in the water should not be allowed to enter the water intake, as far as possible.

v) Accumulated objects should be easily flushed downstream.

vi) The flow velocity should be controlled to protect the structure from erosion.

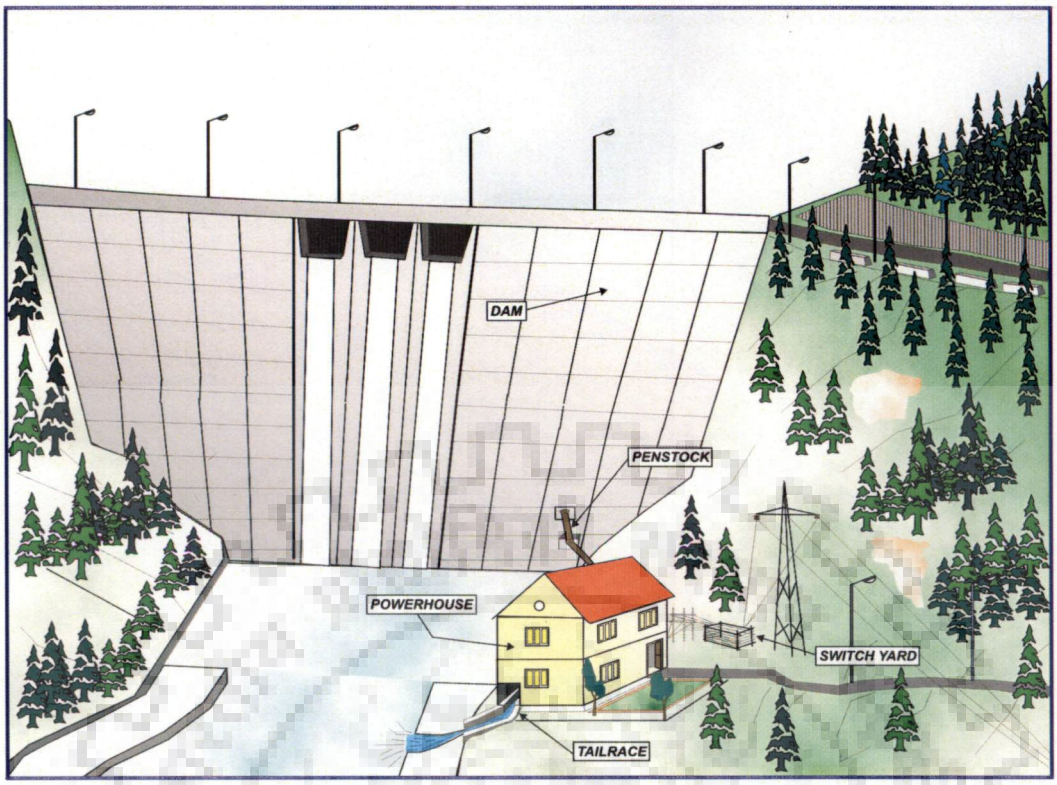

Fig.1.3 Dam based small hydro power scheme

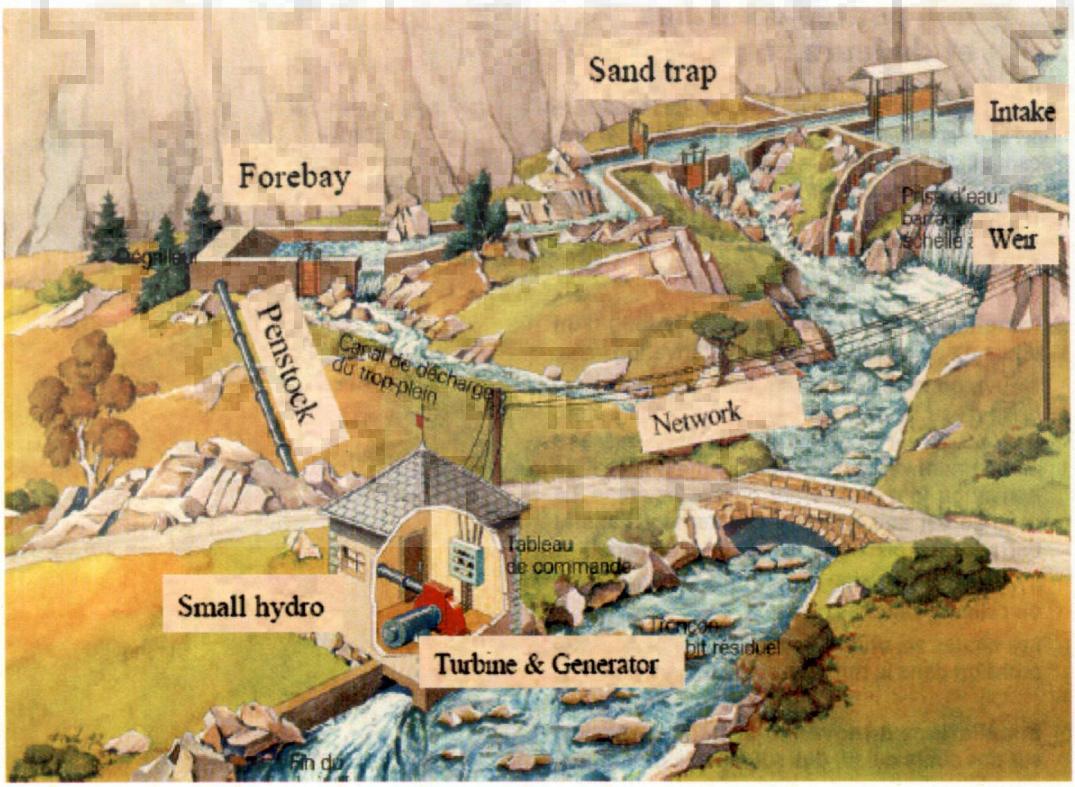

Fig.1.4 Various components of a typical SHP scheme

1.4.1.2 Feeder channel and power or head race channel

The channel provided between intake and desilting tank is called feeder channel and channel provided between desilting tank and forebay tank is called power channel or head race channel. The primary requirement for a power channel is to have a slope as mild as possible with proper conveyance of the discharge. It implies that there should be no resistance of channel to flow and therefore power channels should be invariably lined. The alignment of the channel usually follows the contours and cross drainage works should be avoided as far as possible as they result in head loss. Further the length of channel should be as short as possible.

1.4.1.3 Desilting tank (Settling basin)

The desilting tank or settling basin is provided between the feeder channel and power channel. The water drawn from the river/stream is fed to the turbine, which usually carries suspended particles. These sediments are composed of hard abrasive materials such as sand, which causes extensive damage and rapid wear to the turbine components. To remove the suspended particles from the water, flow must be slowed down in the settling basin so that the silt particles get settled on the floor of the basin. Then, these settled particles are flushed away periodically.

1.4.1.4 Forebay tank

The forebay tank is provided at the junction of power channel and the penstock, particularly in case of run-of river scheme. It acts as a transition between open flow in a power channel and the pressurized flow in a penstock. The forebay serves the following purposes.

i) It provides immediate water demand for starting the generation unit.

ii) It serves as a final settling basin where any water borne, which either passed through the intake or was swept into the channel can be removed before the water passes into the turbine.

iii) It provides some storage in case of sudden failure of the system.

iv) It spills the water in case of sudden shut down or extra water coming to forebay during rain etc.

v) It houses the trash rack and penstock entrance.

vi) It facilitates entry of water in the penstock.

The location of the forebay is governed by topographical and geological conditions of the site. However, the site of the forebay and power house should be so selected that the penstock has the minimum length.

1.4.1.5 Spillway

The main function of spillway is to dispose of surplus water from the forebay tank. Design of spillway has a significant effect on the project layout and costs. Its design and capacity depend on capacity of forebay tank, frequency of inflow discharge and geological and other site conditions.

1.4.1.6 Penstock

The penstock is the pipe, which conveys water under pressure from the forebay tank to the turbine inlet. The penstock often constitutes a major expense in the total budget and it is therefore worthwhile optimizing the design. The trade-off is between head loss and capital cost. Head loss due to friction decreases with increasing pipe diameter. Conversely pipe costs increase steeply with increase in diameter. Therefore a compromise between cost and performance is required.

1.4.1.7 Surge tank

Surge tank or surge shaft is a reservoir which furnishes space, immediately available for the acceptance or delivery of water to meet the requirements load changes. It also serves to relieve the water hammer pressure within the penstock, in case of sudden load rejection and sudden load demand. It should always be located as

close as possible to the power house in order to reduce the length of penstock to a minimum and preferably on high ground, to reduce the height of surge tank.

1.4.1.8 Power house

Power house building for small hydropower stations essentially requires a big hall to accommodate machines (turbines, generators and other accessories) with sufficient height to accommodate crane operations, and sufficient space for maintenance and control operations. It can be constructed as a steel structure consisting of columns, beams, trusses etc. or it can be reinforced concrete framed structure with gable frames to accommodate roof (purlins and sheeting). For remote hilly sites prefab buildings can also be used which are easy to transport and quick to install.

1.4.1.9 Tail race channel

From draft tube, water enters into the tailrace channel. Incase of run-of-river plant water is again supplied back to the stream via tail race channel and similarly, in case of canal based plant water is directed towards the main stream.

1.4.2 Electro-Mechanical Equipments

Electromechanical equipment are categorized into two categories; (i) Hydro turbines and gates and valves (ii) Electric generating machines and controls. These components are discussed in brief as follows;

1.4.2.1 Hydro turbines

A hydro turbine is a prime mover that converts potential energy of moving water into mechanical energy in the form of rotation of shaft. The shaft may directly be coupled with electric generator, which converts mechanical energy into electrical energy. The hydro turbines are classified into two categories according to the action of water on the moving blades viz. impulse turbine and reaction turbine.

1.4.2.1.1 Impulse turbine

A turbine that is driven by high velocity jets of water from a nozzle directed on to buckets attached to a wheel. Before reaching the turbine the pressure head of flowing water is converted to velocity head by accelerating the water through the nozzle. The water coming out of the nozzle is in the form of a free jet, which strikes with a series of bucket mounted on the periphery of the runner at atmospheric pressure. The resulting impulse spins the turbine using kinetic energy of the flowing water. The casing in case of impulse turbine do not have any hydraulic function to perform but it is necessary only to prevent splashing and to lead the water to the tail race, and also act as a safe guard against accidents. Examples of impulse turbine are Pelton turbine, Turgo-impulse turbine and Crossflow turbine.

(i) Pelton turbine

A Pelton turbine consists of a set of specially shaped buckets mounted on the periphery of a circular disc as shown in Fig.1.5. The shape of the buckets as shown in Fig.1.6 is decisive for the efficiency of the turbines. Pelton turbine runner spins about it axis by jets of water, discharged from one or more nozzles and strike the buckets. The buckets are split into two halves as shown in Fig.1.7, so that the central area does not act as a dead spot incapable of deflecting water away from the incoming jet. The cutaway on the lower lip allows the following bucket to move further before cutting off the jet propelling the bucket ahead of it and also permits a smoother entrance of the bucket into the jet.

Pelton turbines are normally considered for heads above 150 m, a higher running speed however for micro-hydro applications Pelton turbines can be used effectively at heads about 20 m.

Fig.1.5 Runner of a Pelton turbine

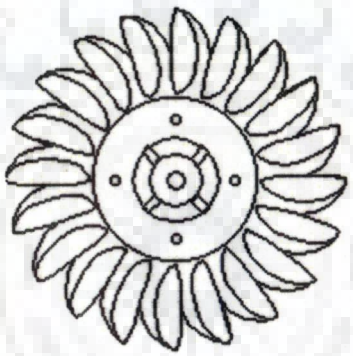

Fig.1.6 Pelton turbine bucket shape

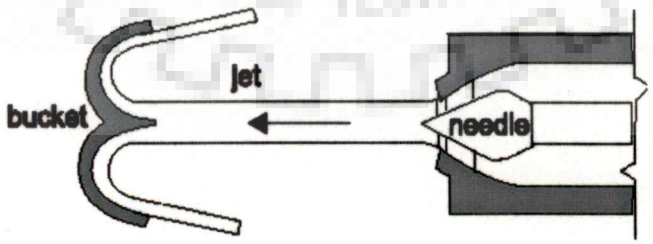

Fig.1.7 Water jet coming out of nozzle strikes bucket

(ii) Turgo Turbine

The Turgo turbine is an impulse turbine similar to a Pelton turbine and has higher specific speed. In this case the jet strikes the plane of the runner on one side and exists on the other. Fig.1.8(a) shows the Turgo runner blades and water jet. A Turgo turbine can have a smaller diameter runner than a Pelton for an equivalent power. With smaller and faster spinning runners, Turgo turbines directly connected to the generator rather than having speed-increasing transmission. A Turgo runner as shown in Fig.1.8(b) is more difficult to make than a Pelton and the vanes of the runner are more fragile than Pelton buckets.

(iii) Cross Flow Turbine

Cross flow turbine is also called a Michell-Banki turbine. A Cross flow turbine has a drum-shaped runner consisting of two parallel discs connected together near their rims by a series of curved blades. Fig.1.9 shows the main parts and the runner of cross flow turbine.

A Cross flow turbine always has its runner shaft horizontal. A rectangular nozzle directs the jet onto the full length of the runner. The water strikes the blades and imparts most of its kinetic energy. Water then passes through the runner and strikes the blades again on exit, impacting a smaller amount of energy before leaving the turbine. Although strictly classed as an impulse turbine, hydrodynamic pressure forces are also involved and a mixed flow definition would be more accurate. At part load, the water can be channeled through either two-third or one third of the runner, thereby sustaining relatively high turbine efficiency.

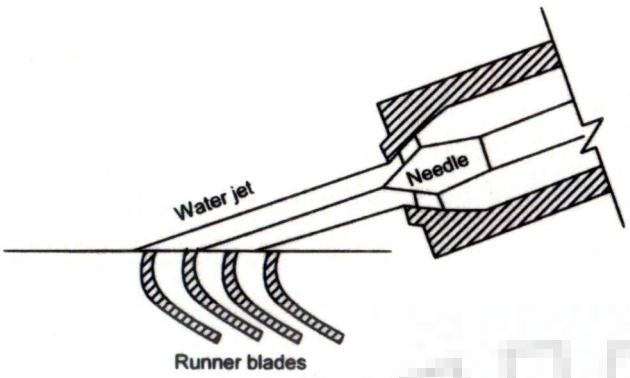

(a) Position of jet with respect to runner blades (b) Runner

Fig.1.8 Turgo-impulse turbine

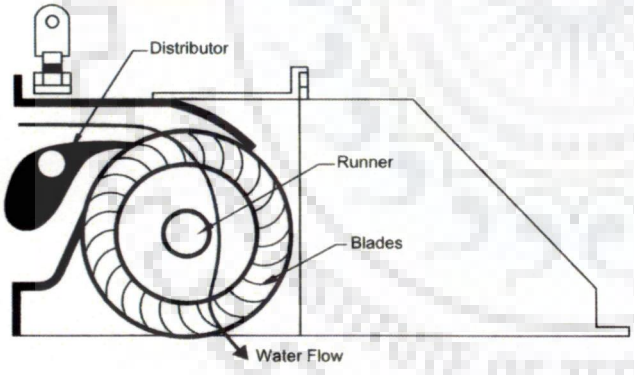

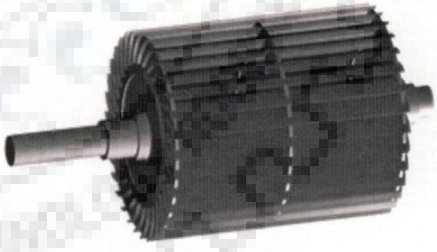

(a) Main parts (b) Runner

Fig. 1.9 Cross-flow turbine

1.4.2.1.2 Reaction Turbine

The water pressure applies a force on the face of the runner blades, which decreases as it proceeds through the runner. The pressure of the fluid changes as it passes through the turbine rotor blades. It operates with its runner submerged in water. The water before entering the turbine has pressure as well as kinetic energy. All pressure energy is not transformed into kinetic energy as in case of impulse turbine. The moment on the runner is produced by both kinetic energy and pressure energy. The reaction turbines can be further classified into two main categories based on the direction of flow of water in the runner as; (i) Mixed flow turbine and (ii) Axial flow turbine.

In case of mixed flow turbine water enters from outer periphery of the runner, moves inwards in radial direction and comes out from centre in axial direction. Example of mixed flow turbine is Francis turbine.

(i) Francis turbine

A Francis turbine is a volute-cased machine. The spiral casing is tapered to maintain uniform pressure around the entire perimeter of the runner and the guide vanes feed the water into the runner at the correct angle. The runner blades are profiled in a complex manner and direct the water so that it exits axially from center of the runner. In doing so the water imparts most of its pressure energy to the runner before leaving the turbine via a draft tube. Fig.1.10 shows main parts and runner of Francis turbine.

The Francis turbine is generally fitted with adjustable guide vanes. These regulate the water flow as it enters the runner and are usually linked to a governing system. When the flow is reduced the efficiency of the turbine falls away.

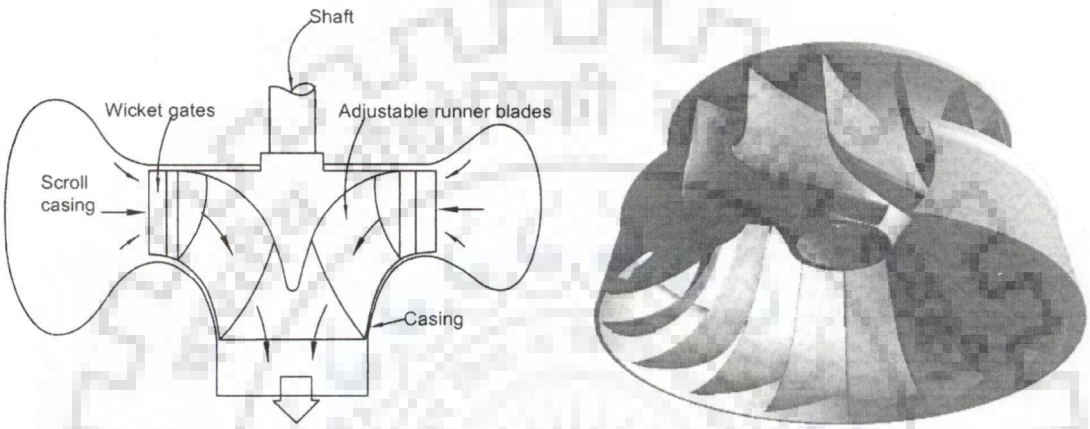

(a) Main parts **(b) Runner**

Fig. 1.10 Francis turbine

In case of axial flow turbine water enters from the wicket gates to the runner in the axial direction, moves along the axial direction and comes out in axial direction. Axial flow turbines utilize low head where large volume of water is available. These turbines provide large flow area and run at very low speeds. Axial flow turbines are classified based on operating condition as; Propeller turbine, semi Kaplan and Kaplan turbine. The axial turbines are also classified depending upon construction and layout as; tubular turbine, Bulb turbine and Straflow turbine.

(ii) Propeller turbine

Propeller turbine consists of an axial flow runner with four to six or at the most ten blades of airfoil shape. These are generally vertical shaft runners, the blades resembling the propeller of a ship. The spiral casing and guide blades are similar to those in Francis turbine. A propeller turbine is suitable when the load on the turbine remains constant. At part load its efficiency is very low; since the blades are fixed.

(iii) Kaplan turbine

Kaplan turbine is also known as a variable pitch propeller turbine. Varying the pitch of the propeller blades together with wicket gate adjustment, reasonable efficiency can be maintained under part flow conditions. It has 4 to 6 blades having no outside rim. Kaplan turbine behaves like a propeller turbine at full-load condition. Fig.1.11 shows various parts of a Kaplan turbine.

(iv) Tubular turbine

Tubular turbines are axial flow propeller type turbines. It has compact structure having turbine and generator with bearings and seals in one unit. The turbine is encased inside a tube, which is a water passage whereas the generator is outside the tube. To permit the installation of generator and speed increase outside the water passage, a bevel is provided in the tube in case of S type and L type turbine.

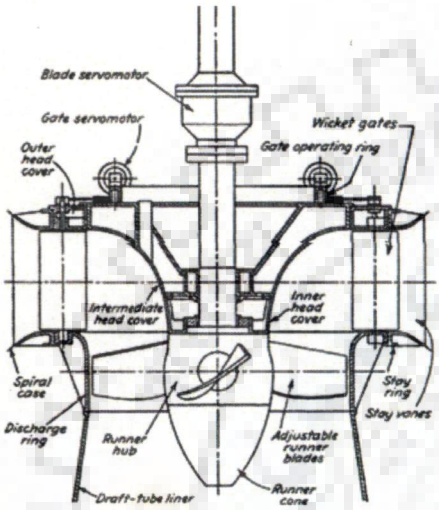

(a) Main parts

(b) Runner

Fig.1.11 Kaplan turbine

The penstock bends just before or after the runner, allowing a straight-line connection to the generator. Installation angle for the unit may vary from vertical to horizontal. It works under heads from 5 to 30 meters. Fig.1.12 and Fig.1.13 show the horizontal axis S-type propeller turbine and vertical axis L type propeller turbine respectively.

(v) Bulb turbine

The Bulb turbine as shown in Fig.1.14 is a reaction turbine of Kaplan type which is used for the lowest heads. It is characterized by having the essential turbine components as well as the generator inside a bulb. A main difference from the Kaplan turbine is moreover that the water flows with a mixed axial-radial direction into the guide vane cascade and not through a scroll casing. The guide vane spindles are inclined (normally 60^{o}) in relation to the turbine shaft. Contrary to other turbine types this results in a conical guide vane cascade. The Bulb turbine runner is of the same design as for the Kaplan turbine, and it may also have different numbers of blades depending on the head and water flow.

(vi) Straflow turbine

In case of Straflow type turbine as shown in Fig.1.15, the turbine and generator form a single unit i.e. the rotor of the generator is mounted on the periphery of the runner.

1.4.2.2 Generator

Generator transforms mechanical energy into electrical energy. In normal practice 3-phase A.C. (alternate current) generators are used. There are basically two types of generators.

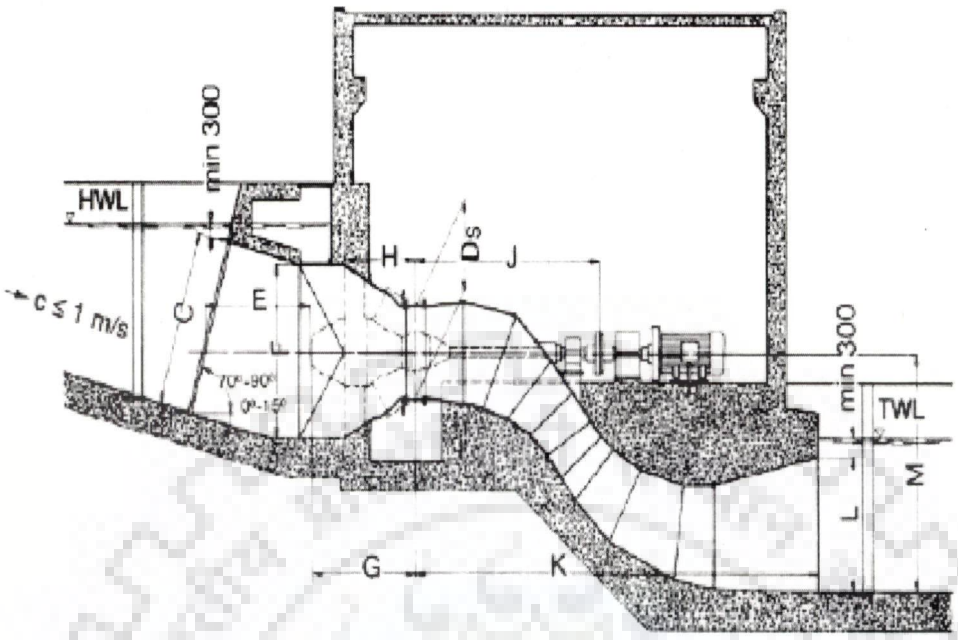

Fig. 1.12 'S' type propeller turbine

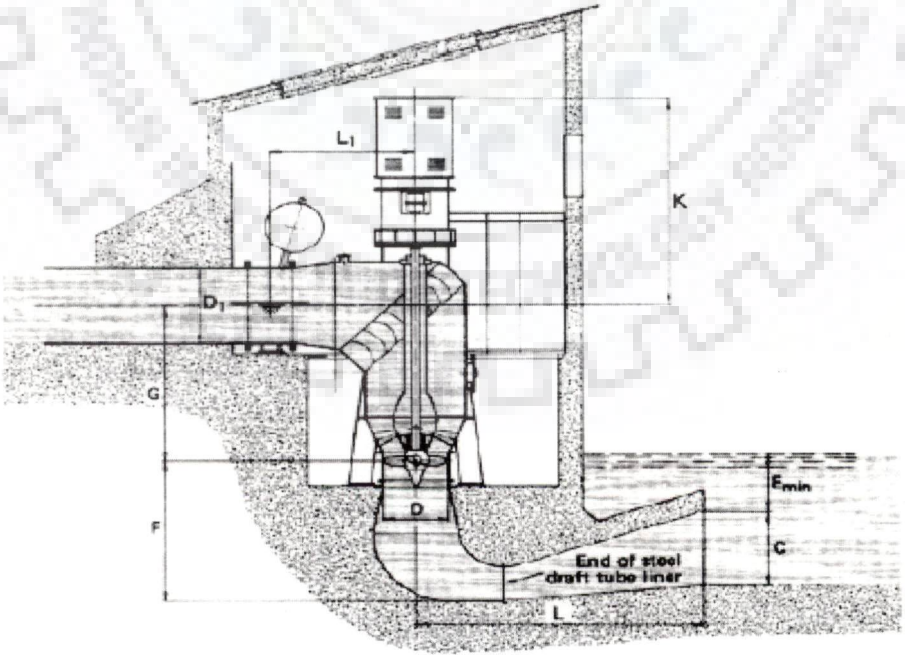

Fig. 1.13 'L' type propeller turbine

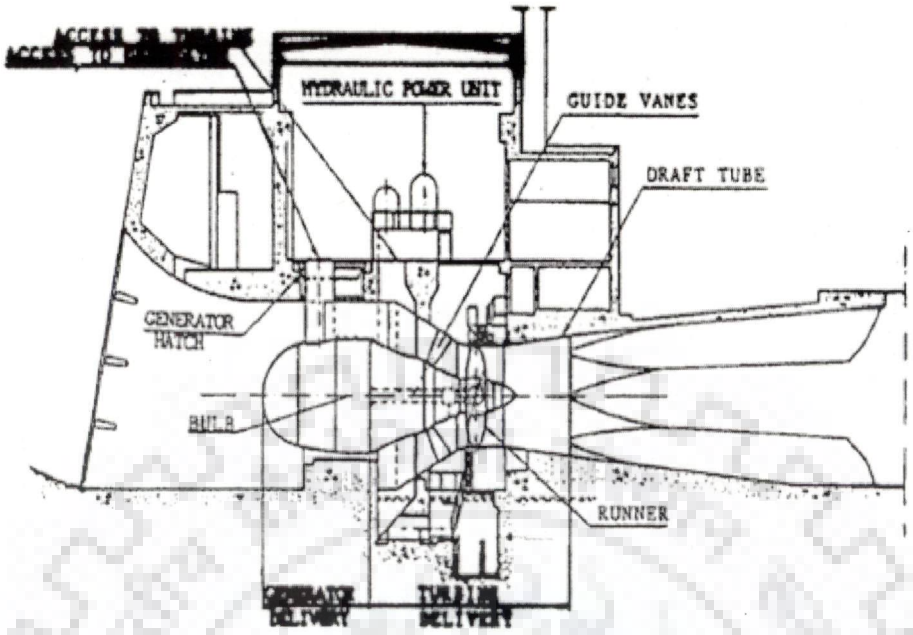

Fig.1.14 Bulb turbine

Fig.1.15 Straflow turbine

1.4.2.2.1 Synchronous generator

The synchronous generator is a rotating machine, generating single or three phase alternating current (A.C.) with a frequency proportional to its rotational speed. It consists of a stationary member called stator comprising winding and a rotating member called rotor, containing magnetic field. The rotor may be permanent magnet or more conveniently an electro magnet whose coils and windings are fed by a D.C. source called excitator. The rotating magnetic field created by the rotor induces voltage and current in the stationary windings. The generator voltage at constant frequency, the speed of the rotor is kept at synchronous speed.

1.4.2.2.2 Induction generator

The induction generator is also called as asynchronous generator as it operates at super synchronous speed. Induction generator basically consists of a stationary winding called stator, enclosed by a machine frame and rotor with a short circuited winding. Rotating magnetic field is created by placing a three phase A.C., on the terminal of the 3-phase stator winding in a machine. The machine rotates at a speed, called synchronous speed n_s, depending on the supply frequency and the number of poles. The rotating field flux cuts the short circuited rotor winding where it induces voltage and current, which in turn produce torque on the rotor. The rotor must always rotate below or above the synchronous speed i.e. at a slip.

1.5 TURBINE SELECTION CRITERIA

Hydro turbines are generally selected based on their specific speeds, but in the range of micro hydro power following criterion are suggested to be considered:

(i) Net Head

(ii) Specific Speed

(iii) Load Characteristics

(iv) Equipment Cost

1.5.1 Net Head

The first criterion to take into account in the turbine selection is the net head. Within the micro hydropower range, the turbines can be classified as high, medium or low head machines as shown in Table 1.7. The operating principle also divides the turbines into two groups.

Table 1.7 Groups of impulse and reaction turbines on the basis of head [9]

Turbine runner	High head	Medium head	Low head
Impulse	Pelton ,Turgo Multi-jet Pelton	Cross-flow, Turgo Multi-jet Pelton	Cross-flow
Reaction		Francis Pump-as-turbine	Propeller Kaplan

1.5.2 Specific Speed

The scientific method for selection of turbine is based on specific speed. The specific speed constitutes a reliable criterion for the selection of turbine. It has been found out that there is a range of specific speed at which each type of turbine is suitable. The specific speed may be defined as the speed of turbine to produce 1 kW of power output when operating under a net head of a meter. Mathematically, specific speed is expressed by the following expression:

$$N_s = \frac{N\sqrt{P_o}}{H^{5/4}} \tag{1.1}$$

where,

N_s is specific sped of turbine

N is speed of the turbine

P_o is power output in kW

H is head in m

Once the specific speed is calculated for a particular site, the turbine is selected from the Table 1.8.

Table 1.8 Specific speed for various types of turbines [9]

Specific speed (N_s)	Type of turbine
10 – 35	Pelton (Single jet)
15 – 70	Turgo Impulse
15 – 80	Cross – flow
70 – 400	Francis
340 – 1000	Axial – flow

1.5.3 Load Characteristics

The load characteristics also have some bearing on the type of turbine to be selected. Fig.1.16 shows the typical efficiency characteristics of different turbines. It indicates that the impulse turbine like Pelton, Turgo and Cross-flow have a flat efficiency curve over a wide range of flow which proves the fact that the Impulse turbines are particularly more suited to part-load conditions.

In hilly-based micro hydropower schemes where discharge varies drastically with the different seasons, these characteristics become all more important while selecting the type of turbine. However, when double regulation of speed is done as in case of Kaplan turbine, part-load efficiency is nearly as good as that of Pelton wheel. But, this improvement in part-load efficiency is obviously costly. Fig.1.17 shows selection chart of turbines on the basis of discharge, head and power output.

1.6 PERFORMANCE OF HYDRO POWER TURBINES

The turbines are generally designed to work at particular values of H, Q, P, N and η_o that are known as the designed conditions. But often the turbines are required to work at condition different from those for which they have been designed. Therefore, it is essential to determine the exact behaviors of the turbine under the varying conditions by carrying tests either on the actual turbines or on their small scale models and the results plotted are known as characteristic curves.

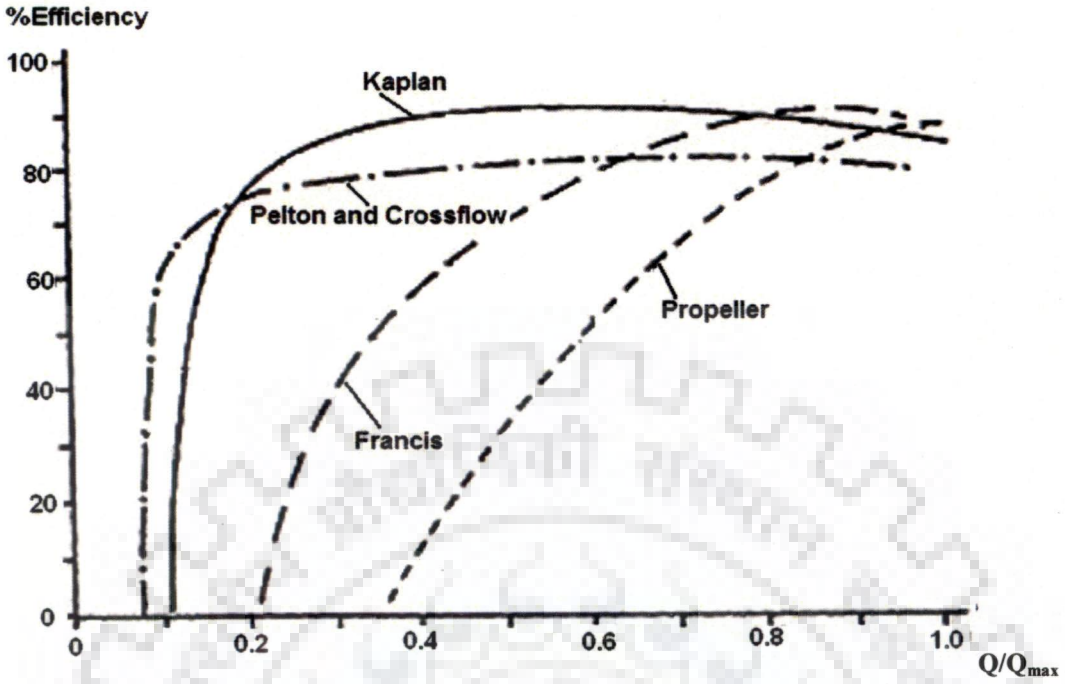

Fig. 1.16 Part-load efficiency of various turbines [9]

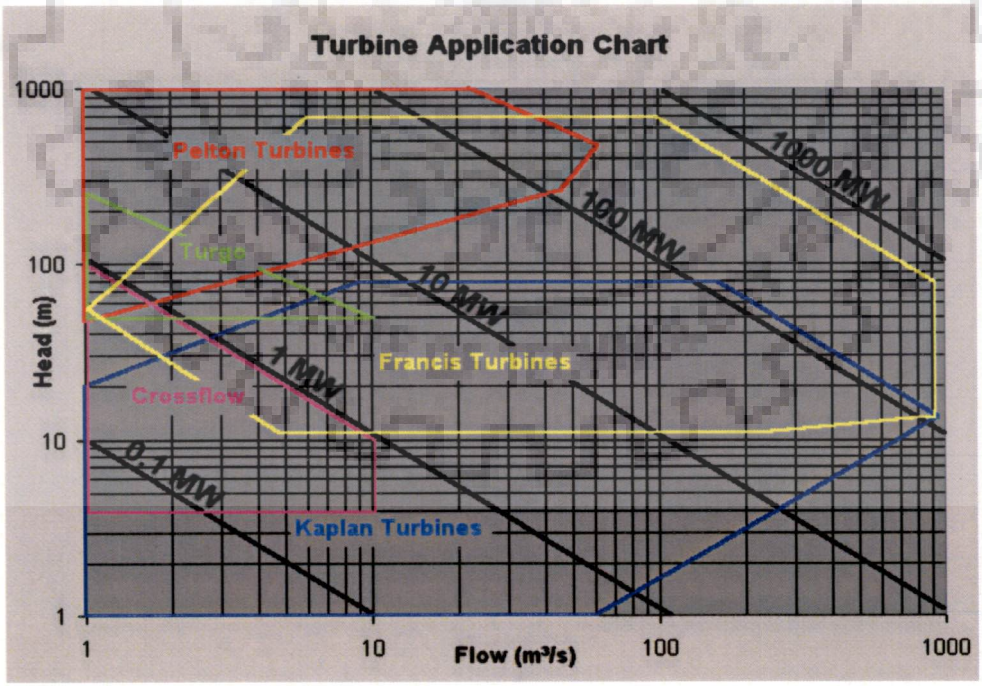

Fig.1.17 Selection of turbine on the basis of head and discharge

The followings are some of the characteristic curves of turbines. The characteristic curves for different turbines are shown in Fig.1.18, Fig.1.19 and Fig.1.20, Fig.1.21 shows percentage of full load versus overall efficiency curves for hydraulic turbines and Fig.1.22 shows percentage of full load versus overall efficiency curves for hydraulic turbines.

1.7 FACTORS AFFECTING THE EFFICIENCY OF HYDROTURBINES

The factors affecting efficiency of hydro turbines is due to several reasons viz. leakage of the water without doing useful work, secondary flow within the flow field or friction loss due to roughness of the surface, erosion of turbine components due to several reasons. The highest efficiency loss in case Pelton turbine occurs at Best Efficiency Point. The loss of efficiency in eroded turbine is due to combined effect of following reasons:

(i) Loss of water through eroded entrance lips.

(ii) Change of flow direction due to erosion at outlet edge of bucket blades and braking effect by back hitting.

Damages concerned to water turbines are caused mainly due to sand erosion, cavitation problems, material defects and fatigue. Erosion occurs primarily in turbines for higher heads than about 250 m.

These problems are consequences essentially of high pressures, pressure variations and high water velocities that to some extent depend on the ever-prevailing search for a minimizing of the costs of the investments. To cope with these problems, studies and research of the phenomena as well as the properties of materials were carried out and are going on.

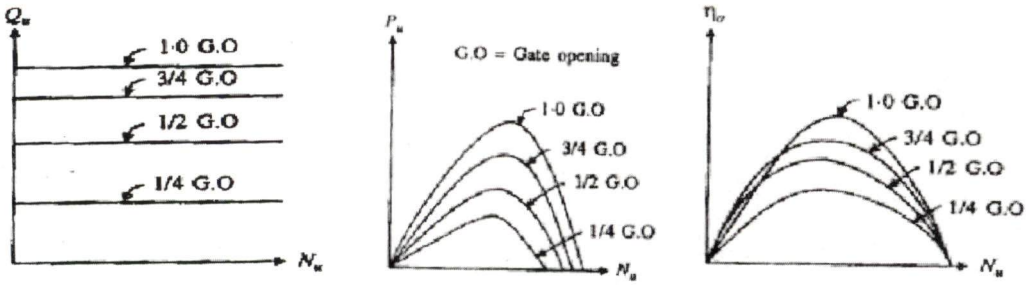

Fig.1.18 Main characteristic curves of Pelton turbine

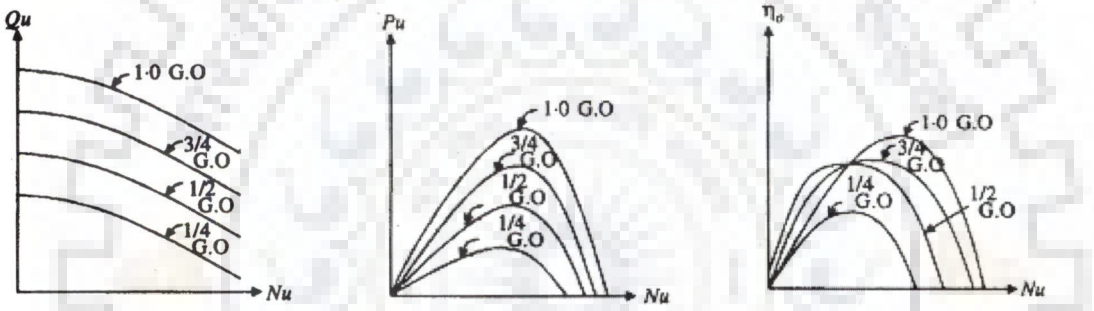

Fig.1.19 Main characteristic curves of Francis turbine

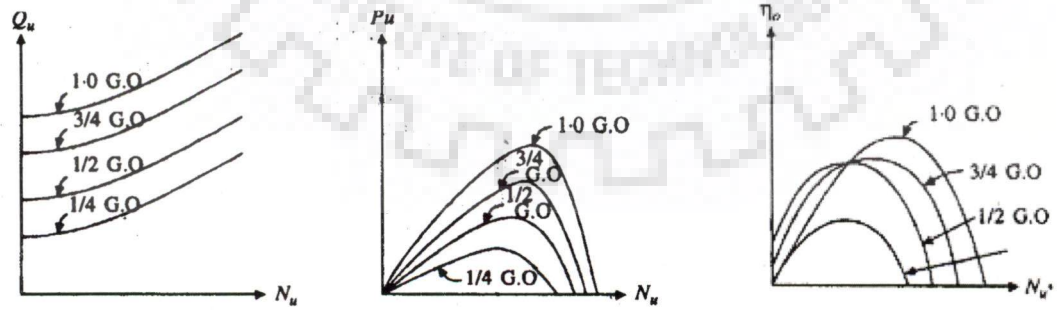

Fig.1.20 Main characteristic curves of Kaplan turbine

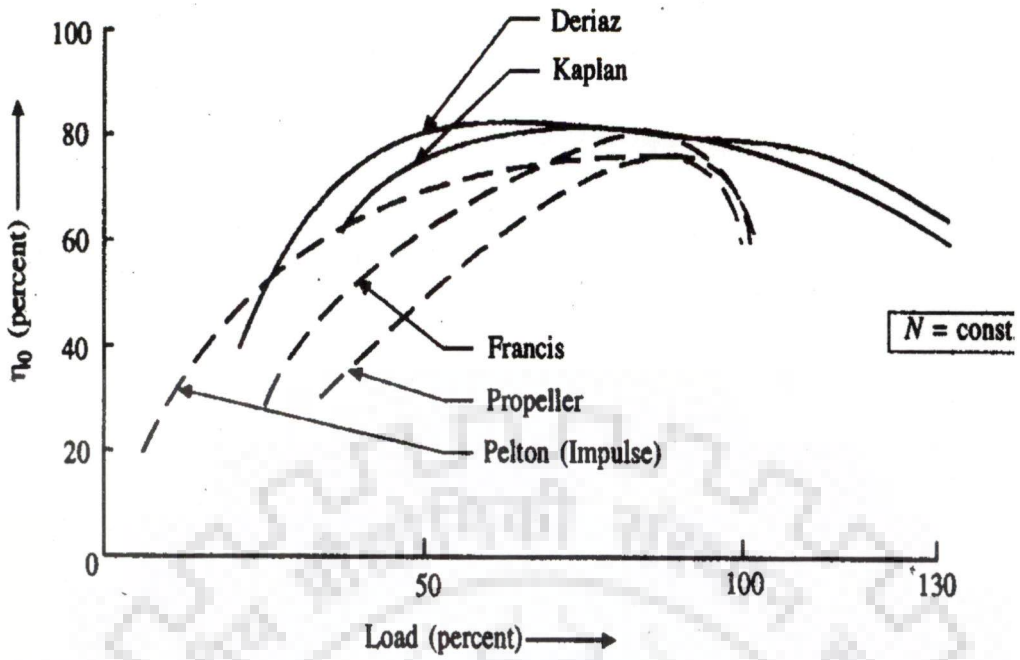

Fig.1.21 Efficiency versus percentage of full load for hydraulic turbines

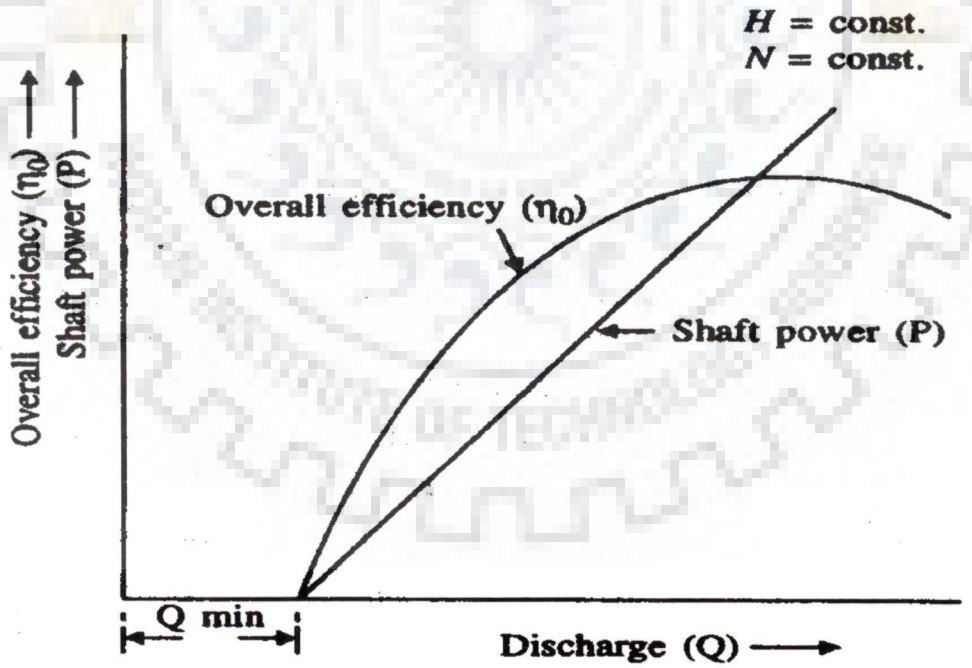

Fig.1.22 Efficiency and power versus discharge curve

1.7.1 Cavitation

The phenomenon of cavitation is concerned with the formation, growth and collapse of small cavities or voids in a liquid flowing of high velocity. The bubbles are formed due to local pressure, resulting in boiling of some liquid particles at the surrounding temperature. When the pressure in any part of the flow passage reaches the vapor pressure of the flowing liquid, it starts vaporizing and small bubbles of vapor form in large numbers. The bubbles are carried along by the flow, and on reaching the high pressure zones these bubbles suddenly collapse as the vapor condenses to liquid again. Due to sudden collapsing of the bubbles or cavities the surrounding liquid rushes in to fill them. The liquid moving from all directions collides at the centre of the cavity, thus giving rise to very high local pressure. The alternate formation and collapse of vapor bubbles may cause severe damage to the surface, which ultimately fails by fatigue and the surface becomes badly pitted. The turbine parts exposed to cavitation are runners and draft tube in case of Francis, Kaplan and bulb turbines and the needles, nozzles and the runner buckets in case of Pelton turbines.

1.7.2 Material Defects

For high head turbines the stress carrying parts are made of fine grain high tensile strength carbon steel. The design criteria of these parts are based on the maximum stress and the number of pressure pulsations cycles. Based on fracture mechanics, design of turbine should fulfill the requirement that unstable fracture from a crack shall not occur until the crack has penetrated the whole plate thickness. This condition is designated as *Leakage Before Rupture* (LBR). As long as a crack has not penetrated the whole plate thickness, an unstable rupture will be prevented. This requirement limits the maximum size of the turbine depending on the toughness of thick materials.

1.7.3 Welding Defects

Defects always occur in a weld due to cracks and lack of fusion of weld material in two dimensions. Three-dimensional defects such as sharp edges of slag and gas cavities may cause micro cracks. The defect becomes dangerous when weld crack propagates and final fracture occurs.

1.7.4 Crack Propagation Based on Fracture Mechanics

Defects may occur in weld or in heat affected zones in the base material, which will grow to rupture under the operational conditions. Based on the theory of fracture mechanics the stress in front of a crack tip in a complete elastic material is expressed by;

$$\sigma = \frac{K}{\sqrt{2\pi r}} \tag{1.2}$$

where, σ is the mean stress which cause the crack to propagate, K is the stress intensity factor and r is the distance from crack tip.

This theory gives at the crack tip that the stress is infinity. This indicates that the crack may propagate even for low average stress value of σ in the surrounding of any small crack with crack-width 'a' for an elastic material. However, all materials suitable for structural design will undergo a plastic deformation at a certain stress level which limits the stress peak value. If the load or stress level and crack depth are within that limit, crack will not propagate beyond the plastic zone. The material will have a certain crack arresting ability depending on the ratio between the elastic energy and the plastic energy stored in front of the crack tip. A crack will propagate only if the loss of elastic energy is equal or greater than the energy needed to initiate a new crack.

1.7.5 Fatigue

Defects of critical size rarely occur in a new turbine. Smaller defects in a new turbine may however, grow to critical size due to fatigue caused by a certain number of load cycles. A turbine during operation however, may be stopped and started, i.e., loaded and unloaded three times or more a day. For a life time of 50 years that leads totally about 50000 cycles. This may come under low cycle fatigue domain. In addition minor stress amplitudes caused by pressure oscillations from the turbine regulation may be superimposed. Based on these conditions the maximum stress must be limited to avoid small-fabricated cracks and other material defects to grow to critical size.

1.7.6 Silt Erosion

Generally, hill streams carry appreciable quantity of silt during rainy season. These are more harmful due to fact that development of such streams is generally, for high heads and abrasion efforts becomes more pronounced with increasing head. To trap pebbles and other suspended sediments desilting tank is generally provided in the initial reaches of water conductor [10].

Sediments are made of fragmentation of rock due to chemical and mechanical weathering. The sediments in river are mixtures of different particle size. Basically it is a sand fraction of the sediment which causes turbine erosion. The sand fraction can be further classified into fine (0.06-0.2 mm), medium (0.2-0.6 mm) and coarse (0.6-2 mm).

Special headwork, sediment settling basins and sediment-flushing system are designed to remove sediment particles and isolate mechanical and structural components from impact by sediments. Sediment settling basins increase the cost of the hydropower projects significantly. Hence they are designed to remove only coarser sediment particles and smaller particles are allowed to pass through the

turbine. Settling of particles smaller than 0.2 mm is costly. However, even with the particles less than 0.2 mm severe erosion of turbine components are observed in high head turbines.

Silt erosion is a result of mechanical wear of components due to dynamic action of silt flowing along with water. However the mechanism of erosion is complex due to interaction of several factors viz. particles size, shape, hardness, concentration, velocity, impingement angle, properties of material and so on. The silt laden water passing through the turbine is the root cause of silt erosion of turbine components which consequently leads to a loss in efficiency thereby output, abetting of cavitation , pressure pulsations , vibrations , mechanical failures and frequent shut downs. Since silt erosion damage is on account of dynamic action of silt with the component, properties of silt, mechanical properties of the component in contact with the flow and conditions of flow are therefore jointly responsible for the intensity and quantum of silt erosion The erosion damages are to some extent different for Pelton and Francis turbines. In case of Pelton turbines, needle, seal rings in the nozzles and runner buckets, splitter is most exposed to sand erosion. In case of Francis turbines runner vane, guide vane cascade and the labyrinth rings are exposed to wear.

1.8 FACTORS AFFECTING EROSION IN HYDRO TURBINES

1.8.1 Operating Conditions

Velocity and impingement angle are the important factors associated with operating conditions and applicable to all type of components where erosion occurs. These terms also appear in almost all models of erosion.

1.8.1.1 Velocity of erosive particle

Most often quoted expression for relation between erosion and velocity of particle is as given below ;

$$Erosion \propto Velocity^{n} \quad (1.3)$$

where, the values of exponent '*n*' vary depending on material and other operating conditions. Considering the impact of particles due to kinetic energy as cause of material removal, theoretically value of 'n' is 3. However, the view and finding of different researchers on the value of this exponent 'n' is not alike and it varies from investigator to investigator.

1.8.1.2 Impingement angle

Normally, the jet angle is considered as impingement angle of particles for practical purpose, but that is not the true impact angle. The impingement angle is defined as the angle between the eroded surface and the trajectory of the particle just before the impact. Impingement angle can range from 0^{o} to 90^{o}.

1.8.2 Eroding Particles

The rate of erosion as well as mechanism of erosion depends upon characteristics of the particles. The knowledge of particle characteristics is very important for estimation, reduction and prevention of erosion. Some of the particle characteristics and their effects are discussed below.

1.8.2.1 Concentration

Concentration is defined as mass (or volume) of particle present in the unit mass (or volume) of fluid. It can also be represented in terms of percentage of particles in a given fluid mass (or volume). Especially for river sedimentation, concentration is presented in term of ppm (parts per million), which is equivalent to mg/liter or kilogram of particles in 1000 m^3 of water (1000 ppm is equivalent to 0.1%). Mostly erosion rate is considered linearly proportional to concentration.

1.8.2.2 Particle size

Particle size can be characterized mainly in two basic dimensions; mass and diameter. For a given velocity, kinetic energy of particle is directly proportional to mass and mass of spherical particle is proportional to cube of diameter or in other words erosion *rate* $\propto$ *diameter*^{3}. The erosion rate ranking depends on hardness in case of erosion due to small particles, whereas in case of large particles, it is dependent on toughness of material.

1.8.2.3 Particle shape

The shape of the particles is one of the important factors which control erosion rate. Beside erosion rate, the shapes of eroding particles are of interest because of its influence in shear strength, density, permeability, compressibility and capacity of sediment transport [12-16]. Generally, particle shapes are described qualitatively such as round, angular and semi-round based on visual observation.

1.8.4 Base Material Properties

The base material for turbine components exposed to high velocity should have material property such as higher yield stresses, improved fatigue life, cavitation and corrosion resistance. The turbine material should have less weight per generation capacity. Erosion is normally not considered for material selection for turbines such as for cavitation and fracture.

However, material selection process should be dominated by erosion resistance of materials where, turbine erosion is a major problem. Basically steels are used for high head turbines, except few low head small turbines are made up of cast iron and bronze.

1.9 MECHANISM OF EROSIVE WEAR

1.9.1 Cutting (abrasive) Erosion

When particles strike the surface at low impingement angle as shown in Fig.1.23 and remove the material by cutting, the erosion mechanism is called abrasive erosion. The abrasive grits roll or slide when they strike on the surface and cause erosion by abrasion or cutting mechanism. The material is removed by scouring or scrapping by sharp edges of the particles forming short track-length scars. Two basic types of cutting mechanisms were suggested [17, 18] while testing on pin on disc wear test rig as: (i). a cutting mechanism called micro cutting and (ii). A wedge build up mechanism with flake like debris called ploughing. Ploughing is found to be less efficient mode of material removal. Beneath the surface of the abraded surface, considerable plastic deformation occurs [19, 20].The material loss is faster if the wear mechanism involves both cutting and fatigue.

1.9.2 Surface Fatigue

This mechanism of erosion is similar to wear due to surface fatigue on rolling surfaces. When the particles strike the surface with large impact angle but at low speed as shown in Fig.1.24, the surface can not be plastically deformed. Instead the surface becomes weak due to fatigue action and cracks are initiated in surface after repeated hitting. The particles will be detached from the surface after several strikes.

1.9.3 Plastic Deformation

Plastic deformation of the surface takes place due to formation of the flakes around the striking point when the particles strike the elastic surface with medium speed and large impingement angle as shown in Fig.1.25. With repeated strike on the flakes, the material will detach as debris.

1.9.4 Brittle Fracture

When particles strike the brittle surface with large impingement angle in medium velocity, erosion takes place by brittle fracture as shown in Fig.1.26. If the particles are sharp, then brittle fragmentation is more likely and the particles detach from the material by subsurface cracking.

1.10 COMPONENTS OF PELTON TURBINE AFFECTED BY SILT EROSION

The Pelton turbine components affected by silt erosion can be classified as (i) inlet system (ii) nozzle and needle (iii) runner and buckets and (iv) wheel pit.

1.10.1 Inlet System

The velocity at inlet system such as manifold and valve is normally, maintained low. The water is slightly accelerated before it enters the valve and velocity is maintained slightly higher in the valve to reduce the size because of cost and weight.

1.10.2 Nozzle and Needle

The water is accelerated in the nozzle and comes as a high velocity jet of magnitude close to $\sqrt{2gH}$. Pelton turbine installed with the head of 1200 m can have jet velocity up to 150 m/s. Such extremely high velocity damages both nozzle and needle. High velocity creates strong turbulence in the boundary layer close to needle tip. The fine particles bombarding due to turbulence, strikes the needle surface several times and severe erosion can be seen in short time. The cavitation can follow in short duration and severe damage of needle can take place. Figs.1.27-1.31 show Pelton needle and nozzle ring after severe erosion damage as typical cases.

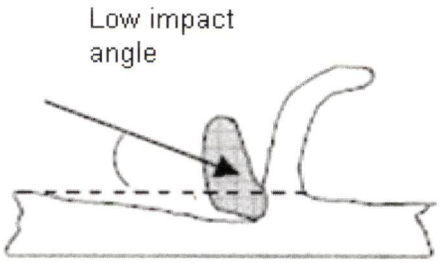

Fig.1.23 Cutting (abrasive) erosion mechanism

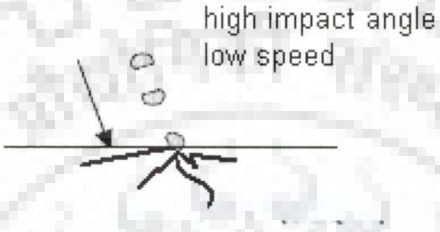

Fig.1.24 Fatigue erosion mechanism

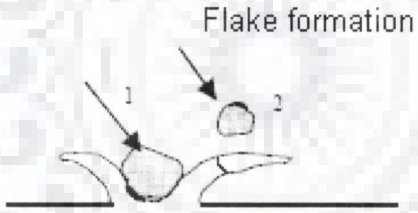

Fig.1.25 Plastic deformation

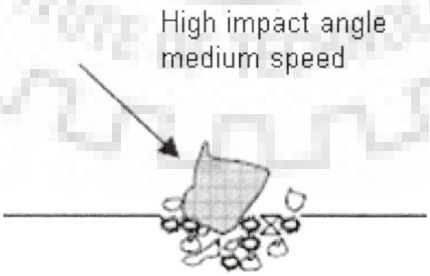

Fig.1.26 Erosion by brittle fracture

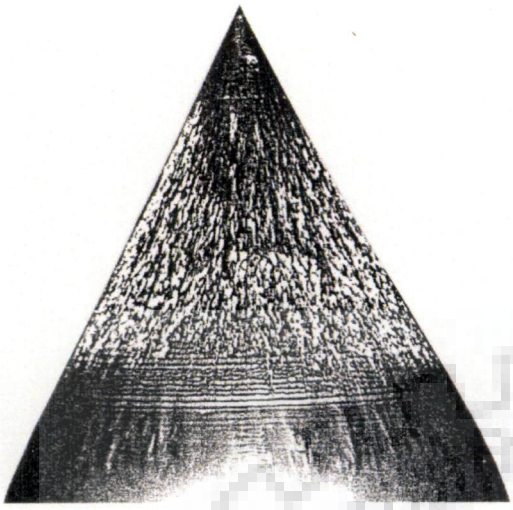

Fig.1.27 Eroded needle of Pelton turbine of Mel power plant, Norway (P=52 MW, H=810 m) [21]

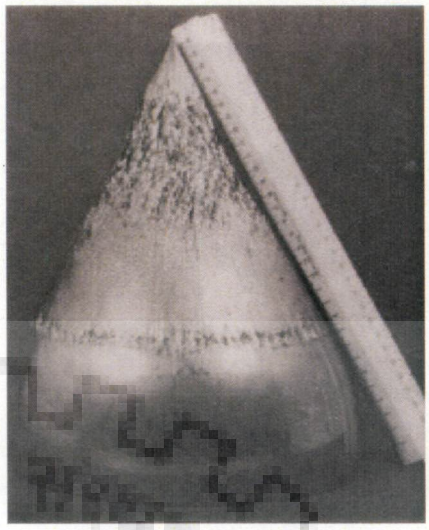

Fig.1.28 Eroded stainless steel nozzle of Pelton turbine without coating of Bhabha Hydro Power station after one monsoon.; P=8.4MW; H=540m.[22]

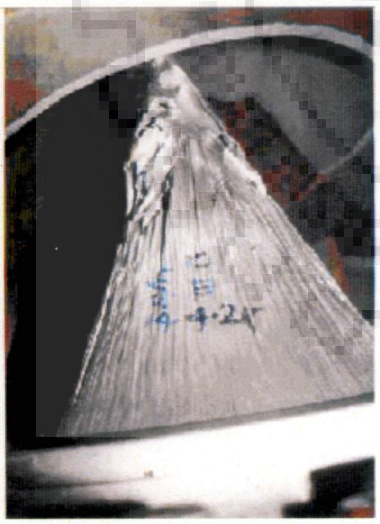

(a) Boronised

(b) HVOF coated

Fig.1.29 Eroded stainless steel nozzle of Pelton turbine with coating of Bhabha hydro power station after one monsoon[22]

Fig.1.30 Damaged needle [23]

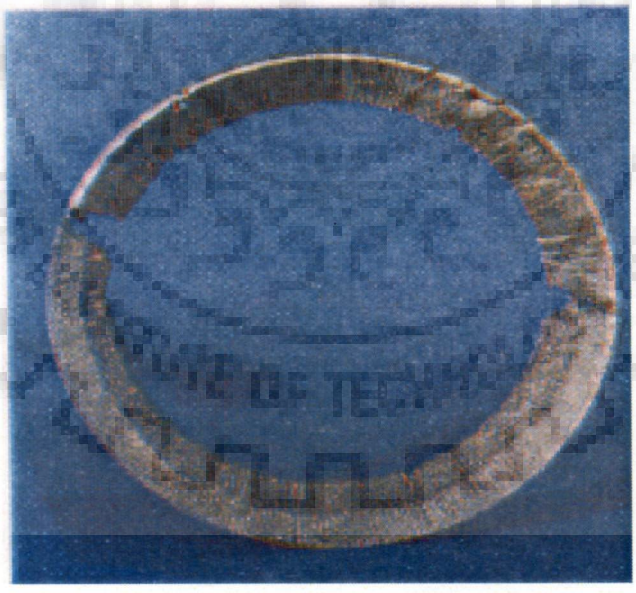

Fig.1.31 Damaged Pelton nozzle ring [24]

1.10.3 Runners and Buckets

Sand erosion has impact on both performance and reliability of the Pelton runner. Bucket is the most affected part of the Pelton runner. The change of bucket profile alters the flow pattern causing loss of efficiency. Similarly loss of material weakens highly stressed parts increasing probability of fracture. Figs.1.32-1.35 show the damage of Pelton turbine components due to acceleration of large particles and turbulence of fine particles. Such a high acceleration separates the particles from streamline. The curvature of the Pelton bucket is very important because of very high acceleration. The nature of damage of Pelton turbine erosion with fine or coarse sand is different. With coarse particles, most of the damages are in the area where the jet directly hits at the bucket inlet. Surface damage is not of the nature of cutting action by sharp edge, but is more like hammering [21].

1.10.4 Other Parts

The jet directly hits the deflector, but because of short exposure time the erosion of deflector is not serious. Moreover it can be replaced easily; hence deflector erosion is not crucial. Similarly turbine pit liners can also be eroded with the deflected water. This can be considered minor because impact energy on liner is not very high. Normally there is no problem of sand erosion in runner disc, because water and particle does not strike.

Fig.1.32 Pelton bucket surface erosion (P=32MW, H=360m) [24].

Fig. 1.33 A Pelton runner destroyed (P=10MW, H=410m) [24].

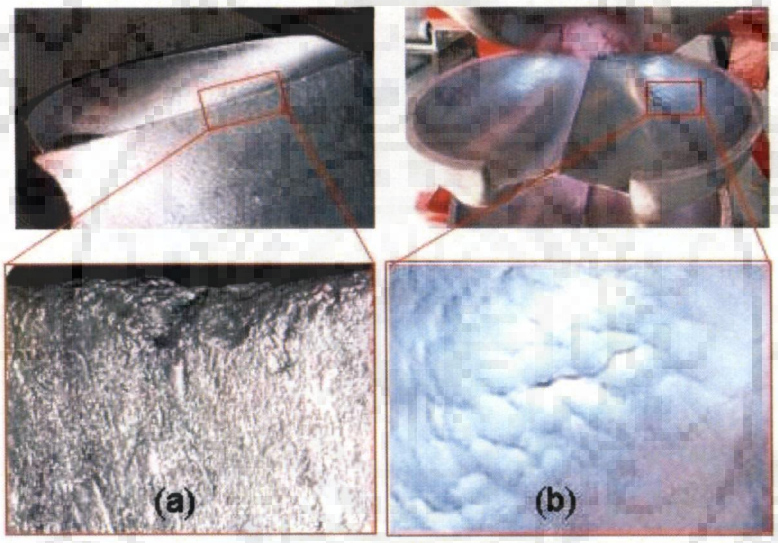

(a) Skagen (b) Khimti

Fig.1.34 Eroded Pelton buckets [23]

(a) Rangjung power plant, Bhutan [24] (b) Alfalfa power station Chile [25].

Fig.1.35 Badly eroded Pelton bucket

CHAPTER-2

LITERATURE REVIEW

2.1 GENERAL

Most of the hydropower plants in the Himalayan Rivers are run-of-river type and affected by excessive silt due to Himalayas' immature geology and tropical climate [26-30]. Under a study, Naidu [30] reported that about 22 large hydropower stations in India are facing silting problem. These power stations have been classified into three categories based on quantum of damage as; (i) category A – indicates intensive damage and needs renovation every year, (ii) category B – indicates substantially high damage and needs renovation in every 3 years and (iii) category C – indicates considerable damage and needs special efforts and resources after 15–20 years. In another study, Naidu [30] stated that Baira Siul project (3 × 66 MW) in Himachal Pradesh in India, handles nearly 10,000 tons of silt per day, per machine during critical monsoon days and more than 90% of the silt passing through these machines is quartz.

Nepal is also facing severe silting problem in hydropower plants with specific sediment yield of about 4240 tonnes/km^2/year. Marshyangdi river is one of the sediment-laden rivers in Nepal. The sedimentlogical study performed in 1981 has revealed an average annual load of 26.7 million tonnes and bed load of 2.9 million tonnes. Out of this total load, 90% of the sediments are transported in the river during the monsoon season from May to October. Similar conditions also prevail in rest of the rivers [31].

Erosive wear of hydro turbine components become a complex problem as there are so many variables involved in the erosive wear. This depends upon type of erodent, base material and flow conditions. In most of the cases, problems of erosive wear can be minimized by controlling these parameters. But during monsoon season,

it becomes impossible to control these parameters, which cause erosion. Complete elimination of erosion of the turbine components is not possible, but the study of material characteristics and failure mechanisms help in understanding the cause of material failure which helps to minimize the damage of the material. It therefore, becomes essential to investigate their effects. Under this Chapter-2 an extensive literatures related to silt erosion in various components of hydro turbines are discussed.

2.2 THEORETICAL INVESTIGATIONS

Silt erosion was designated as abrasive wear and this type of wear will brake down the oxide layer on the flow guiding surfaces and partly make the surfaces uneven which may be the origin for cavitation erosion. Wear or erosion is defined as the damage to a solid surface, generally involving progressive loss of material, due to relative motion between the surface and a contacting substance or substances [32]. However, Bhushan [33] emphasized that the material displacement on a given body with no net change in weight or volume should be considered as wear. Sand erosion may be both, a releasing and contributing cause for damages which are observed in power plants with a large transport of wearing contaminants in the water flow. Erosion models are useful for design of turbine components, sediment settling basin and optimization of hydropower plant operation in sand-laden river. The actual mechanism of erosive wear was not fully understood. Therefore a simple, reliable and generalized quantitative model for erosion could not be developed. Most common expression for the erosive wear was based on experimental experiences. The hydro-abrasive wear was commonly quantified by means of wear rate W, which is defined by the loss of mass per unit time and generally, it is expressed by the following equations;

$$W = f\begin{Bmatrix} properties\ of\ particles, \\ properties\ of\ substrate, \\ operating\ condition \end{Bmatrix} \quad (2.1)$$

Truscott[34] surveyed literature of 20 years on abrasive wear of hydraulic machinery and reported the relationship between material erosion and velocity can be expressed as;

$$\text{Erosion} \propto (\text{velocity})^n \quad (2.2)$$

Different models developed based on theoretical investigation are discussed as follows;

2.2.1 General Erosion Model

2.2.1.1 Finnie's model

Finnie [35] derived expressions for ductile materials by assuming the target material as plastic, eroding particles as rigid with sharp edges and ideal case of hitting by single particle. The developed expressions were further extended to the equations for impacts by several free moving particles of total mass, M considering only 50% of the total impinging particles. The expressions for total volume removed by cutting wear are expressed as follows;

$$Q = \frac{MV^2}{8P}(Sin2\alpha - 3\sin^2\alpha) \quad (2.3)$$

if $\alpha \leq 18.5^\circ$

and

$$Q = \frac{MV^2}{24P}(Cos^2\alpha) \quad (2.4)$$

if $\alpha \geq 18.5^\circ$

where V is velocity of particles, α is impingement angle and P is plastic flow stress.

For impact angles lower than 18.5°, he assumed that the particles will leave the surface while they are still in the cutting action, whereas for higher angles the horizontal motion of particles cease. The ratio of the vertical to horizontal force component in particle face was assumed to be as 2 with the experience of grinding. The ratio of length to depth of the scratch was also assumed to be as 2 from the analogy of metal cutting experiment.

The equations had angular dependence and were agreed well with the experimental results at low angle. However, these equations had limitation of underestimating the erosion above the impact angles of 45°. At normal impact the equation showed no erosion, which is contradictory to the real life experience. This deviation could be due to deflection of impinging particles to smaller angles because of rebounding particles or irregularities of surfaces at micro-level. Similarly, impacts at high impingement angle may cause fracture of work hardened surface and hence may have brittle failure. The erosion of brittle materials cannot be estimated by this equation, since material failure mechanism is different than the one assumed by Finnie.

2.2.1.2 Bitter's models

Bitter[36] stated that basically two types of erosive wear are involved, viz. (i) Deformation wear (W_D)- due to repeated impact of particles normal to target and (ii) Cutting wear (W_C)- due to cutting action by free-moving particles striking surface on acute angle. These two types of erosive wear are discussed as;

(i) Deformation wear (W_D)

Deformation wear is caused by repeated deformation during collisions, eventually resulting in infringement of a piece of material, later caused by the cutting action of the free-moving particles. Cutting wear component was considered as

negligible in erosion of brittle materials whereas deformation wear component was considered as negligible in ductile materials.

The plastic deformation of material takes place when collision exceeds elastic limit due to repeated hitting, elastic limit increases because of hardening of plastically deformed surface. Once the surface becomes relatively hard and brittle, it cannot be deformed plastically anymore with increasing load and surface layer will be destroyed by detachment of fragments. The deformation wear was expressed as;

$$W_D = \frac{\frac{1}{2} M[VSin\alpha - K_T]^2}{\varepsilon} \quad (2.5)$$

where ε is deformation wear factor, which is the ratio of energy absorbed by the surface layer during collision and amount of energy needed to remove one unit volume of material. Equation 2.5 is valid *if* $V\ Sin\ \alpha \geq K_T$, where K_T represents the maximum particle velocity at which collision is still purely elastic.

(ii) Cutting wear

When particles strike the horizontal surface in acute angle, the material is subjected to shear stress and indent through surface. When this stress exceeds material shear strength, material is removed by scratching, which is known as cutting wear. The magnitude of scratching depends upon velocity and impingement angle of particles. The velocity of impinging particles can be resolved in two components; normal to the surface (W_D) and parallel to surface (W_C). The energy possessed by particle is exhausted during deformation and scratching, resulting decrease in both horizontal and vertical component of particle velocity. Bitter [36,37] suggested two possibilities of particle velocity after scratching the surface and corresponding erosion; (a) Wc_1 in which horizontal velocity component is still present when particle leaves the body surface and (b) Wc_2 in which particle horizontal velocity component vanished during the collision. These are expressed by the following expressions as;

$$W_{c1} = \frac{2MK(VSin\alpha - K_T)^2}{\sqrt{(VSin\alpha)}}\left[VCos\alpha - \frac{K(VSin\alpha - K_T)^2}{\sqrt{(VSin\alpha)}}\varsigma\right] \quad (2.6)$$

$$W_{c2} = \frac{\frac{1}{2}M[V^2Cos^2\alpha - K_1(VSin\alpha - K_T)^{3/2}]}{\varsigma} \quad (2.7)$$

where,

ς is the cutting wear factor, K and K_1 are expression constants and K_T is threshold velocity, which are dependent on material properties.

The total wear at any instant is given as;

$$Wt = W_D + Wc_1 \quad (2.8)$$

or

$$Wt = W_D + Wc_2 \quad (2.9)$$

Fig.2.1 shows the curves for total wear for soft and ductile material, hard and brittle material based on Bitter's model.

2.2.1.3 Neilson and Gilchrist model

Neilson and Gilchrist [38] compared their experimental results with the analyses of Finnie[35] and Bitter[36] and recommended that the following factors to be accounted for any erosion damage viz. (i) The normal component of kinetic energy of the impacted particles is absorbed in the specimen surface and accounts for deformation wear, (ii) When hard materials subjected to deformation wear, no erosion takes place below a critical velocity and limiting value of velocity is dependent on particle shape, (iii) The velocity component parallel to the surface is associated with cutting wear and (iv) For cutting wear at large angles of attack the particles come to rest in the surface and the total parallel component of kinetic energy contributes to cutting wear.

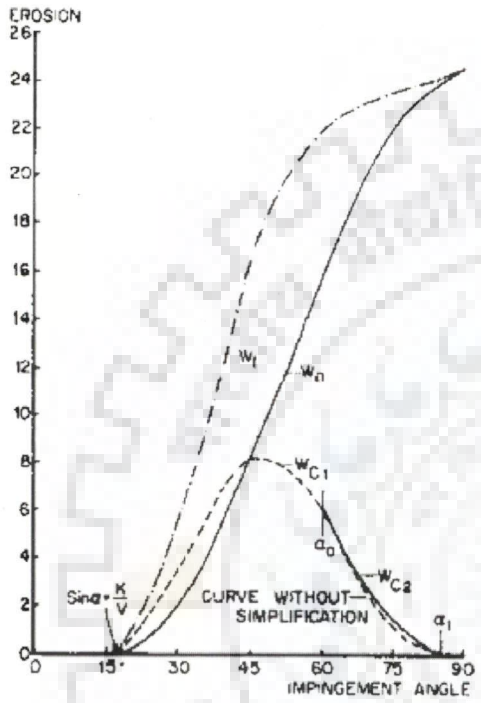

Fig. 2.1(a) Erosion of a soft and ductile material [36].

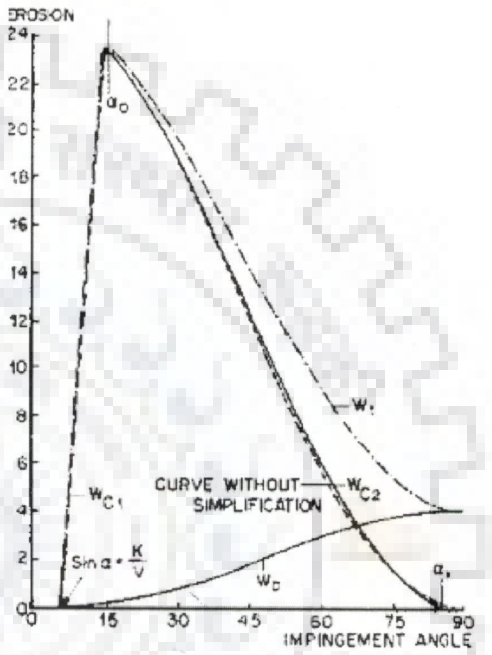

Fig. 2.1(b) Erosion of a hard and brittle material [36]

For small angles of attack, however, the particles may sweep into the surface and finally leave again with a residual amount of parallel kinetic energy.

By assuming a simplified ductile erosion model, they simplified Bitter's combined model. Based on their model [38], the erosive wear produced is expressed by the following expression as;

$$W = \begin{cases} \dfrac{MV^2\cos^2(\alpha)}{2\phi_c} + \dfrac{M[V\sin(\alpha) - V_{el}]}{2\varepsilon_b}, \alpha \geq \alpha_o \\ \dfrac{MV^2\cos^2(\alpha)\sin(n\alpha)}{2\phi_c} + \dfrac{M[V\sin(\alpha) - V_{el}]^2}{2\varepsilon_b}, \alpha \leq \alpha_o \end{cases} \quad (2.10)$$

where, W is the erosion produced by mass of particles M, α is angle of attack, V is particle velocity, K is the velocity component normal to the surface below which no erosion takes place in certain hard materials, v_p is the residual parallel component of particle velocity at small angles of attack, α_o is the angle of attack at which v_p is zero. However, the simplification made still did not provide any mean of eliminating or reducing the experimental work required to determine the erosion constants.

2.2.1.4 Hutchings model

Hutchings model [39] employed a criterion of critical plastic strain to determine the material removed from target material surface by spherical erodent. The values of velocity exponents as 3 for erosion and -2 for the mass of spherical particles were obtained. The failure strain may be predicted either assuming low cycle fatigue and using the Coffin-Manson equation[40], or using random walk theory to give the expected value of strain at a point. The failure criterion is expressed as;

$$\Delta\varepsilon_p N_f^{\frac{1}{2}} = \varepsilon_c \quad (2.11)$$

where, ε_c is the critical strain, the mean number of plastic strain cycles needed to remove a wear fragment, N_f is number of spherical projectiles distributed at random over the surface, each traveling at the same velocity and causing the same pattern of plastic deformation in the target on impact and $\Delta\varepsilon_p$ is plastic strain increment.

Based on the assumption that all the kinetic energy of the particle is expended as work done in creating the indentation, an expression for the erosion rate E (mass loss of target per unit mass of impinging particles) is expressed as;

$$E = 0.033\frac{\alpha\rho\sigma^{\frac{1}{2}}}{\varepsilon_c^2 P^{\frac{3}{2}}} \tag{2.12}$$

where, ρ and σ are the density of target material and particle respectively, V is the velocity of particles and P is the dynamic hardness of the target material.

2.2.1.5 Hashish's model

Hashish [31] modified Finnie model for erosion to include the effect of the particle shape and the velocity exponent predicted by Finnie [36]. The final form of the model, which is more suitable for shallow angles of impact, is expressed as follows;

$$W = \frac{7}{\pi}\frac{M}{\rho_p}\left(\frac{V}{C_k}\right)^{2.5}\sin(2\alpha)\sqrt{\sin\alpha} \tag{2.13}$$

where, C_k can be computed as;

$$C_k = \sqrt{\frac{3\sigma_f R_f^{\frac{3}{5}}}{\rho_p}} \tag{2.14}$$

Where, R_f is the particle roundness factor.

One of the main advantages of this model is that it does not require any experimental constants. In addition, it is the only model that accounts for the shape of particles. However, the author did not perform any validation or experimental investigation to investigate the accuracy of the model and its boundaries. This model is based on the ductile behavior of material only and is suitable for shallow impact angles for ductile materials.

Meng and Ludema [42] reported a number of fundamental studies of erosion behaviors carried out by prominent researchers [36-39, 43-68].

Bardal [69] described a general formula as a function of velocity, material hardness, particle size and concentration for pure erosion which is expressed as;

$$W = K_{mat} K_{env} C V^n f(\alpha) \tag{2.15}$$

where, W is erosion rate (material loss) in mm/year, K_{mat} is material constant and K_{env} is constant depending on environment, C is concentration of particles, $f(\alpha)$ is function of impingement angle α. V is the velocity of particle and n is the exponent of velocity.

2.2.2 Erosion Models for Hydraulic Machines

The erosion models are basically developed for specific purpose or condition. Some researchers have presented models specifically for hydraulic machinery. These erosion models are discussed as follows.

Bergeron [70] presented the predictive equation for the erosion rate of pump with simplified assumptions such as pure sliding of spherical particles over the surface. The erosion equation was expressed by the following expression as;

$$erosion \propto \frac{V^3}{D}(\rho_p - \rho) d^3 pK \tag{2.16}$$

where, V is the characteristic velocity of liquid, D is the characteristic dimension of the machine, ρ_p is density of particle, d is diameter of particle, p is number of particles per unit surface area, ρ is density of liquid, K is experimental coefficient depending upon nature of abrasive particles. This equation is proportional to experimental coefficient, which is dependent on abrasive nature of particles.

Schneider and Kächele [71] proposed that wear rate is a function of a multitude of parameters as expressed by the following algebraic relationship as;

$$W \sim cqf(d_{50})v^n \tag{2.17}$$

where, W (kg/hr) is wear rate, c (kg/m^3) is sand concentration, q (kg/kg) is hard particle contents, d_{50} (m) is median particle size, v (m/sec) is flow velocity. By conducting a number of experiments, the authors suggested the value of n, varied considerably from about 2.1 to more than 3. This range of values was reported to reflect the limitations of the algebraic relation given above, which considered neither material parameters of the eroded body nor the flow and silt parameters.

Bain et al. [72] developed a correlation for the estimation of erosion rate based on extensive data collected in a bench scale test rig. The general form of the correlation can be represented as;

$$W = KV^{\beta}d^{\gamma}C^{\phi} \tag{2.18}$$

where, W is erosion rate, V is velocity of particle, d is particle size, C is solid concentration, K, β, γ and φ are constants whose values depend on the properties of the erodent as well as the target material. For different erodent, the effect of particle size has been normally considered as a parameter affecting the wear and the exponent value γ was found to lie between 0.3 and 1.6.

Naidu [73] suggested the following expression for predicting the silt erosion rate as;

$$W = S_1 S_2 S_3 S_4 M_r V^x \tag{2.19}$$

where, S_1 is coefficient of silt concentration, S_2 is coefficient of silt hardness, S_3 is coefficient of silt particle size, S_4 is coefficient of silt particle shape, M_r is coefficient of wear resistance of base material, V is relative velocity of water. Based on experience, the authors have suggested the following values for the exponent x as 3 for Francis runner, 2.5 for guide vanes and pivot ring liner, 2.5 for Pelton nozzle and 1.5 for Pelton runner buckets.

Krause and Grein [74] reported that the abrasion rate on conventional steel Pelton runner made of X5CrNi 13/4 was as given below;

$$\delta = pqcv^{3.4} f(d_{p50}) \tag{2.20}$$

where, δ is abrasion rate (μm/h), p is a constant, q is quartz content, c is mean silt concentration, v is relative jet velocity, $f(d_{p50})$ is function defining particle size. Since the above equation was proposed for X5 CrNi 13/4, it may be applicable to turbine components made of this material.

The hydraulic performance tests on a Francis turbine model with sediment laden flow were conducted in Japan and reported by Okamura and Sato [75]. It was concluded that the turbine best efficiency decreased in direct proportion to the increase in solids concentration as expressed below;

$$\eta_m = (1 - 0.085 C_w)\eta_w \tag{2.21}$$

where, η_m is turbine peak efficiency with sediment laden flow, η_w is turbine peak efficiency with clean water, C_w is fraction of solid by weight.

The turbine abrasion was expressed by Asthana [76] as;

$$TA = f\left(PE, v^{z}\right) \tag{2.22}$$

where, PE is modified suspended sediment content, v is relative velocity between flowing water and turbine parts when abrasion is severe, z is exponent for relative velocity.

The modified sediment content (PE) is expressed by the following equation;

$$PE = P^{X} a^{\beta} k_1 k_2 k_3 \tag{2.23}$$

where, P is the average annual suspended sediment content in gm/l. It is based on the long term measurements in the river; x is exponent of 'P' representing correction factor for suspended sediment concentration. It is taken as 1 for concentration up to 5 g/l, a is average grain size coefficient of suspended sediment with a base of 0.05 mm, β is exponent of 'a' representing correction factor for average particle size, which was taken as 1 for particle up to 0.6mm and curved flow, k_1, k_2, k_3, represent the coefficient to account for shape, hardness and abrasion resistance of base metal, respectively. k_1 is taken as 0.75, 1.0 and 1.25 depending on irregularities ranging from few to severe, k_2 was taken as 1 for hardness greater than 3 (on Moh's scale) and 0.5 for less than 3 and k_3 was taken as 1 for 13Cr4Ni steel.

Mack et al. [77] suggested a numerical model to predict the erosion on guide vanes and in labyrinth seals in hydraulic turbines. The prediction of erosion was based on the Lagrangian calculation of particle paths in a viscous flow. It was described for two components of a Francis turbine for which results of field tests were available. It was shown that the erosion level was strongly dependent on the particle size. A fully 3D flow and erosion calculation around the guide vanes of the same Francis turbine was presented. There was a good agreement between the numerically obtained erosion pattern and the field test measurements.

Date at el.[78] explored the performance characteristics of a simple reaction hydro turbine for power generation for an ideal case of no frictional losses using principles of conservation of mass, momentum and energy, the governing equations.

Doujak[79] made an effort to obtain Practical experiences in preaparing a feasibility study for refurbishing a small hydro power station in Austria. Doujak et al.[80] applied PIV for the Design of Pelton Runners for RO-systems.

Chaishomphob et al. [81] undertook a preliminary feasibility study on run-of-river type hydropower project in Maehongson province, Thailand.

Keck et al. [82] presented a study of the utilization of CFD method to predict the erosion pattern in a hydraulic turbine and results were compared with field measurements of the erosion. Sand erosion was modeled by applying the LaGrange method i.e. tracking a large number of individual particles in the flow field. The motion of the particles was described by the Basset-Boussinesq-Oseen equation [83]. The experimental study based correlations were used for the drag and the influence of turbulent motion. During the Lagrangian tracking the number of particles impinging on a surface was recorded. Out of these data the removal of the wall was calculated. Calculations were performed for different particle sizes. The result showed a good correlation for the erosion pattern with the field observation. However, the authors concluded that CFD simulation did not provide accurate absolute erosion, though it could be used to obtain relative erosion intensities and to evaluate different designs relative to each other.

Majumdar [84] carried out dynamic stability analysis of a remote small hydropower station connected to infinite bus through transmission line. Varun et al. [85] evaluated life cycle green house gas (GHG) emission from the run-of-river SHP plants from India. Mehta et al. [86] developed a methodology using unsteady flow conditions behind axial and mixed flow turbine runner for performance of turbines.

2.3 EXPERIMENTAL INVESTIGATIONS

Many investigators reported their experimental results on erosive wear conducted with different base materials and different type of erodent. These experimental studies carried out by various researchers are discussed below;

Chattopadhyay [87] conducted experiments to determine the slurry erosion characteristics of AISI 316L, 15wt. % Cr-15wt% Mn stainless steel and Stellite powder alloy applied as an overlay to cast ferritic stainless steel of CA6NM type, which is used as a normal turbine runner material.

The tests were conducted on specially designed test rig as shown in Fig.2.2. The different wear rates of the alloys were explained in terms of the microstructure, hardness and work hardening rate. The samples were rectangular in section and having size of 65mm x 14mm x 20mm. Thick sand slurry was taken as the erodent. The author concluded that 15wt% Cr- 15wt% Mn stainless steel and Stellite powder alloy applied as an overlay showed better erosion resistance properties as compared to the base material CA6NM steel.

Krause and Grein [74] conducted model tests under varying parameters forX5 CrNi 13/4 steel which is normally used in hydro plants. The test rig was designed to simulate the flow conditions in a turbine. A natural sand/water mixture taken from a power plant reservoir and sand containing 99 percent quartz in various grain sizes were used for the tests. They concluded that the abrasion rate was found to be a function of velocity, sand content, proportion of hard components and size of the sand particles. The maximum abrasion occurred within an approximate particle size range of 40 to 70μm.

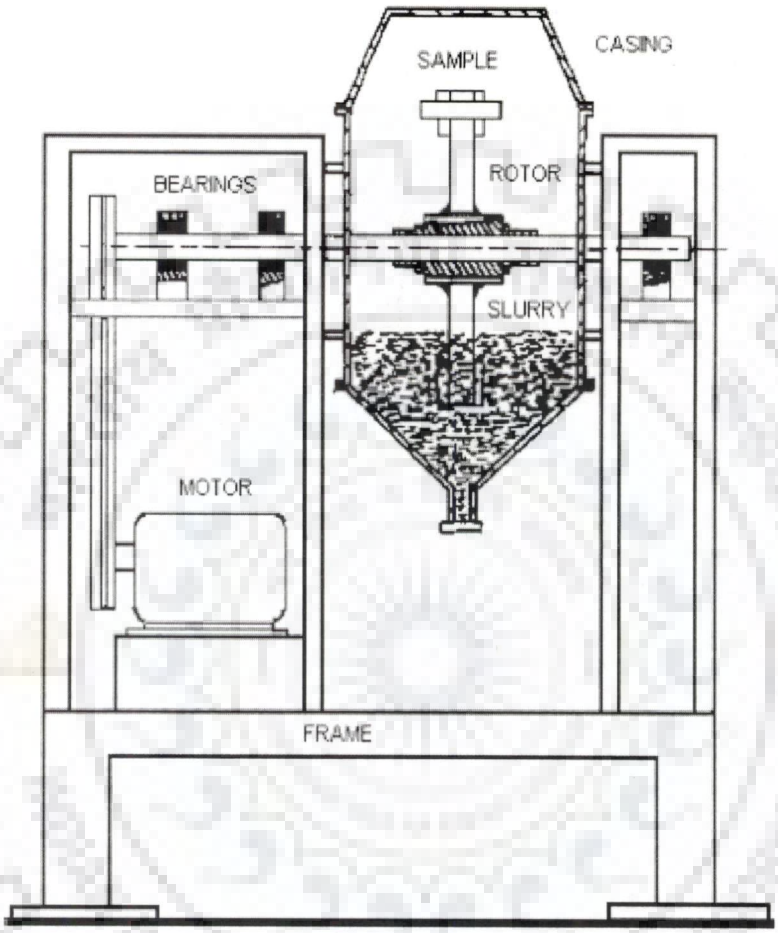

Fig. 2.2 Test Rig used by Chattopadhyay [87]

Roman et al. [88] reported the development of a new erosion resistant coating NEYRCO—a composite coating with ceramic and organic matter base, designed to combine hardness and ductility. In order to find the effectiveness of the coating against erosion, they carried out a series of model tests in a specially designed test rig as shown in Fig.2.3. Four values of water velocities were used as 20m/s, 25m/s, 36m/s, 48m/s. The water flow rate was 2.5l/s. The abrasive material was high silica content having the following chemical composition,

SiO_2	:	>99.5%
$Al_{12}O$	:	>.2%
Fe_2O3	:	>.2%
$CaCO_3$	:	>.04%
Size	:	200 to 400μm
Hardness	:	7Moh
Concentration	:	20gm/l

They observed that the coated samples gave better performance as compared to the uncoated when both the samples subjected to same erosive condition samples. Fig.2.4 shows the surface condition of, uncoated stainless steel sample and stain steel sample coated with Neyrco.

Mann [89] carried out an experimental study. Schematic of the test rig used by them is as shown in Fig.2.5 They studied the erosion resistance characteristics of different hard coatings such as hard chrome plating, plasma nitriding, D-gun spraying, boronising with commonly used steel in hydro turbines. The wear test facility was designed considering the low and high impact wear of hydro turbine components. The samples used were cylindrical shapes to simulate the angle of impingement from 0° to 90°, which occurred in hydro turbine blades and vanes. Sand was used as the erodent, the concentration varied from 1500 to 10,000 ppm. Performance of borided T410 steel was found to be much better than others.

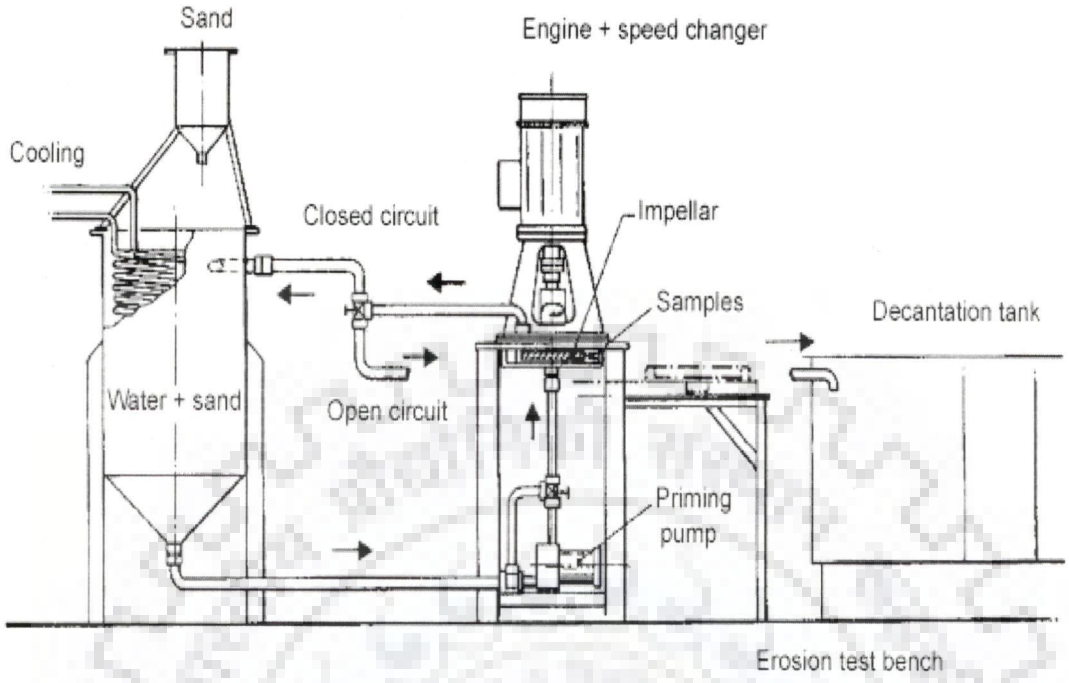

Fig.2.3 Test rig used by Roman et al. [88]

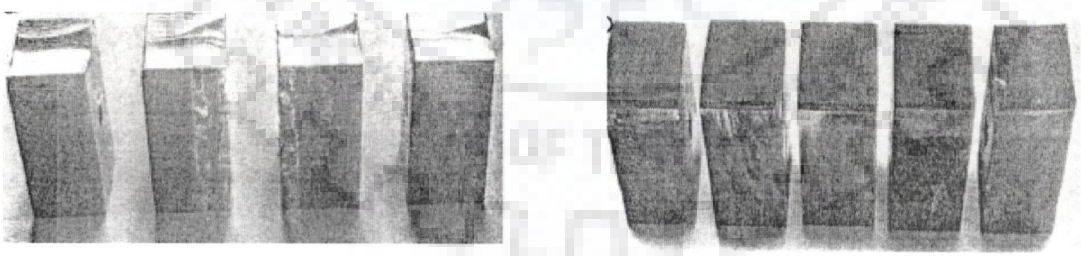

(a) Uncoated **(b) Coated with Neyrco**

Fig.2.4 Surface condition of stainless steel sample [88]

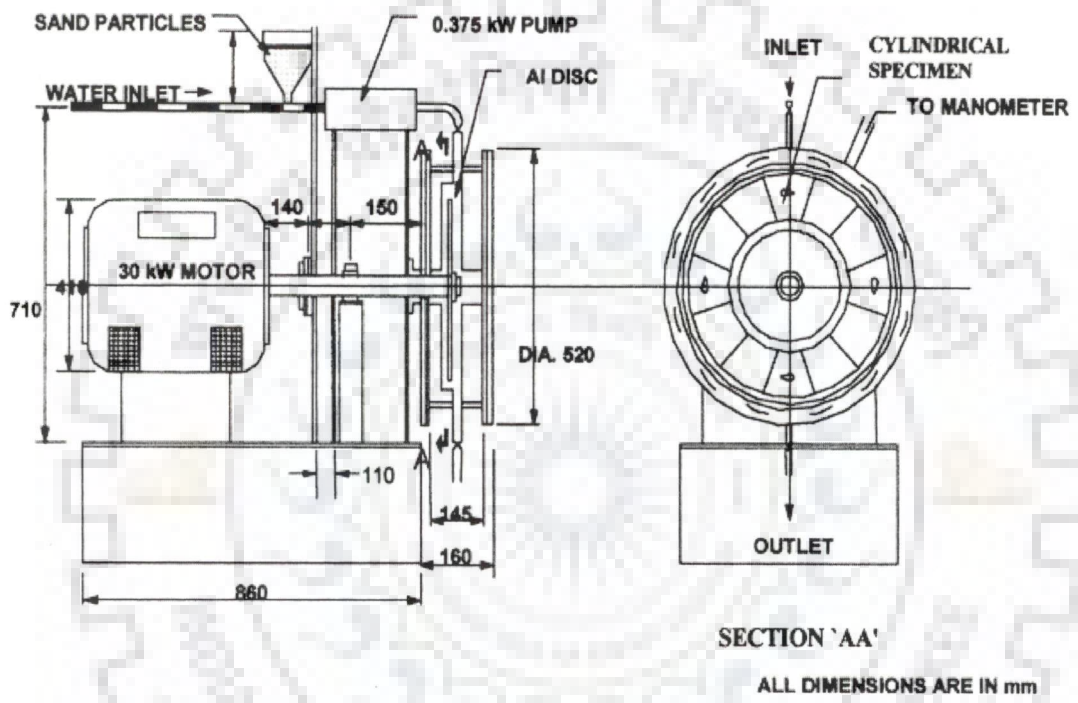

Fig. 2.5 Test rig used by Mann and Arya [90,91]

Mann and Arya [90] studied the silt erosion characteristics of plasma nitriding and HVOF coatings along with commonly used steel in hydro turbines. The abrasive wear characterization was carried out as per ASTM G-65. Angle of incidence, velocity and Reynolds numbers were maintained similar to those that commonly occur in hydro turbines. Simulation was made for low as well as high-energy impingement wear. The test parameters adopted under the study were as given below;

(i) 1 kg mineral sand of hardness: 1100 HV

(ii) Size of erodent : 180–250 μm

(iii) Erodent flow rate : 5.5 g/s

(iv) Sample size : 75mm × 25mm × 6mm

HVOF coating showed superior performance than Plasma nitrided steel, but the demerits of HVOF coating was that it showed micro cracking, debonding and digging out of WC particles. There was ductile mode of erosion for plasma nitrided steels.

Engelhardt and Oechsle [91] examined different materials and coatings to evaluate their resistance to the hydraulic turbine surface. A hard, HVOF-applied TC/CoCr coating named Diaturb 532 and a soft PU-based coating called Softurb 80 were taken for testing.

The samples were tested on a test rig. Later the San Men Xia hydro power plant in China's Henan province was selected for full scale testing of the improvements found during the laboratory research programmes. The project included a monitoring phase of two years, during which the turbine parts were inspected several times. Except for some mechanical damage to the protection systems, wear rates on the HVOF-coated runner blades were determined to be within the accuracy of the thickness measurement gauge (<40μm). The wear rate on the PU-coated surface of the runner blades and the guide vanes was determined to be around 0.15mm per

year. The unit was in operation during the two-year monitoring phase and also during the flooding season with an average sand concentration of 20–30kg/m^3.

Thappa and Brekke [23] carried out experimental studies for erosion on curved specimens. The effect of particle size was investigated by simulating the flow condition of Pelton bucket in a high velocity test rig as shown in Fig.2.6. Aluminum specimens with different curvature as shown in Fig.2.7 were used for the experiment. Baskarp-15 foundry sand with 66% free quartz (fine sand) of size 174μm and artificial silica sand (coarse sand) of size 256μm were used as the erosive particles. The results were presented in the form of erosion rate for different profiles and surface roughness at different locations of curved specimens. By visual observation of eroded particles the authors concluded that most of the coarse grains strike close to the splitter, where as the fine grains were observed far away from splitter. The erosion rate in terms of weight loss per unit striking particle found smaller with fine particles. This was due to low particle impact energy of smaller particles and might be because of escaped gliding without striking the surface by some of the fine particles. Further they observed that erosion rate (mg/kg) was increased with the increase in curve radius.

Wear characteristics of a ductile material, namely brass was investigated by Desale et. al.[92]. Experimentation was carried out by orienting the flat specimens at different orientations relative to the velocity direction in a pot tester containing a solid–liquid suspension. The erosion behavior was studied at various orientation angles, defined as the angle between the tangent to the plane surface and its velocity. Results at different orientation angles showed that the wear at any orientation angle increases with increase in velocity and particle size but decreases with increase in solid concentration. It was also considered that the wear at various operating conditions increases with increase in the orientation angle till 30° attaining the maximum value and then decreased up to 90°. It was further observed that the maximum wear was around 3–4.5 times higher than the surface wear measured at 90° orientation angle.

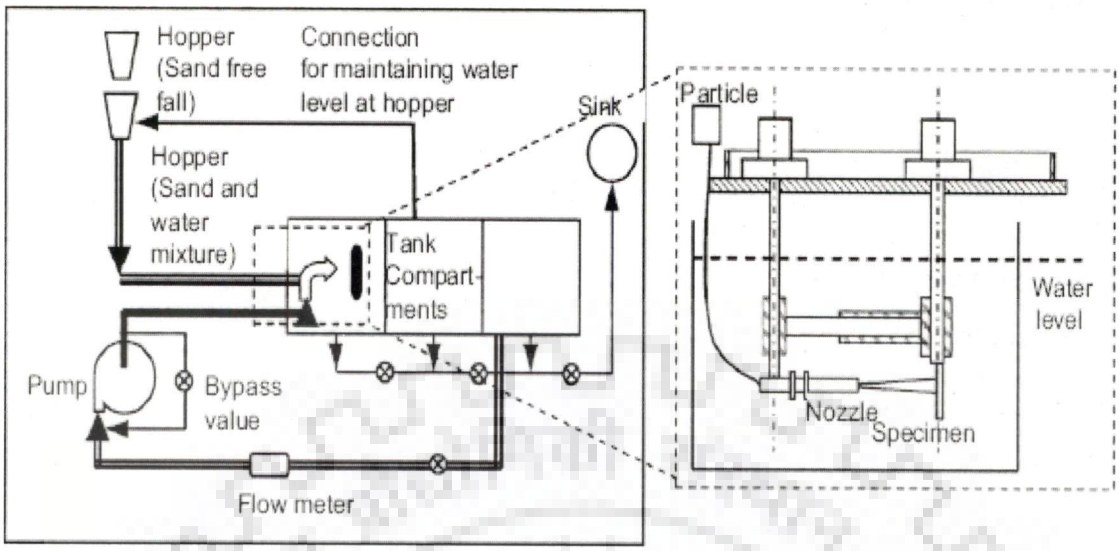

Fig.2.6 High velocity test rig used by Thappa and Brekke [23]

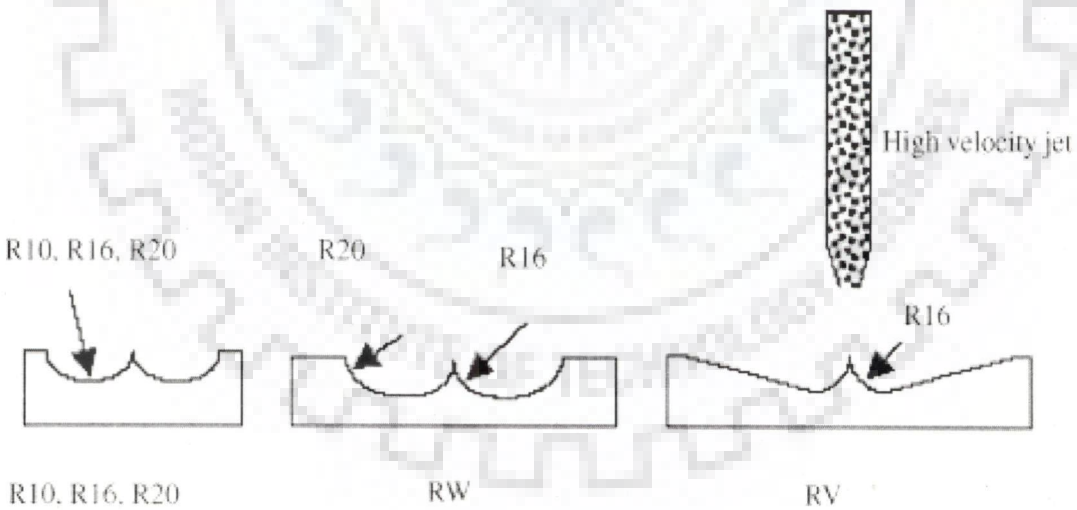

Fig.2.7 Specimens of different curvature used by Thappa and Brekke [23]

Several mechanisms proposed for the removal of material from a metal surface by solid particle impact. Finnie [35] suggested a process involving cutting or displacing material. Tilly et al. [93-96] considered erosion to be a two stage process: the initial stage being the formation of raised lips, and the second stage the removal of these by a radial flow of fragments resulting from the combination of other particles impacting nearby. Sheldon and Kanhere [49] observed that the metal removed had flowed around the sides of the impacting particle until it was strained sufficiently to break off.

Spherical and angular particles have shown different material removal rate due to change in wear mechanism [12, 38, 55, 61, 97-99].Winter and Hutchings [99] observed ploughing or smearing type of impact crater with large rake angles and a cutting mechanism at small rake angles. The term rake angle is defined as the angle between the front face of the particle to the normal to the target surface and is dependent on the particle shape. For a spherical particle, the rake angle is always large and negative. Angular particles are generally found to cause a greater proportion of cutting type of material removal. If the angle between the surface and the leading edge of the particle is larger, a micromachining action occurs. However, rather than scooping out material as a chip, the cutting edge of the particle tends to bury itself deeply into the specimen. Material can be removed as a result of a particle breaking up during its cutting action. Here, a lip raised during the early stages of the impact is subsequently cut off by fragments of the particle. They predicted particle rotation takes place during impact and that when this happened the particle's effectiveness in removing material is diminished.

Hutchings and Winter [55] observed oblique impact by an individual spherical particle formed a lip from surface material sheared in the direction of motion of the particle and that above a critical velocity this lip can become detached.

Stachowiak and Batchelor [100] discussed seven different possible mechanisms for solid particle erosion as abrasive erosion, surface fatigue, brittle fracture, ductile deformation, surface melting, macroscopic erosion and atomic erosion. But among all these, from the point of view of erosion of hydraulic machinery, only first four (abrasive erosion, fatigue, plastic deformation and brittle fracture) are applicable.

Sharma et al. [101] conducted wear experiments for Al-Pb alloys on a pin-on-disc machine and the worn-out test pin surface topography, sub-surface damage and debris were studied by SEM. They found that a number of wear processes, such as delamination, adhesion and abrasion, take part in removal of metal as debris, and no single wear process is responsible for metal removal from sliding surfaces. The presence of lead in base alloys is found to reduce wear and friction.

Roy Chowdhury et al. [102] presented the wear equations for polymer in two groups, one representing primarily abrasive wear and the other the fatigue mechanism, since the two mechanisms operate in distinct roughness ranges, and validated the proposed model experimentally. Roy Chowdhury et al. [103] studied mechanical and tribological properties of UHMWPE and HDPE composites with improved biocompatibility.

2.4 CASE STUDIES

Darling [104] studied the refurbishment of the Svartisen hydroelectric plant (Norway). Hydro turbine at this project experienced more erosion than other Francis units in Norway due to the unusually high levels of silt in the water. From the commissioning of the plant in 1993 until 2003, the efficiency of the turbine was dropped by 2-2.5%. Tungsten-carbide thermal spray coating was applied on surface as an effort to increase the time for refurbishments and to increase the lifetime.

Thapa et al. [105] investigated the effect of suspended sediments in hydropower projects based on a case study of 60MW Khimti hydropower plant. Due to presence of high amounts of sediments, the hydropower plant was designed with settling basins to screen 85% of all particles with a diameter of 0.13 mm and 95% of all particles with a diameter of 0.20 mm. The plant was commissioned in July 2000 and the damage to the turbine components was investigated in July 2003. The investigators observed that a significant amount of erosion had appeared in the turbine bucket and needles. Even though the settling basins were performing satisfactorily, particles smaller than the design size passed through the turbines and caused the damage. The bucket thickness was reduced by about 1 mm towards the root of the bucket, which was critical from the point of view of strength and hence the reliability of the component. Similarly the splitter of the bucket was eroded to saw tooth form from the original straight edge. The sharp edge of the splitter had blunted and the width became approximately 4 mm due to which the efficiency of the turbine had decreased. To minimize the effect of erosion hard ceramic coatings were applied on the bucket and needle surface at the cost of around US$ 25000 per runner, but the performance had not been obtained at promising end.

Pradhan [106] conducted case studies and observed during his studies that in run of river power plants in steep sediment loaded rivers the conventional design criteria to trap 0.2 mm size sediment particles did not seem to function satisfactorily. In general, projects were having damages to runners due to severe erosion caused by silt. In case of Jhimruk Project (Nepal), the wear on runner was so high that it required repair after every monsoon. Case studies were carried out for Jhimruk Hydro Plant (Nepal), a 12 MW run-of-river type project built and commissioned in 1994. The settling basin was designed to trap 90% of 0.2 mm size particles.

Singh [107] reported the case study of the Tiloth hydro power station (3 x 30 MW) on river Bhagirathi (India). The three units were commissioned in the last

quarter of 1984. The turbines were found to be seriously damaged after about 2600hours of operation. They were repaired, but again within 3000 to 5000hours of operation, extensive damage was observed. The sedimentation chamber was designed to arrest silt particles larger than 0.3mm. Based on petrographic studies carried out, the presence of highly abrasive quartz having hardness of 7 on Mohr's scale was revealed. The concentration of the silt particles during rainy season was found maximum which was reached up to 4000ppm. Initially there was a proposal to provide another sedimentation chamber to arrest particles up to 0.15mm. But due to very high cost and as the settling chambers could not completely remove the silt particles, the proposal was not implemented. The investigators, rather, suggested improving the metallurgy of the turbine blades. The new runner was manufactured with stainless steel (13 Cr 4 Ni), which was supposed to give a better performance regarding erosion. However, it was observed that there was no appreciable reduction in the erosion compared to the older runners.

Yan [108] studied the effect of silt abrasion in different hydropower plants of China and had drawn the following conclusions.

i. The abrasion remained moderate for all particles smaller than 0.05mm and rises sharply for larger sizes.

ii. The product of operating head,H and content of harmful sediment, S_d (d>0.05mm) must be less than 7, so that the abrasive erosion in the turbine would be minimum.

Wood [109] reported a field study carried out by China North West Electric Power by mounting coated specimens in different places in Kaplan and Francis turbines and left during the flood season. Coated region had reduced the worn out thickness between 5μm to 43μm, whereas, the surrounding uncoated metal had been worn out within 1mm and 10 mm. The research programme concluded that minimum

loss of efficiency can only be reached by combination of design optimization based on erosion prediction and protection of surfaces with wear reducing coatings.

Saini et al. [110-130] carried out analytical, experimental and case studies for the development and improvement of small, mini and micro hydro power plants in Himalayan range of India and Nepal.

Duan and Karelin [131] tried to expound the fundamental theory, research situation, and achievements from laboratory and practice engineering of the abrasive erosion and corrosion of hydraulic machinery.

Bajracharya et al. [132-137] undertook experimental study and case studies of 19 hydropower plants in Nepal with generating capacity of 2MW and more. Mostly these projects are run-of-river (ROR) except Kulekhani hydropower plant and are affected by sand erosion. From the collected field data they predicted the relationships between the erosion rate of spear and the particle size at different quartz content levels as expressed below;

$$Erosion\ rate \propto a(size)^b \tag{2.24}$$

where,

$a = 351.35, b = 1.4976$ for quartz content of 38%,

$a = 1199.8, b = 1.8025$ for quartz content of 60%,

$a = 1482.1, b = 1.8125.$ for quartz content of 80%.

Erosion rate with particle size was obtained as shown in Fig.2.8. They observed severe erosion both in the spur needle and the buckets in Kulekhani-I, a reservoir type hydropower plant, during maintenance period as shown in Fig.2.9.

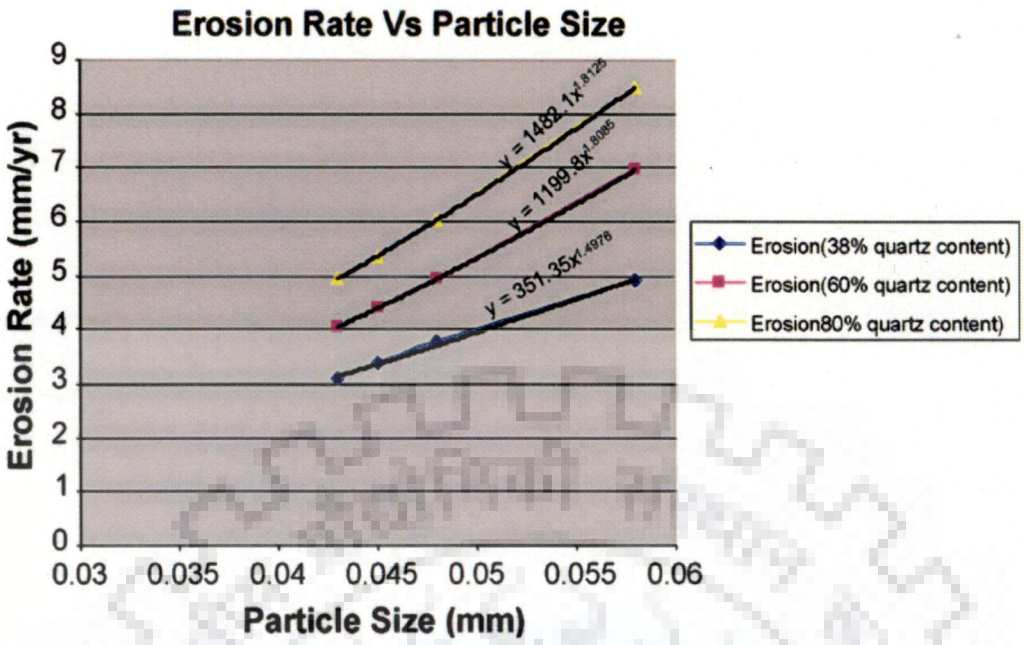

Fig.2.8 Relationships between the erosion rate and the particle size [132]

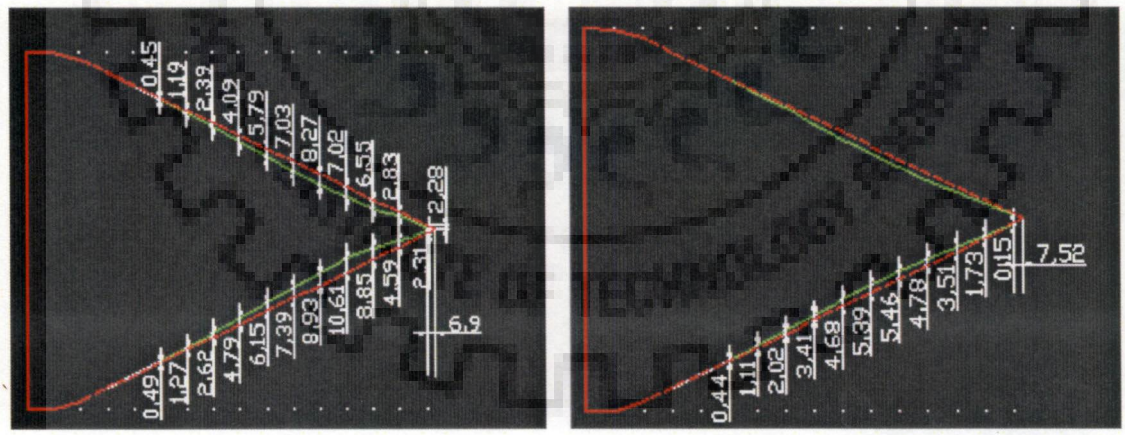

(a) Severely eroded surface **(b) Uniformly eroded surface [132]**

Fig.2.9 Erosion profiles of needle

The dotted line in the figure shows the actual profile of the spur needle, while the profile in the continuous line shows the eroded surface. Further, a groove along the radialy opposite part of the conical spur needle was observed.

A relation between the erosion rate of spear and the reduction of efficiency from the field data was predicted [132] as shown in Fig.2.10. The prediction was expressed by the following expression;

$$Efficiency\ reduction \propto a \times (Erosion\ rate)^b \tag{2.25}$$

where,

$a = 0.1522$ and $b = 1.6946$

Erosion rate of spear needle of Chilime Hydro Electric Project, Nepal was observed as 3.4mm per year which predicted from the Eq.2.24 that the reduction in the efficiency of the turbine was 1.2% for the first year of operation and around 4% in the next year for the continuous operation and without maintenance of the plant.

Brekke [138] undertook a case study on Driva Power Plant and observed that abrasive erosion of facing plates on head cover and lower cover of a Francis turbine leads to an increased leakage between the guide vane facing and covers. The increased loss in efficiency caused by abrasive erosion of 2 mm in a high head turbine at 540 m net head resulted about 10 % relative efficiency loss as shown in Fig.2.11.

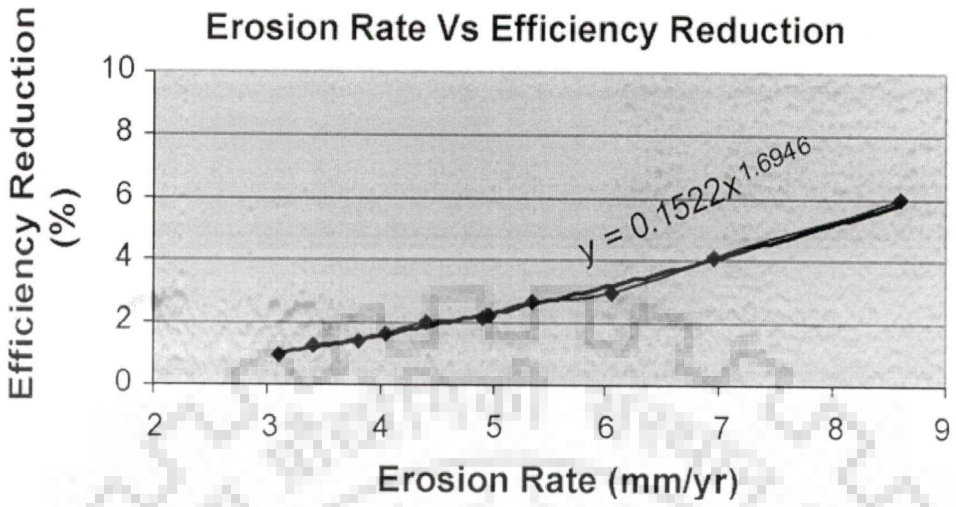

Fig.2.10 Efficiency loss versus erosion rate [132]

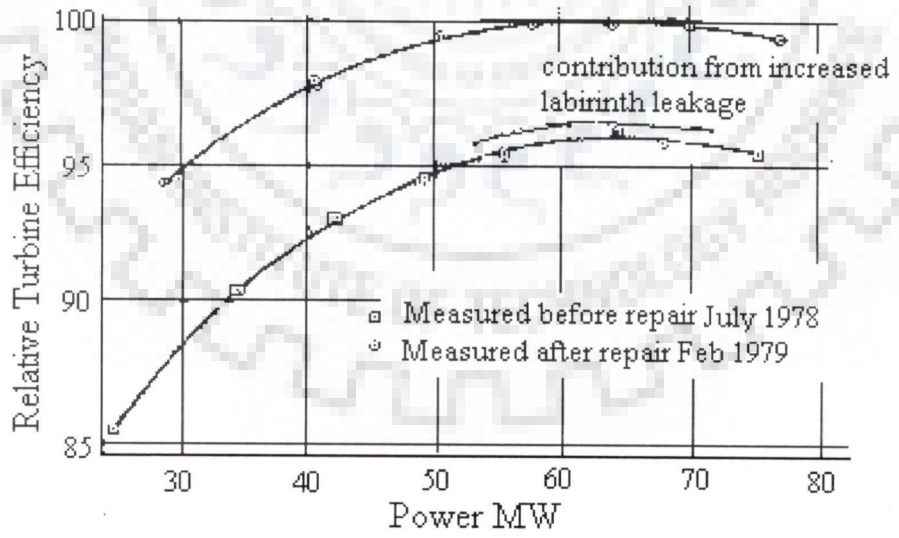

Fig.2.11 Efficiency loss due to erosion (Francis turbine, P=71.5 MW, H=540m,N=600 rpm)[138]

Brekke [139] suggested a thumb rule to estimate the drop in efficiency by measuring the thickness of splitter. The height of splitter gradually decreases due to erosion which is proportional to the erosion depth in the bucket. This thumb rule was stated as "When the thickness of the splitter increases to 1% of the bucket width, the drop in relative efficiency at full load is 1%". This condition was observed when needle was not damaged. In case of Pelton turbine, the highest loss is at best efficiency point which is shown schematically in Fig.2.12.

Pradhan et al. [106] under a case study in Jhimruk river, observed that average values for suspended sediment concentration in Jhimruk river during the peak monsoon ranges from about 2,000 to 6,000 ppm with upper values ranging from about 20,000 to as high as 60,000 ppm, which indicated that sediment transport in Jhimruk river during the monsoon was quite significant. The runners were significantly worn out after every monsoon. They concluded that the efficiency loss was 4% at best efficiency point and 8% at 25% load. The results obtained based on the thermodynamic efficiency measurements and are shown in Fig.2.13.

Thapa et al.[23] undertook a case study of damage of Pelton turbines from hydropower plants, (i) Mel (Norway) with sand particles size equal and less than 60 micron, (ii) Khimti (Nepal) with particles size less than 150 micron and (iii) Fortun (Norway) with large particles (gravel hitting). They observed that fine particles caused erosion on the needle but not much erosion in the buckets. Coarse particles caused erosion in the buckets but less erosion in needles. Medium size particles caused erosion in both needle and bucket.

They concluded that fine particles may glide along with water inside the bucket and strike the surface toward outlet edge, causing severe erosion around outlet. Due to distortion of bucket profiles near the outlet. This phenomenon was schematically explained in Fig.2.14.

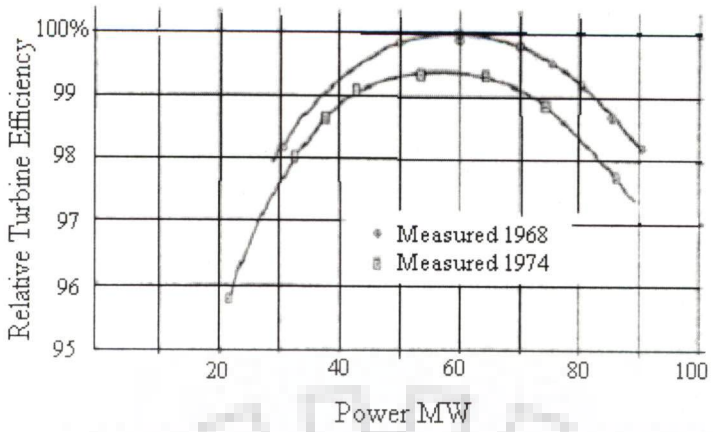

Fig.2.12 Efficiency curve for 81 MW vertical Pelton turbine before and after sand erosion (H= 645 m, N=500 rpm)[139]

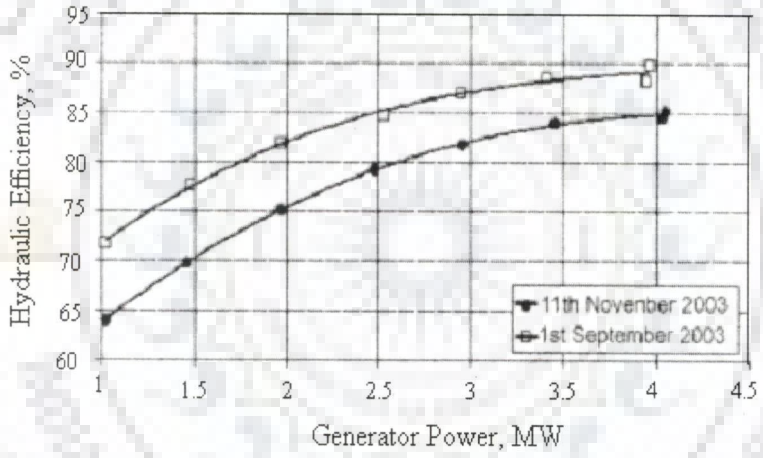

Fig.2.13 Efficiency loss due to erosion at Jhimruk hydro power plant [106]

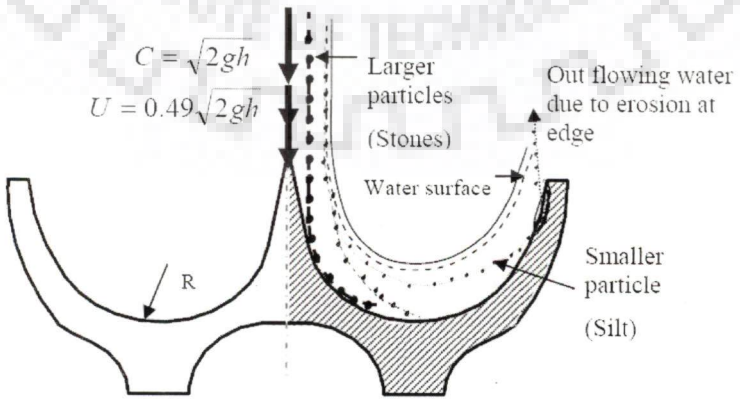

Fig. 2.14 Particle separation at high acceleration [23]

CHAPTER-3

OBJECTIVE AND METHODOLOGY OF THE PRESENT STUDY

3.1 GENERAL

A number of hydro electric project sites in the Himalayan range and in the northeastern region of India face severe silt erosion problems in turbines which over a period of time drastically reduce the overall efficiency of power generation system. A study of several existing hydro electric power stations located in these regions has confirmed the severity of silt erosion on the critical underwater parts of turbines and other components of the power stations. Himalayan rivers contain very high sediment concentration during the monsoon season. Major components of this sediment are hard abrasive sand and silts which severely damage the turbine components.

For efficient operation of hydropower plants in order to meet the electricity demand the hydro energy is stored either in reservoirs for dam based schemes or settling basins for run-of-river schemes. These reservoirs or settling basins are filled with sediments over a period of time. This problem must be taken care of by sediment settling systems in power plants. However, lot of unsettled sediment pass through the turbines every year and turbine parts are exposed to severe erosion. The erosion of hydro turbine components is a major problem for the efficient operation of hydropower plants. These problems are more prominent in power stations which are of run-of-river types. The problem is aggravated if the silt contains higher percentage of quartz, which is extremely hard. Nepal is also facing severe silting problem in hydropower plants with specific sediment yield of about 4240 tonnes/km^2/year.

Silt erosion is a result of mechanical wear of components due to dynamic action of silt flowing along with water. However, the mechanism of erosion is

complex due to interaction of several factors viz. particles size, shape, hardness, concentration, velocity, impingement angle, properties of material and so on. The silt laden water passing through the turbine is the root cause of silt erosion of turbine components which consequently leads to a loss in efficiency thereby output, abetting of cavitation , pressure pulsations , vibrations , mechanical failures and frequent shut downs. Since silt erosion damage is on account of dynamic action of silt with the component, properties of silt, mechanical properties of the component in contact with the flow and conditions of flow are therefore, jointly responsible for the intensity and quantum of silt erosion The erosion damages are to some extent different for Pelton and Francis turbines. In case of Pelton turbines, needle, seal rings in the nozzles and runner buckets, splitter is most exposed to sand erosion. In case of Francis turbines runner vane, guide vane cascade and the labyrinth rings are exposed to wear. The hydraulic machines, working under medium and high head are normally exposed to erosion. High head Francis and Pelton turbines are highly affected by sand erosion. Even low head Kaplan turbine and propeller turbines are also found eroded in rivers with high sediment contents. Bucket, nozzle and needle are most affected parts in case of impulse turbines and guide vanes, faceplates, runner blades and seal rings in case of reaction turbines.

It is revealed from the literature survey that various researchers have studied the process of silt erosion in hydro turbines and the effect of different parameters on erosive wear. Details of these studies have been discussed in previous Chapter-2. Under this Chapter-3 objective of the present study has been discussed. A methodology adopted to carry out the investigation has also been presented.

3.2 OBJECTIVE OF THE STUDY

Based on analytical and experimental studies, different correlations were proposed by different investigators to predict the erosive wear in hydro turbines. The

effect of different parameters on erosive wear was discussed. These correlations are mostly based on experiments on small specimens, which do not match actual turbine components. The flow conditions created in the test rigs used in such experiments did not represent the real flow conditions in turbines. The models based test results obtained during such experimental studies in laboratories may not be able to predict the silt erosion of actual turbines in practice. It is therefore, more theoretical and experimental studies are required to incorporate the actual flow conditions inside the turbines. It becomes necessary to investigate the effect of different parameters, i.e., concentration and size of silt, jet velocity, operating conditions and properties of base materials on erosion of turbine components with a view to predict silt erosion more accurately.

The most common type of impulse turbine is Pelton turbine, which operates under high head. The available potential energy of water is converted to kinetic energy at the nozzle, which furthermore depend on the mass of water and available head. The energy available in the water is converted into mechanical energy in the form of turbine rotation at the cost of reaction to the turbine components. During this process, the sediment present in the water exerts force on the turbine components; as a result the turbine components get deformed. The dimensional change of the components leads to efficiency loss and eventually the system failure. Various terms such as erosion, hydraulic abrasion, abrasion and hydro-abrasion were used in the literature for describing the process of gradual change in the shape and state of the surface due to silt particles in flowing water.

The Pelton turbine components affected by silt erosion can be classified as (i) inlet system (ii) nozzle and needle (iii) runner and bucket and (iv) wheel pit.

Silt erosion has impact on both performance and reliability of a Pelton runner. Bucket is the most affected part of the Pelton runner. The change of bucket profile alters the flow pattern causing loss of efficiency. Similarly loss of material weakens highly stressed parts increasing probability of fracture. The damage of Pelton turbine components occurs due to acceleration of large particles in the bucket, turbulence of fine particles in needle and impact in splitter.

The present investigation was carried out for erosive wear on Pelton turbine buckets. The objective to investigate the erosive wear of Pelton buckets is based on the consideration, that the maintenance of buckets after erosion is costly in comparison of other components. The maintenance of the eroded turbine mainly depends upon dismantling time of the runner.

Keeping this in view, the present study is undertaken to investigate the effect of silt erosion on Pelton turbine buckets. In order to predict the effect of different parameters on erosive wear due to silt laden flow in Pelton buckets, following are the objectives for the present study.

i) To design and fabricate the experimental setup for actual flow conditions in the Pelton turbine.

ii) To investigate the effect of the following parameters on erosive wear of Pelton buckets.

   a.) Silt concentration

   b.) Size of silt particles

   c.) Jet velocity

   d.) Operating hours of the turbine

iii) To establish correlations for normalized erosive wear as a function of silt related parameters.

iv) To investigate the effect of silt parameters on turbine efficiency.

3.3 METHODOLOGY ADOPTED

The investigation was carried out in two stages discussed below;

i) Identification of wear hot spots

a) The Pelton turbine buckets were coated with easily erodible material. The wear hot spots were identified after running the turbine over a period of time.

b) Thin pieces of soft material (Brass) specimens were fixed at the hot spots with adhesive.

ii) Measurement of wear

a) The pattern of erosive wear of Pelton turbine bucket was examined by taking magnified photographs of bucket surface.

b) The mechanism of erosive wear for the specimens placed at different hot spots were examined through SEM (Scanning Electron Microscope) micrographs and discussed.

c) Tests were conducted to determine the quantum of erosive wear and the effect of different parameters on erosive wear. The quantum of erosive wear was determined by measuring the mass of buckets before and after the experimentation for different operational hour.

d) Based on the experimental data collected, correlation for normalized erosive wear was developed as a function of silt parameters.

e) Based on the power generation data recorded and experimental data collected, further, the effect of considered parameters was discussed for loss of percentage efficiency of turbine. Correlation was developed for turbine efficiency as a function of silt related parameters.

3.4 STRUCTRE OF THE THESIS

The work carried out under the present study has been presented in the following 7 Chapters.

CHAPTER-1 INTRODUCTION

CHAPTER-2 LITERATURE REVIEW

CHAPTER-3 OBJECTIVE AND METHODOLOGY OF THE PRESENT STUDY

CHAPTER-4 EXPERIMENTAL INVESTIGATION

CHAPTER-5 RESULTS DISCUSSIONS AND DEVELOPMENT OF CORRELATION

CHAPTER-6 INVESTIGATION OF TURBINE PERFORMANCE

CHAPTER-7 CONCLUSIONS

CHAPTER-4

EXPERIMENTAL INVESTIGATION

4.1 GENERAL

It is revealed from the literature survey presented in Chapter-2 that a number of researchers have conducted experiments to study the effect of silt parameters on erosive wear. Most of these experiments are on small size samples in different types of test rigs to simulate the flow conditions in the turbine. However, actual flow conditions and the phenomenon of erosive wear is too complex to simulate. In order to take into account the factors (i) the actual flow conditions, (ii) operating hours of the turbine, (iii) the curvature of the Pelton turbine bucket, (iv) the variation of the size and the concentration of the eroding particles and (v) jet velocity, the present investigation has been carried out on a small scale Pelton turbine.

Under the present study an experimental set up was designed and fabricated keeping in view with the actual turbine conditions and to investigate the effect of the considered parameters on the erosion. Silt related parameters and operating conditions i.e. concentration, size of silt particles, jet velocity and operating hours of the turbine were considered.

This Chapter-4 presents an extensive experimental study that has been carried out to collect the experimental data in order to develop the correlation for wear rate as a function of particle size, concentration, jet velocity and time of operation of the turbine. Experimental data have been generated taking into account all the parameters contributing their effect on erosion of Pelton turbine bucket. The silt samples from the river basin close to a severely affected powerhouse were collected. Various aspects related to the experimental study such as experimental setup, instruments, experimental procedure, range of parameters and experimental data have been discussed in this Chapter-4.

4.2 EXPERIMENTAL SETUP AND INSTRUMENTATIONS

An experimental setup was designed and fabricated to carry out the proposed investigation. Fig.4.1 shows a schematic of the test set up. The set up consisted of; (i) Pelton turbine runner, (ii) Water tank, (iii) Stirrer, (iv) Cooling jacket, (v) Service pump-motor set, (vi) Penstock pipe, (vii) Spear valve and nozzle, (viii) Control valve, (ix) Channel with weir, (x) Generator and a control panel with resistive load and (xi) the instrumentation. A photograph of the experimental set up is shown in Fig.4.2

4.2.1 Pelton Turbine Runner

The most important part of the setup was the Pelton turbine runner. Pelton turbine runner having pitch circle diameter of 245mm and nozzle diameter 10mm, mounted with 16 numbers of buckets was used for the experiments. The Pelton turbine buckets made up of brass were chosen as specimen to get measurable amount of erosion in a short time period. The weight of each specimen bucket was 205 ± 1.5g. The shaft of the runner was directly coupled with the generator shaft. A photograph of the runner used under the present study is shown in Fig.4.3.

4.2.2 Water Tank

A steel tank having size of 600 mm long, 510 mm wide and 780 mm deep was used to circulate water through turbine under different operating conditions and to mix silt with water. Water was stored up to a depth of 450mm and the upper portion of the tank was connected to a channel. The tank was provided with an inlet water tap for pouring water to the required level and at the bottom an outlet valve was provided to drain out silt water mixture when it was required to replace after each set of experimentation.

4.2.3 Stirrer

A stirrer connected with a 0.5 hp motor was provided in the middle of the tank. It was operated continuously during experiments so as to provide uniform mixture of silt and water.

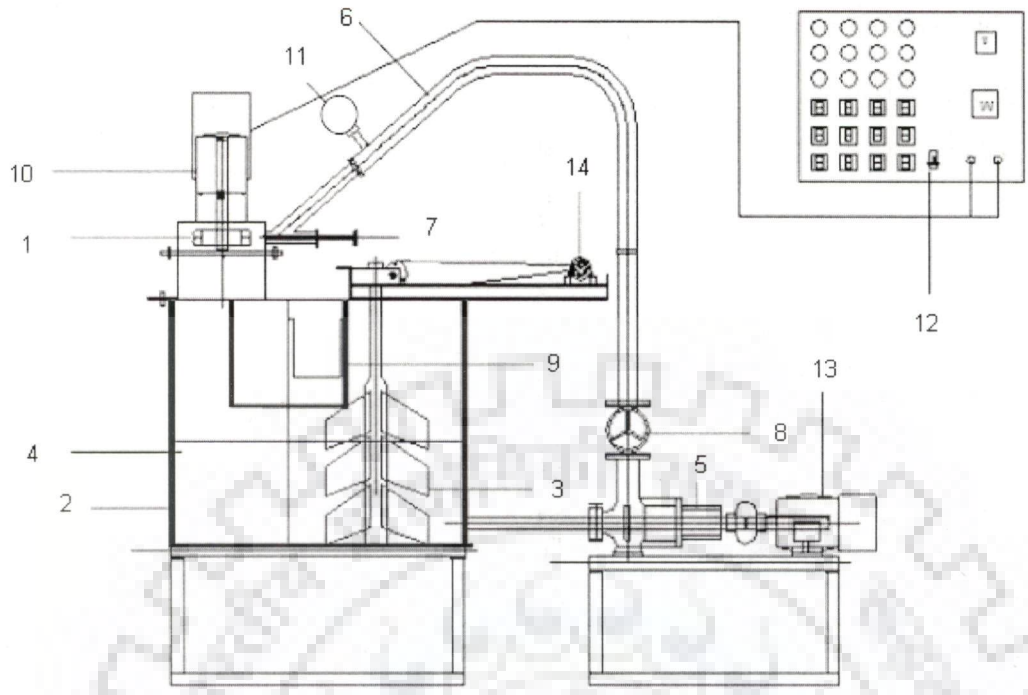

Fig.4.1 Schematic of experimental set up

Description:

1: Pelton turbine runner

2: Water tank

3: Stirrer

4: Cooling jacket

5: Service pump

6: Penstock pipe

7: Spear valve

8: Control valve

9: Channel with weir

10: Generator set

11: Pressure transducer

12: Control panel with ballast load

13: Driving motor

14: Motor for driving stirrer

Fig.4.2 Photograph of experimental setup

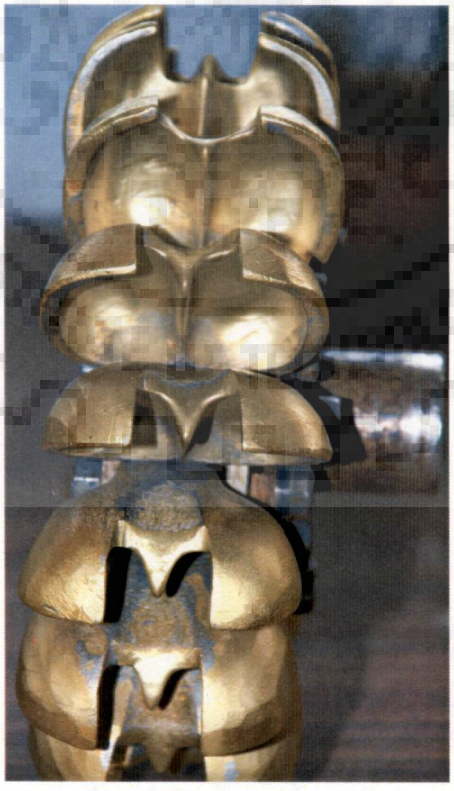

Fig.4.3 Photograph of Pelton turbine runner

4.2.4 Cooling Jacket

In order to maintain the temperature of the silt laden water constant, a cooling water jacket was provided on three sides of the tank. The other side was connected to the service pump through a pipe. The width of the cooling water jacket was 315 mm and the depth was kept as 335 mm. Cooling water was circulated in the cooling jacket continuously so as to maintain constant temperature of the silt water mixture in the tank.

4.2.5 Service Pump-Motor

In order to create the head to be applied to the turbine under desired conditions a centrifugal pump (Type: CD65-40-200 of Gita Flopump Pvt. Ltd., India) having 50m rated head and rated discharge of 8 lps was used for circulating water silt mixture to create hydro potential. Water from the turbine outlet was allowed to flow back to the water sump. The pump was driven by a Kirloskar make (7.5 kW) three phase induction motor.

4.2.6 Penstock Pipe

A penstock pipe of 60 mm outer diameter and 4 mm wall thickness was used for supplying water under pressure to turbine nuzzle.

4.2.7 Spear Valve and Nozzle

A spear valve was used at the end of the penstock pipe with a nozzle having a diameter of 10 mm to convert the potential head of water into velocity head.

4.2.8 Control Valve

A control valve on the penstock pipe just above the service pump was provided to maintain the required head and discharge to the turbine.

4.2.9 Channel with Weir

A channel was designed and fabricated with 10 mm thick perspex sheet to measure the discharge at the turbine outlet. The channel having length as 5700mm, width as 200 mm and depth of 400 mm was connected to the upper portion of the tank. During the discharge measurement the water from the turbine was allowed to flow through this channel. A thin plate rectangular weir was fixed at the end of the channel to measure the discharge by observing the head over the weir. The rectangular wear was designed according to IS:9108-1979 [140].

4.2.10 Generator and Control Panel

A generator was directly coupled to the runner shaft. An electrical load was connected with the generator through a control panel, to measure the electrical power output. The control panel consisted of a Wattmeter, a Volt meter and electric bulbs used as ballast load. Photographs of the generator and the load control panel are shown in Fig.4.4 and Fig.4.5 respectively.

4.2.11 Instrumentations

The instruments used to measure the different parameters for the experimental investigation are discussed as follows;

4.2.11.1 Digital pressure transducer

A digital pressure transducer of ABB make was used to measure the pressure (Head) at the inlet of the turbine. The pressure transducer was 600 T series model with span ranging from 267KPa to 8000KPa and accuracy ± 0.075% which had integrated display of 4-digit LCD. A photograph of the same is shown in Fig.4.6.

4.2.11.2 Digital balance

A digital analytical balance of METTLER TOLEDO make with a span range from 10 g to 210 g and having an accuracy of 0.1mg was used to measure the mass loss of the buckets. The values of the weight measured with an accuracy up to four decimal points. A photograph of the balance is shown in Fig.4.7.

Fig.4.4 Photograph of generator set

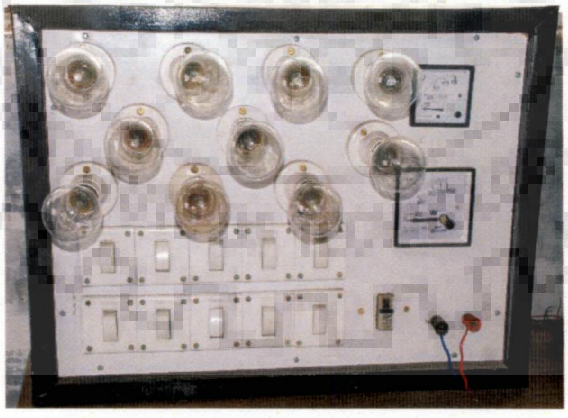

Fig.4.5 Photograph of control panel

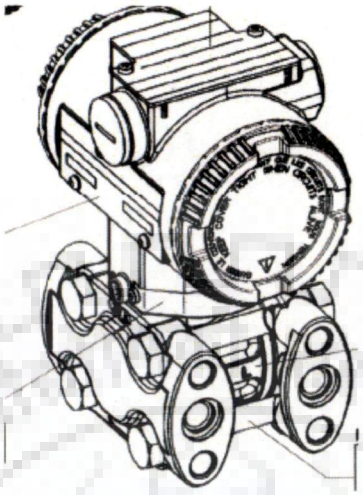

Fig.4.6 Digital pressure transducer

Fig.4.7 Photograph of digital analytical balance

Another digital balance of Citizen Make with span range from 10 g to 6 kg and least count of 0.5 g was used to measure the weight of silt having different parameters used for the investigation. The values of weight were measured with accuracy up to ± 0.5 g. A photograph of the digital balance is shown in Fig.4.8.

4.2.11.3 Sieve analyzer

A sieve shaker of Lab Line Instruments make was used for grading silts to different sizes. The different sizes of sieves having a 20 cm diameter, spun brass frame and best quality wire meshes of 355μm, 215 μm, 180 μm and 90 μm sieve opening were used.

4.3 SYSTEM AND OPERATING PARAMETERS

As discussed above, silt size and concentration, are the parameters related to silt erosion. The working parameters considered under present study are the jet velocity (head) and operating hours of the turbine. In the present investigation runner bucket has been considered in order to study the effect of erosive wear for different silt parameters. The silt related parameters considered under the present study are discussed as follows;

4.3.1 Silt Concentration

Concentration in general is defined as mass (or volume) of the solid particle present in unit mass (or volume) of fluid. It can also be defined in terms of percentage of particles in a given fluid mass (or volume). Parts-per notation is often used as the measure of concentrations for measuring the relative quantity of dissolved minerals or pollutants in water. Particularly the expression parts per million (ppm) remains widely used in technical disciplines. For river sedimentation concentration is generally presented in terms of ppm, which is equivalent to one milligram of sediment per liter of water (mg/l). 1000 ppm is considered to be equivalent to 0.1%.

Fig.4.8 Photograph of digital balance

Different values of silt concentrations have been used under the present study. Different silt concentrations were prepared in the tank by mixing the silt of appropriate amount with water. The silt concentrations considered for the present study were 10,000 ppm, 7,500 ppm and 5,000 ppm, which correspond to 1%, 0.75%, 0.5% by weight respectively.

4.3.2 Silt Size

Particle size can be characterised mainly in two basic dimensions mass and length. For a given velocity, kinetic energy of particle is directly proportional to mass. The mass of spherical particle is proportional to cube of diameter. Theoretically, erosion rate is proportional to cube of diameter. The literature review reveals that the mode of erosion changes from ductile mode to brittle mode when the particle size changes from smaller to bigger. Small size particles have more cutting effect while bigger particles deform material by plastic deformation and fatigue. The erosion rate ranking depends on hardness in case of erosion due to small particles, whereas in case of large particles, it is dependent on toughness of material.

In the present study, the different values of the silt size are considered on the basis of silt diameter. Different sizes of sieves as; 355 μm, 250 μm, 180 μm and 90 μm were used for grading the silt for the size range of 250-355 μm, 180-250 μm, 90-180 μm and below 90 μm.

4.3.3 Jet Velocity

In actual practice, material damage due to plastic deformation and cutting occur simultaneously. The quantum of these damage mechanisms depends on velocity of particles, impingement angle and on silt parameters. The modes of erosion also vary depending on velocity of the particles. At low velocity, the particles do not have enough energy to erode the material by cutting action, but elastic deformation or fatigue effect may be observed. A relation between erosion and velocity of particle is

expressed as erosion proportional to (velocity)^n, where the values of exponent '*n*' vary with tested material and other operating conditions. The velocity at which the jet from the nozzle strikes the Pelton turbine bucket depends upon the operating head. The whole potential head of water is converted into velocity head at the nozzle outlet before the jet striking to the Pelton turbine bucket. The available potential head or net head at the spear valve is responsible for the jet velocity. The gross head, H_g or total head in situ is considered as the difference between the water level at the reservoir or head race and water level at the tail race. The head available at the inlet of the turbine is known as net or effective head. It is denoted by *H* and is given as;

$$H = H_g - h_f \tag{4.1}$$

where, h_f is total loss of head between head race and entrance of the turbine,

For the present experimental study the potential head is generated by pumping water at different pressure as per the requirement. From the gross head created by the pump the net head can be calculated by considering the losses in the pipe bend, pipe length and nozzle. A pressure transducer was fitted with the penstock pipe at the inlet of turbine near to the spear valve to monitor the pressure. The pressure head readings in pressure transducer were recorded. The pressure transducers are designed to measure the net head, so all the losses in the penstock pipe measured up to the measurement point are already considered automatically in the measured readings.

4.3.5 Discharge

Discharge of the Pelton turbine is defined as the volume of water passing through the turbine bucket per second, which is equivalent to the volume of water passing through the nozzle per second or quantitatively it is expressed as the cross sectional area of nozzle multiplied by the jet velocity. Under the present investigation discharge was measured by using a thin plate rectangular weir fitted in the channel. The detail of the discharge measurement is discussed as follows.

Discharge was measured with the help of a rectangular notch having the specifications as shown in Fig.4.9. A free fall of water from the weir to the tank was ensured. A pointer gauge was used to measure the height of water over the notch. The discharge of the pump corresponding to each head was recorded. Then the channel was closed and during experiment the silt water mixture was not allowed to pass through the channel. The control valve was set to maintain the constant head and discharge during the particular set of experimental run.

4.4 RANGE OF PARAMETERS

As discussed above different parameters considered in the present study are silt concentration, silt size and jet velocity. Silt was collected from river Bhagirathi (India), near the head works of Maneri Bhali Hydro Electric Project, Phase I, which is one of the most silt affected power house in India. The quartz content in the sand sample is more than 90% [71]. Petrography analysis of sand samples was carried out and are as given in Table 4.1. Sand was dried in an oven for twenty four hours and then sieved to different sizes before mixing with water.

Table 4.1 Petrographic analysis of suspended load collected from Maneri Bhali project (Uttarkashi)[71]

Sl.No.	Constituents	Weighted Compositions of Sample (below 0.3 mm size) (%)	Hardness(Moh's scale)
1.	Garnet	0.46	7.5
2.	Tourmaline	1.67	7.5
3.	Quartz(quartzite)	90.37	7.0
4.	Zircon	0.46	7.0
5.	Basic rock	0.10	6.0
6.	Hornblende	0.52	6.0
7.	Biotite	1.92	5.0
8.	Chasephrite	0.02	4.0
9.	Schist	3.86	3.0
10	Muscovite	0.82	2.25

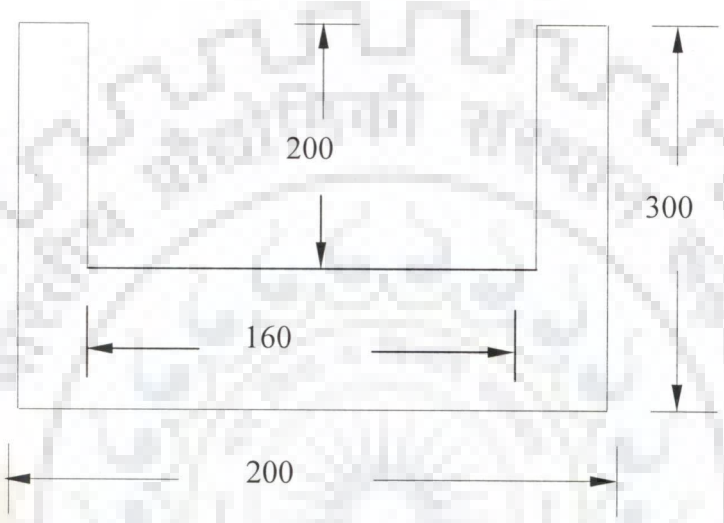

Fig.4.9 Dimensions of rectangular notch weir for flow measurement

The range of parameters considered under the present investigation is given in Table 4.2.

Table 4.2 Range of parameters

No	Parameters	Range
1	Concentration	5,000 to 10,000 ppm
2	Silt Size	Up to 355μm
3	Jet Velocity	26.62 m/s to 29.75 m/s
4	Operating Time	8 hr run for each set

4.5 PLANNING OF EXPERIMENTAL INVESTIGATION

As discussed earlier, most of the researches conducted earlier were on small scale test rigs in order to simulate the flow conditions of different hydraulic machines. A very few investigators tried to simulate flow conditions on Pelton turbine buckets based on the data collected from the plants as case study. It is difficult to simulate the flow conditions inside a Pelton turbine bucket considering all the system parameters.

Under the present study an attempt has been made to carryout an experimental study in more realistic way by considering a small scale Pelton turbine at a test rig. All the system parameters and silt parameters were considered in order to simulate actual operating condition of a turbine.

The experimental investigation was divided into two parts. In the first part of the study wear hot spots were identified inside the Pelton buckets. The Pelton buckets were coated with two layers of easily worn-out material. First the surface was nickel painted with a micro layer and again dipped in a paint. The turbine was operated under silt laden water over a period of time. A very high concentration was used for identifying the hot spots. The mechanisms of erosive wear at the hot spots were analyzed by fixing of the thin pieces of soft material as specimen at the hot spots with

the help of some adhesive. Scanning Electron Microscope, (SEM) photographs of small specimens were used to study the mechanism of wear in the Pelton buckets.

The second part of the experiment involved the investigation of the effects of silt parameters i.e. silt concentration, silt size and operating parameters (jet velocity and operating hour) on erosive wear in Pelton bucket. The efficiency loss of the Pelton turbine due to bucket erosion is also studied. Quantity of erosive wear of buckets is calculated by measuring the weight of Pelton buckets before and after the experimentation. The effect of efficiency loss of Pelton turbine due to bucket shape change as a result of alteration of Pelton buckets has also been discussed.

4.6 EXPERIMENTAL PROCEDURE

The experimental set up was designed and fabricated according to the Pelton turbine model design [141] for 1 kW power out put. All the accessories and instruments were mounted at their respective location, as shown in Fig.4.1. A Pelton turbine runner having pitch circle diameter as 245 mm, nozzle diameter as 10 mm and having 16 numbers of buckets has been used for the present study. In order to get measurable amount of erosion in a short period of time, the turbine buckets were made of brass. A tank made of MS was used to circulate silt water mixture through turbine runner under different conditions. The depth of water in the tank was maintained at 450 mm with the upper portion of the tank connected to the channel. The tank was provided with an inlet and an outlet tap to fill water to the desired level and to drain out the used silt water.

A stirrer was attached over the water tank to be operated continuously during the experiments so as to supply a uniform mixture of silt water to the turbine. A penstock pipe having 60 mm outer diameter and 4 mm thickness was used for supplying water to the turbine nozzle under desired pressure. A spear valve was used at the end of the penstock pipe with 10 mm nozzle diameter to convert the potential

head of circulating water into velocity head. The net head was measured by the digital pressure transducer fitted with the penstock just before the spear valve. The operating position of the spear valve was kept constant during the experimentations in order to maintain the desired head and discharge to the turbine for a set of experiment. A control valve was also used on the penstock pipe just above the service pump to maintain the head and discharge as per the requirement.

A trial test was conducted to verify the proper functioning of the whole set up. Proper functioning of all the instruments was also verified. Initially service pump drew water from the tank and supplied it to the turbine. Water from the turbine was allowed to flow through a channel and then the rectangular weir for discharge calibration. The height of water over the crest of the weir was recorded by a pointer gauge and the discharge of the pump corresponding to each head was determined. The calculation of discharge was made based on the height of water flowing above the crest (h).

In order to prepare the silt water mixture having various concentrations, required quantity of silt having desired parameters was added to a known volume of water in the tank. The stirrer was rotated at a speed of 60 rpm with the help of a motor of 0.5 H.P. capacities through a gear box. In order to create turbulence throughout the volume of water and silt mixture in the tank the length and diameter of stirrer was designed and fabricated, keeping clearance of 5 mm at the bottom and 15 mm at the sides of the tank. In order to prevent the settling of silt at the bottom of the tank, silt was mixed with the water in the tank after creating sufficient turbulence. Further, discharge from the outlet of the turbine was allowed to fall directly into the tank which created more turbulence in the tank and helped in preventing settling of silt particles. It was observed that there was no trace of silt particles after releasing the slurry from the tank.

A digital balance with span range of 10g to 6 kg and least count of 0.5 g was used to measure the weight of silt. In order to maintain a constant temperature of the silt water in the tank, a cooling water jacket was provided on three sides of the tank. In order to investigate the effect of silt parameters on erosive wear silt laden water was supplied to the turbine operated under a given head.

After every 2 hours of experiment, the buckets were dismantled from the runner, cleaned with detergent, washed in clean water and wiped with tissue paper. Then these buckets were rinsed with acetone and allowed to dry inside an oven for 2 hours at a temperature of 60^0 C. The quantum of erosion under the present study was measured in "mg" with the help of a very high precision digital analytical balance having a least count of 0.1 mg with span range of 10 to 210 g. The mass loss of the buckets was measured after every two hours of run. One run of experiment consisted of two hours and after every one hour the silt slurry was drained away completely and after cleaning the tank properly fresh silt slurry was prepared for the next one hour. Keeping one parameter as variable and others as fixed, one set of readings was taken for four values of considered parameter, at a time interval of two hours. It is therefore, for considering different values of concentration, three sets of experiments were conducted. Similarly, for silt size, four sets and for jet velocity, three sets of experiments were conducted. In order to maintain the jet velocity constant, throughout the experiment, the control valve was adjusted to get a constant head reading. By maintaining the constant head on turbine, it was ensured that jet velocity through the nozzle remained constant. However, the impeller of the service pump got eroded due to circulation of slurry after certain period of operation. The impeller was replaced with a new impeller to ensure the required input (head and discharge) to the turbine.

4.7 EXPERIMENTAL DATA

Considering the range of parameters discussed above experimental data were collected under different conditions.

The data were collected for all the concentration, silt size and head for a time interval of two hours of turbine operation. Table 4.3 gives sample data of erosive wear for all the sixteen buckets for a typical set. Table 4.4 gives observations for a typical bucket.

4.8 DATA REDUCTION

4.8.1 Calculation of Silt Concentration

Size of the tank

Length : 60cm

Width : 50cm

Height : 40cm (water level)

For Sand concentration : 10,000ppm

(i) Volume of water in the tank

= 60×50×40 cc=120,000 cc

=120 L

(ii) 10,000 ppm =10,000 mg in one litre

10,000 ppm in 120 L =10x120 gm =1.2 kg

= 1.2 kg of silt

Similarly

For 5000 ppm concentration, quatity of silt will be determined as 600 g for the same quatity of water.

Table 4.3 Data of silt erosion for a typical set (H = 45m, concentration = 10,000 ppm, size = 302 micron, time=2 hrs)

No. of buckets	Bucket mass before experiment (g)	Bucket mass after experiment (g)	Bucket mass loss(g)
Bucket no. 1	205.7134	205.5780	0.1354
Bucket no. 2	204.5702	204.4383	0.1319
Bucket no. 3	204.5028	204.3726	0.1302
Bucket no. 4	206.2431	206.1082	0.1349
Bucket no. 5	205.8257	205.6825	0.1432
Bucket no. 6	205.8638	205.7168	0.1470
Bucket no. 7	205.9752	205.8316	0.1436
Bucket no. 8	206.0694	205.9360	0.1334
Bucket no. 9	206.1818	206.0554	0.1264
Bucket no. 10	204.7889	204.6459	0.1430
Bucket no. 11	204.6602	204.5223	0.1379
Bucket no. 12	205.6893	205.5510	0.1383
Bucket no. 13	205.0339	204.9025	0.1313
Bucket no. 14	205.9212	205.7904	0.1308
Bucket no. 15	204.6180	204.4706	0.1474
Bucket no. 16	205.8242	205.9615	0.1373

Table 4.4 Table for observations for a typical bucket

Size range 255-350 μm, concentration 10,000 ppm						
Time, t (h)	Flow, Q (m^3/s)	Head, H (m)	Mass loss, (g)	Power, P (W)	Power input =9.81×Q×H	efficiency
2	0.00378	45.27	0.1373	1060	1670.28	63.46
4		45.32	0.1309		1670.28	
6		45.15	0.1294		1670.28	
8		45.21	0.1351		1670.28	

4.8.2 Determination of Silt Size

Silt size ranges considered in this investigation are below 90 micron, 90-180 micron, 180-250 micron and 250-355 micron. Silt was sieved between two successive size ranges.

4.8.3 Determination of Jet Velocity

The jet velocity was calculated from the reading of pressure transducer observed during the experimentation as follows ;

Pressure head $P=\rho gH$ (4.2)

Or $H=\frac{P}{\rho g}$ (4.3)

and $V=\sqrt{2gH}$ (4.4)

Hydraulic losses taking into account

$V=k_v\sqrt{2gH}$ (4.5)

where,

P is pressure KPa,

ρ is density of water (1000 kg/m^3),

H is net head in m,

V is jet velocity in m/s, g *is* acceleration due to gravity in m/s^2 (9.81 m/s^2) and k_v *is* velocity coefficient (=0.98 as 2% losses are considered in the nozzle).

4.8.4 Measurement of Bucket Mass Loss

(i) Bucket mass loss = Mass of bucket before experiment – Mass of bucket after experiment

The bucket mass loss was normalized with the bucket mass before the respective experimental run.

(ii) Normalized bucket mass loss

$$= \frac{\textit{Mass of bucket before experiment - Mass of bucket after experiment}}{\textit{Bucket mass before the respective experimental run}}$$

4.8.5 Discharge Calculation

The formula used for calculating the discharge is as given below ;

$$Q = \frac{2}{3} C_e b_e \sqrt{2g} h_e^{\frac{3}{2}} \tag{4.6}$$

where,

Q is the discharge,

C_e is coefficient of discharge,

b_e is effective width,

h_e is effective head

The effective width and head are defined by the following equations;

$$b_e = b + k_b \tag{4.7}$$

$$h_e = h + k_h \tag{4.8}$$

where,

b is the length of the weir crest(perpendicular to flow)

h is the measured upstream head over the weir

k_h is the head correction factor

k_b is the width correction factor

g is the acceleration due to gravity

The coefficient of discharge was calculated from the chart shown in Fig.4.10. This chart is applicable for "Liquid Flow Measurement in Open Channels using Thin Plate Weirs" according to Indian Standard [143].

4.9 ERROR ANALYSIS

An error analysis of experimental measurements has been carried out on the basis of method proposed by Kline and McClintock [142]. The details of the error analysis are given in Appendix-I .The maximum possible uncertainties in the values of major parameters of present investigation are obtained given below;

i) bucket mass loss (M_{bl}) : 1.41%

ii) flow rate (Q) : 1.75%

iii) jet velocity (V) : 0.77%

iv) silt size (S) : 1.35%

v) silt concentration (C) : 0.21%

vi) operating hour (t) : 1.18%

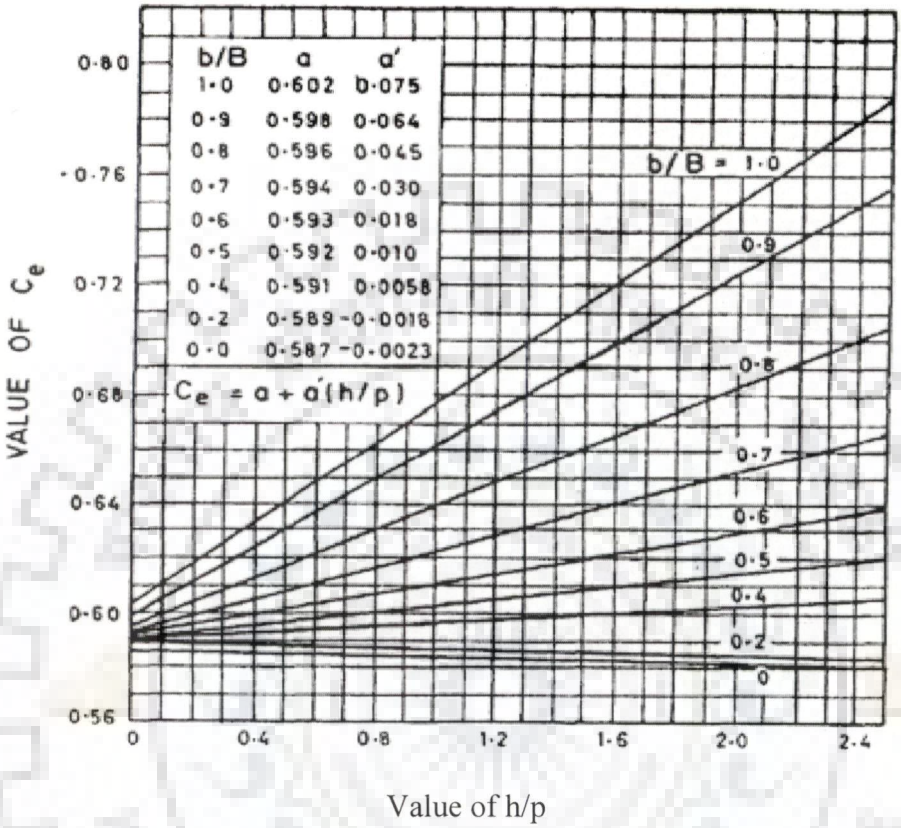

Fig.4.10 Chart for calculation of the value of C_e [140]

CHAPTER-5

RESULTS DISCUSSIONS AND DEVELOPMENT OF CORRELATION

5.1 GENERAL

Details of the experimental set up, instrumentations, experimental procedure, range of parameters investigated and data collected during experiments have been discussed in previous Chapter-4. Based on the experimental data, effect of silt size and silt concentration on erosive wear in Pelton turbine bucket has been discussed and presented in this Chapter-5.

Under the first part of discussions silt erosive mechanism in Pelton bucket for the given conditions has been discussed. Pattern of erosive wear in Pelton bucket has been observed and analyzed under different conditions of silt and operating parameters.

In the second part of the discussions, the effect of different parameters on silt erosion has been discussed and an attempt has been made to develop a correlation for erosive wear as a function of considered parameter.

5.2 PATTERN OF EROSION IN PELTON BUCKET

The erosion rate is commonly given in terms of mass or volume of material removed per unit mass of impacted erodent. Nevertheless, investigators implicitly assume that the dimensions of the eroded area and the particle concentration are not important [143-144]. However, monitoring of the turbine erosion is difficult task and there is no standard procedure for measuring the erosion effect in the turbine components. In laboratory tests, the specimens are small in size and they are of regular shape or flat plates. Therefore, it is easy to measure the effect of erosion in terms of weight loss, volume loss, surface roughness or dimensional deformation. Since the sizes of turbines in actual hydropower plants are big and the runner blades

or buckets are not flat, it is therefore, difficult to measure the extent of erosion damage by above mentioned procedures [145]. The present investigation has been intended to study the erosion behavior of Pelton turbine buckets with respect to the silt concentration, silt size, jet velocity and operating hours of the turbine.

As discussed earlier in Chapter-4 that under first part of the experimental study, the bucket surface was provided with two layer of easily worn out material. First the surface was nickel plated with a micro layer and again buckets were dipped in a paint. After this process buckets were air dried.

In order to get hot spots in a shorter period of turbine operation a solid concentration of 5% weight was prepared with silt and water and the turbine was operated for one hour. Within a few minute the paint over the turbine buckets peeled out to small pieces. It was clearly observed from paint pieces floating over the water in the tank. It was, therefore, inferred to be inadequate to obtain productive results. Since, there was a coating below the paint; the experiment was continued up to one hour. The turbine runner was dismantled from the set up. Photographs of turbine runner were taken and wear hot spots are now clearly visible.

Fig.5.1 shows the marked portions as wear hot spots on the turbine bucket. At these marked portions both the coatings were washed away after one hour of turbine running with silt laden water. The paintings peeled out improperly but the nickel coat helped in finding out the wear hot spots. Further, the remaining portion of the painting was cleaned properly for further experiments. In order to study the erosive mechanism small specimen pieces of metal were fixed at the marked portion of wear hot spots.

Fig.5.2 shows the specimen fixed on the identified wear hot spot. Mechanism of erosion on Pelton bucket under the present investigation is discussed as follows;

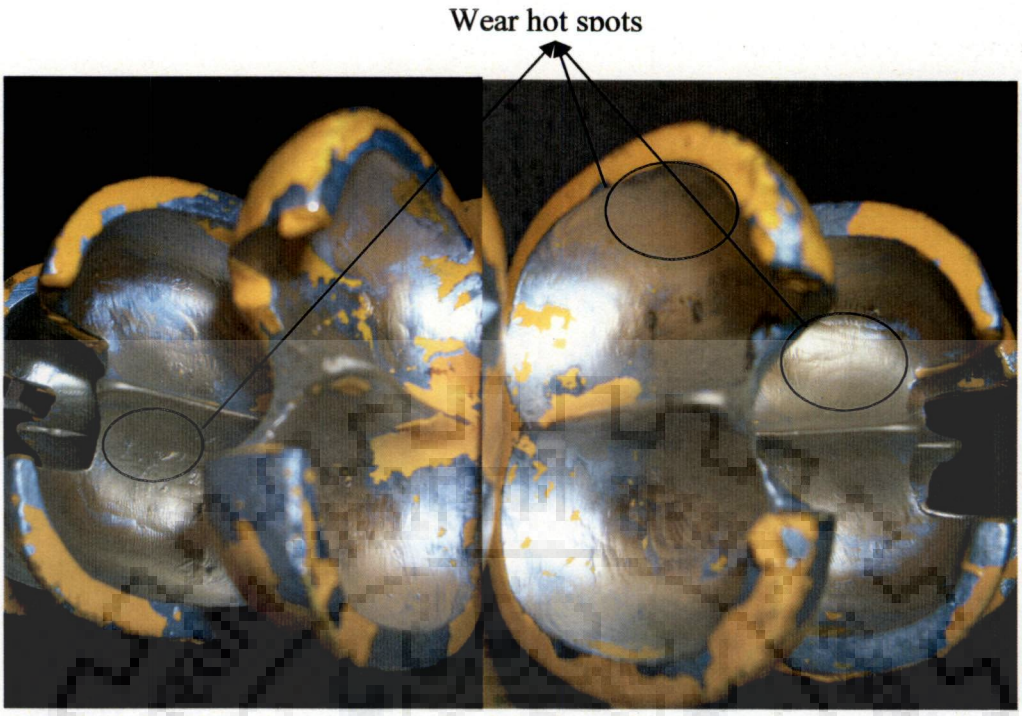

Fig.5.1 The marked portion of the Pelton bucket indicating wear hot spots

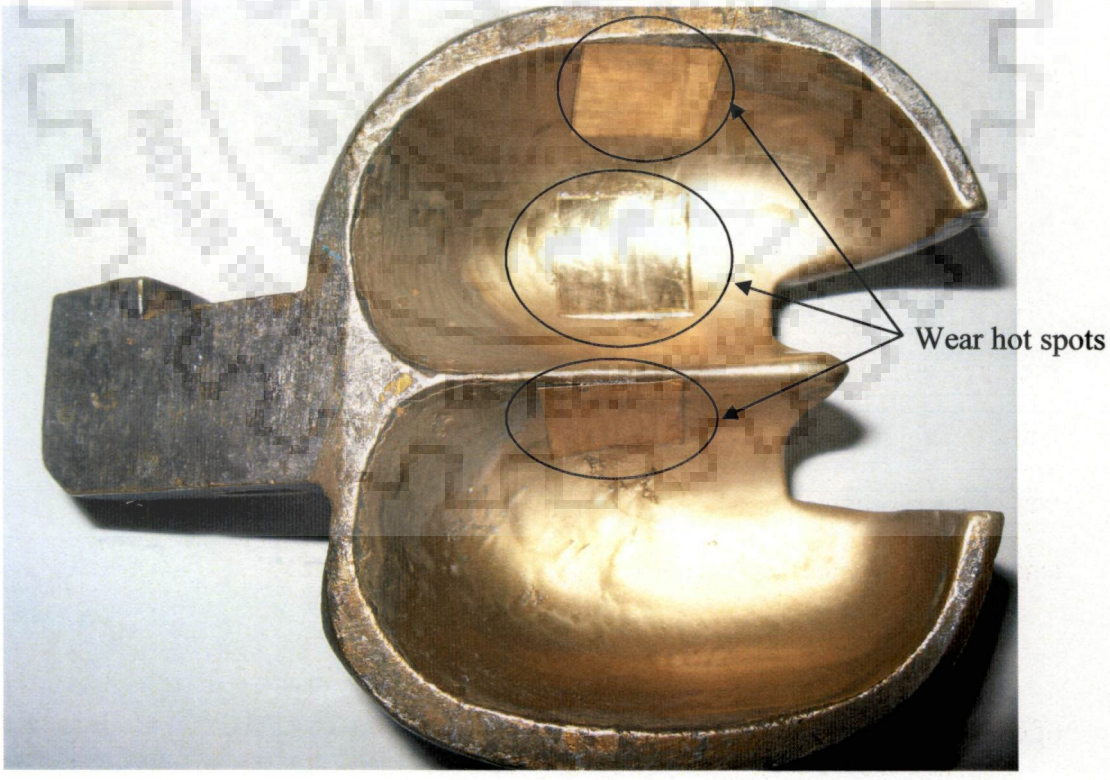

Fig.5.2 Locations showing specimen glued on bucket surface

5.3 MECHANISM OF EROSION IN PELTON BUCKET

In order to investigate the wear mechanism in different parts of Pelton turbine bucket, specimens are glued at these specific places of bucket. The specific places were chosen according to the wear hot spots established in the first part of experimental study.

Three specimens were glued by adhesive at the inlet, outlet and along the depth of the two different Pelton buckets. Fig.5.3 shows the Scanning Electron Microscopy (SEM) micrograph of wear specimen before experiment. Fig.5.4 shows the E-DAX analysis of the wear specimen and Table 5.1 gives the composition of wear specimen obtained from E-DAX analysis.

The SEM micrographs of eroded specimen placed at specified places of the Pelton bucket were obtained after experiment. The mechanisms of erosion of turbine bucket at different hot spots were studied from the SEM micrographs.

Table 5.1 Composition of wear specimen

Element	Wt%	At%
OK	01.19	04.60
CuK	64.12	62.52
ZnK	34.69	32.88
	Correction	ZAF

The SEM micrographs of wear specimens at 5000 ppm solid concentration and different size range of silt particles viz., 302 micron, 215 micron, 135 micron and 45 micron; placed at inlet, outlet and along the depth of the bucket are presented in Fig.5.5-5.7 and discussed as follows ;

Fig.5.3 Micrograph of wear specimen before experiment

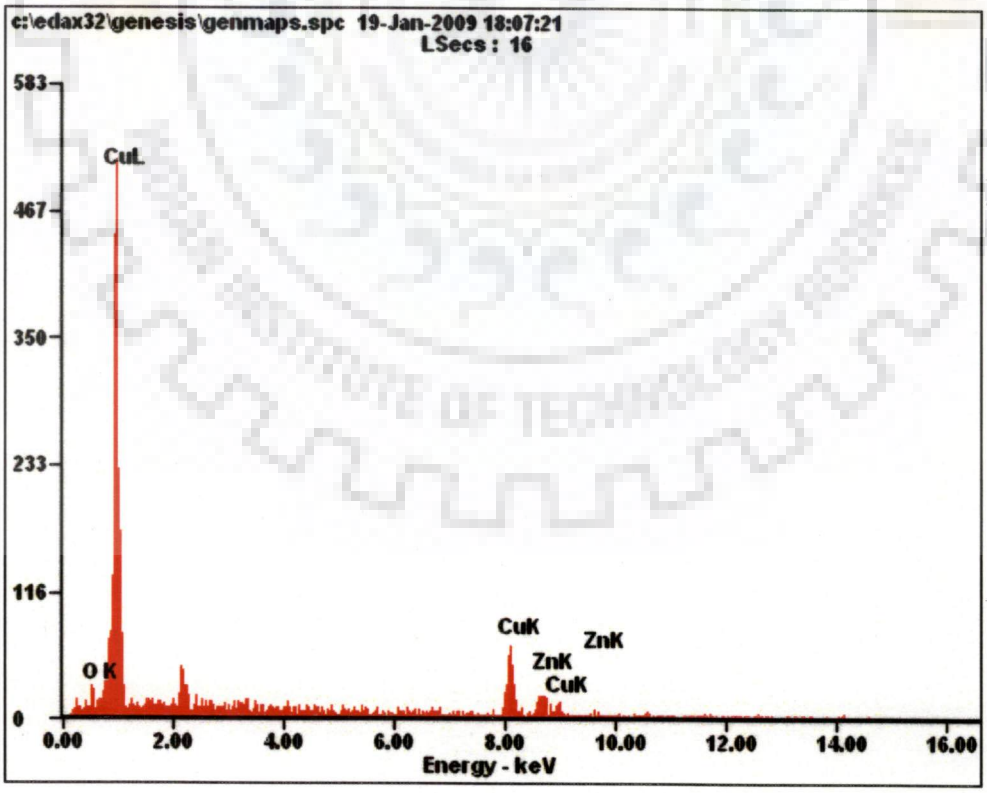

Fig.5.4 E-DAX Analysis of wear specimen

5.3.1 Inlet of the Bucket

Fig.5.5 (a) shows the material removal from the inlet of the Pelton bucket for silt sizes of 302 micron and a given value of concentration. From the micrographs it is seen that the material removal occured due to shearing action of silt particles. Lips are observed to be raised on the sides along the travel path of the silt particles. At few places materials displaced at the front of the cut with raising of lip. Wide cuts seem to be present with lower depth of cut. This may be due to shearing action taken place by the surface of silt particles at small angles ($< 22.5^0$) of impact. At small impact angle the particles have higher horizontal component of velocity which seem to be deformed at the surface by spreading material in the direction of motion.

Fig.5.5 (b) shows the micrograph of specimen placed at the inlet of Pelton bucket for the erodent having 215 micron mean silt size in the range of 180-250 micron. In this case the plowing action takes place by sharp edges of the silt particles. It has been observed that the silt particles displaced the material in the side way along with the travel path of the silt particles. The raised lip formations are seen in the side way as well as in front of the crater in some cases. The sharp edges of the silt particles seem to be pierced into the specimen surface. The locations for the same are shown in Fig.5.5.

Fig.5.5(c) shows the micrograph of specimen placed at the inlet of Pelton bucket for the erodent having 135 micron mean silt size in the silt particle range of 90-180 micron. In this case the scratches obtained due to silt particles are found densely on the specimen. However, the length of cut is turned to be smaller than the length of cut obtained in earlier cases. Silt particles seem to be embedded into the specimen thus causing raise in lip along the flow path of silt particles. It is seen from the micrograph that smaller particles cause micro indentations with shorter length and embedded into the surface loosing their kinetic energy. The embedded silt particles may flow out of the surface of the substrate by the incoming jet of water.

Fig.5.5 (d) shows the micrograph of specimen placed at the inlet of Pelton bucket for the erodent having 45 micron mean silt size in the range of silt particles below 90 micron. It has been observed that micro indentations are obtained on the substrate due to the erodent having 45 micron mean size. These particles are of smallest sizes among all. In this case a principal mode of erosion seems to be plowing and leaflet formation along with micro indentations. The mechanism of erosion is almost similar to the previous case of 135 micron silt size.

5.3.2 Outlet of the Bucket

Similarly the micrographs of specimen fixed at outlet of Pelton bucket can be discussed under different conditions. Fig.5.6 shows the micrograph of the silt erosive wear for silt size of 302 micron, 215 micron, 135 micron and 45 micron in different range of particle sizes. In case of particle size having 302 micron silt size, it is observed from the Fig.5.6 (a) that scratches due to erosion are appeared on the specimen surface as compared to the specimen placed at the inlet of the Pelton bucket. The material from the specimen surface seems to be displaced on the side ways along the travel path of the silt particles. This indicates the plowing mechanism of material removal. Further, smaller marks of scars and small indentation marks are found on the specimen surface. It seems that most of the erodent particles flow close to the splitter and seems to loose their kinetic energy at the inlet and producing lower impact force on the outlet surface. This results in less material removal at the outlet surface.

In case of erodent having mean silt size of 215 micron in the range of silt particles of 180-250 micron, the shearing of target surface and scar marks by the sharp edges of erodent are found to be present on the surface. The mode of erosion seems to be plowing and by formation of new surface as shown in Fig.5.6 (b). The scar marks observed on the target surface are densely found than that in earlier case of 302 micron erodent.

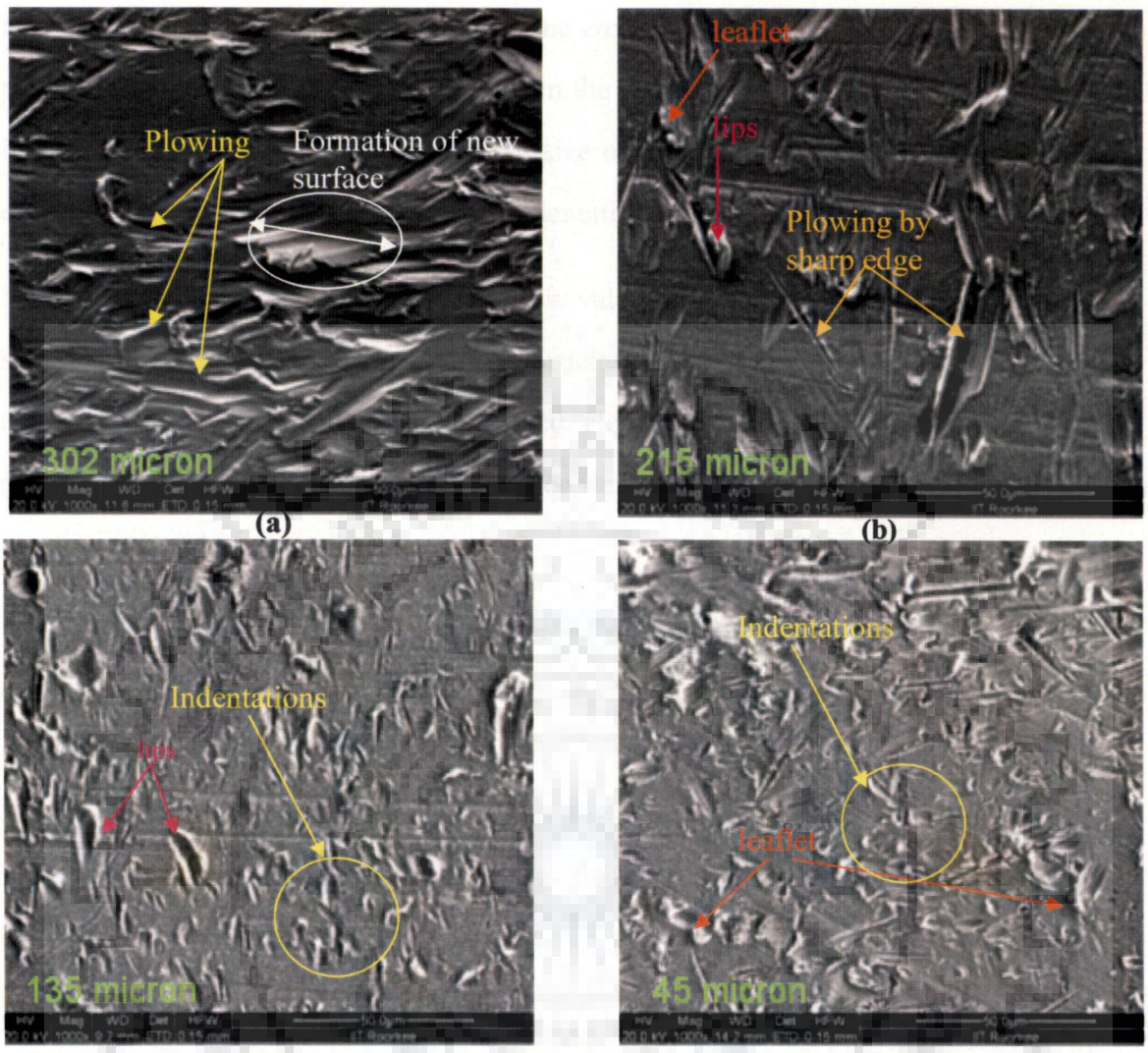

Fig.5.5 Micrographs of wear specimen placed at inlet of the Pelton bucket

Fig.5.6(c) shows the micrograph of specimen placed at the outlet of Pelton bucket for mean silt size of 135 micron. The erodents used were silt particles for size range of 90-180 micron. It is observed from the figure that the outlet of the surface is heavily eroded by the erodent having silt size of 135 micron. The principal mode of erosion seems to be due to plowing and indentation by the erodent.

The smaller scars may be due to low value of kinetic energy possessed by the smaller particles. In case of smaller size particles the number of particles are more for the same values of concentration considered. However, comparing with the specimen placed in inlet of the bucket, the same size erodent caused less erosion at inlet than the specimen placed at outlet.

Further, Fig.5.6 (d) shows the micrograph for the erodent having silt particle of silt size below 90 micron. The erodent particles flow parallel to the outlet surface along with the water. The impact of erodent seems to be at very small angle, thus causing surface shear of the substrate. Very tiny micro debris from the surface of the substrate is appeared to be detached through the kinetic energy of the incoming water jet.

5.3.3 Along the Depth of the Bucket

Fig.5.7 (a) shows the micrograph of specimen placed along the depth of Pelton bucket and the erodent used were silt particles in the range of 250-355 micron. It is seen from the Fig.5.7 (a) that the erosion mechanism is found to be different from all the cases of erosion at inlet and outlet of the Pelton bucket as discussed earlier. In this case the erodent particles strike to the target surface at normal impact angle which cause of developing craters. At these places surface looks like to be pressed deep into the surface. At some places pit holes are seen and the material from these places seems to be lost as wear debris. It appears that erosion took place at a higher rate along the depth of the bucket than the inlet and outlet. Scars of shorter length also appeared densely over the surface. The close examination of the wear surface gives an idea that the erodent impact to the surface is at a higher impact angle close to the normal impact angle.

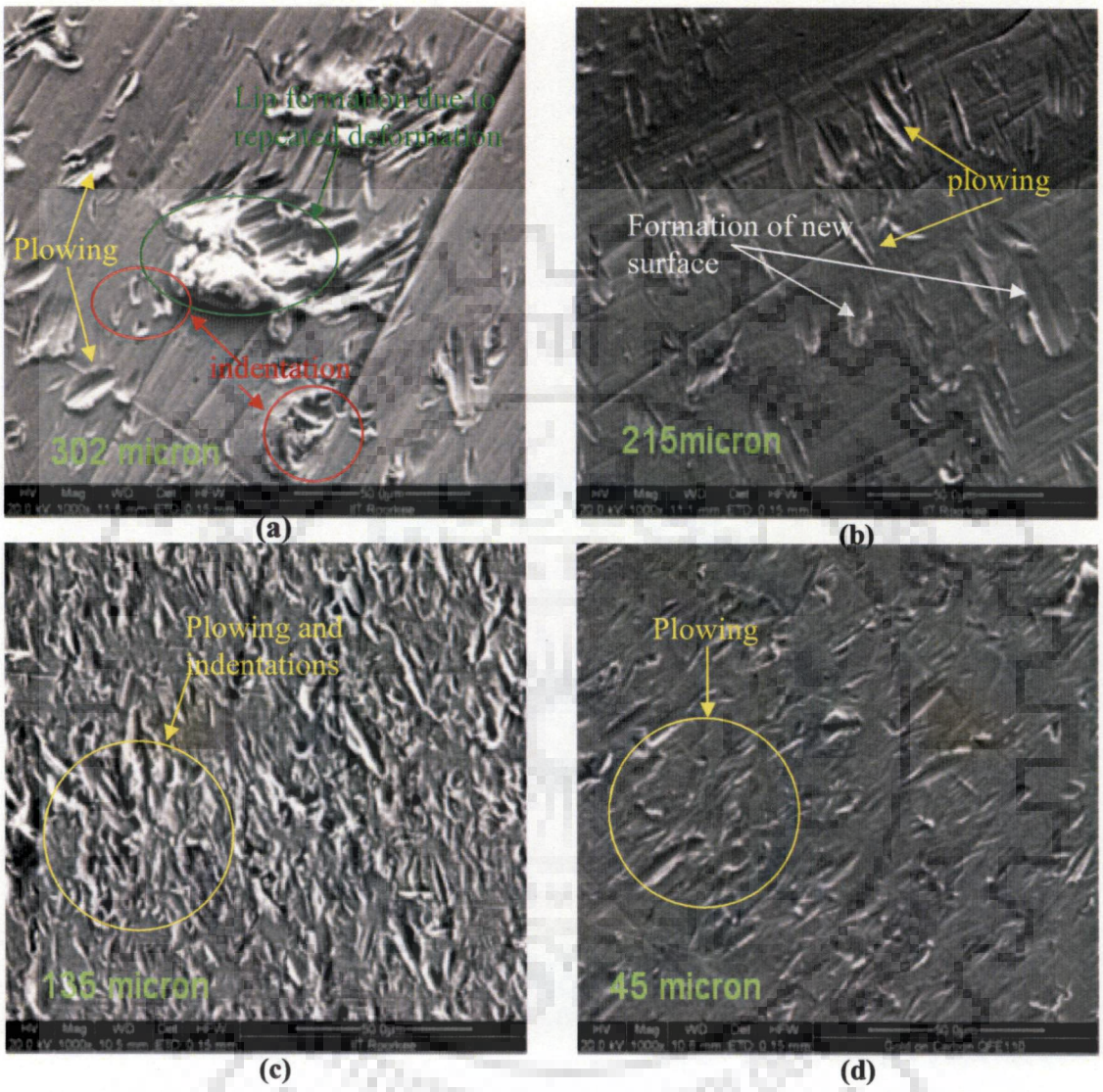

Fig.5.6 Micrographs of wear specimen placed at outlet of the Pelton bucket

Fig.5.7 (b) shows the micrograph of specimen placed along the depth of Pelton bucket and the erodent having silt size of 215 micron, in the range of silt particles size of 180-250 micron. It is observed from the Fig.5.7 (b) that small scar marks are densely found over the surface. Tiny micro craters are appeared over the surface. The loss of material seems to be due to leaflet formation, indentation and plowing of material. In this case also, erosion rate appears to be more than the inlet and outlet of the bucket.

Fig.5.7(c) shows the micrograph of specimen placed along the depth of Pelton bucket and the erodent having mean silt size of 135 micron in the range of silt particles of 90-180 micron. It is observed from the figure that the specimen is heavily eroded and the scar marks appear to be overlapping to each other. The primary mode of erosion seems to be plowing and leaflet formation. In some places erodent particles seems to be embedded into the target surface creating longer crater.

Fig.5.7 (d) shows the micrograph of specimen placed along the depth of Pelton bucket and the erodent having 45 micron mean silt size in the range of silt particles of mean size below 90 micron. The mechanism of erosion in this case is found to be similar to the earlier case of 135 micron. The erosion of specimen seems to be occurred due to plowing and leaflet formation.

Close examination of the micrographs of the specimens placed at different hot spots of Pelton bucket shows that the bigger particles cause more erosion at the inlet and along the depth of the bucket. The mode of erosion seems to be plowing by forming wide new surfaces. The surface of the silt particles may be responsible for erosion at inlet in case of bigger particles.

Smaller particles are turned to be more responsible for causing erosive wear at the out let of the turbine bucket. Craters and pit are found along the depth of the bucket in case of larger particles while plowing and shearing of specimen surface are observed in case of smaller size particles. These findings are found to be on similar lines of the theory developed by Harry et al. [146].

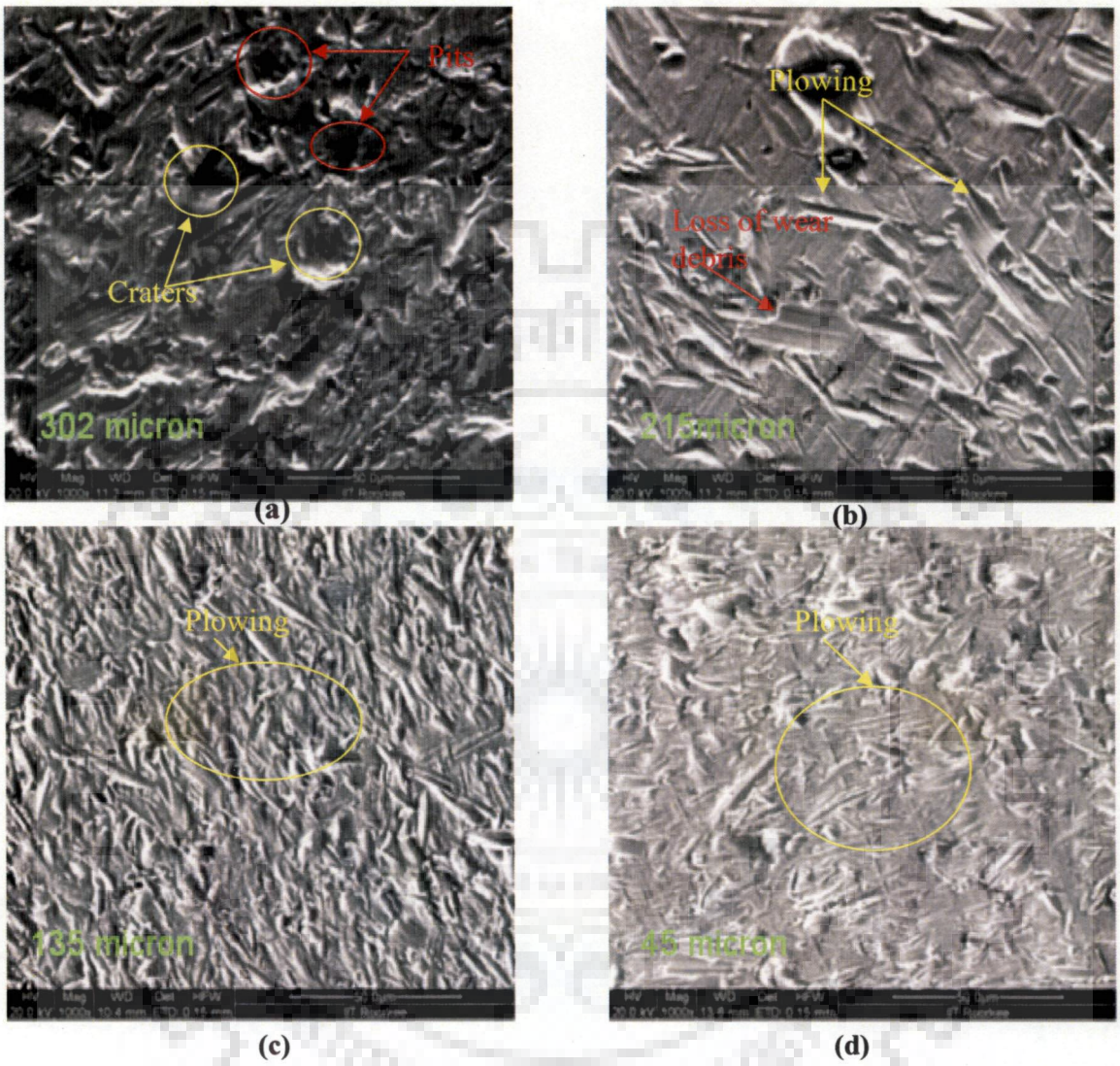

Fig.5.7 Micrographs of wear specimen placed along the depth of the Pelton bucket

Based on the observations made, it can be concluded that bigger particle flow at a higher velocity and impact along the depth of the bucket at higher impact angle caused pits and craters on the surface. While, the particles flowing close to the splitter caused erosion due to the shearing action of the surface of the silt particles. However, smaller particles have less relative velocity with respect to water jet and flow along with the water jet causing abrasive type of erosion. These findings are found to be on similar lines as the observations made by Thapa et al. [19,145]

Fig.5.8 (a) and Fig.5.8 (b) show the surface condition of Pelton bucket before and after the experimentation respectively. Fig.5.8 shows the most effected portion of the bucket. These effected portions are magnified. Maximum erosion has been observed at the splitter and some portions of the notch of the buckets. The splitter is found to be eroded significantly and the sharp edges have become blunt. The marked portion of the splitter was found to be eroded to a considerable depth. Also the thickness of marked portions near the notch got reduced which can be observed even with necked eye visualization.

The micrographs of splitter tip and surface along the depth of the Pelton bucket are shown in Fig.5.9 and Fig.5.10 respectively. The splitter tip is found to be eroded by plastic deformation and indentation. Overlapping craters are found on the splitter tip and erosion took place by plastic deformation as well as plowing at the surface along the depth of the bucket.

The magnified view of the outlet edge of the eroded Pelton turbine bucket is shown in Figs.5.11 and Fig.5.12. It is observed that the erosion has occurred due to a typical cutting action of silt particles in their flow path. A number of channels have been created in the flow path of the continuously flowing silt particles. In other words ripples were formed in the flow path of silt laden water jet. These ripples are nearly normal to the flow direction as shown in Fig.5.11 and Fig.5.12. These observations are found to be on similar lines with field observations and experimental studies of other investigators [17,19, 147-157].

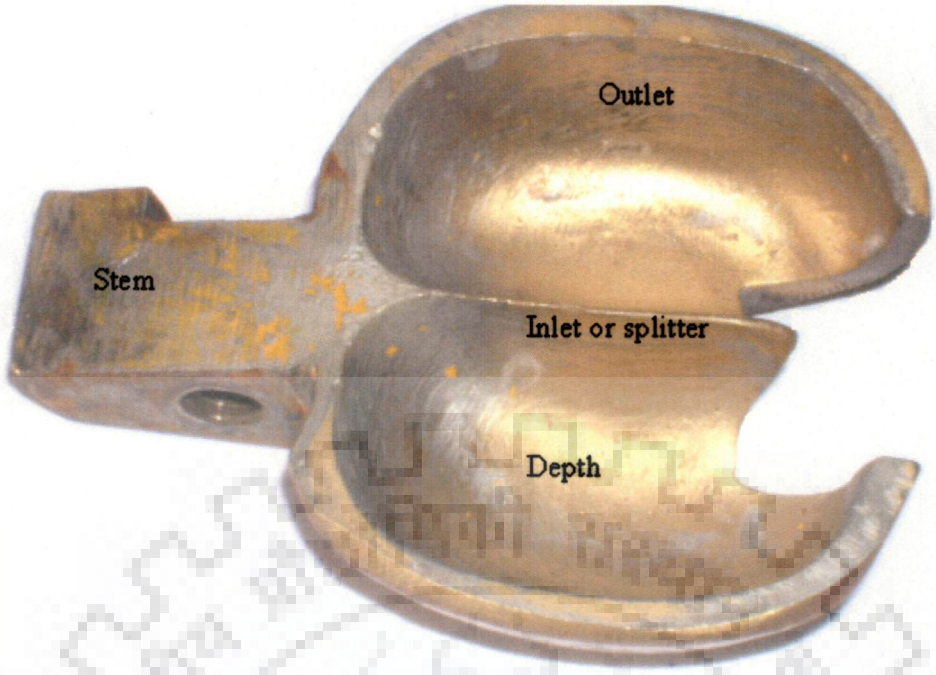

Fig.5.8 (a) Condition of surface of Pelton bucket before experimentation

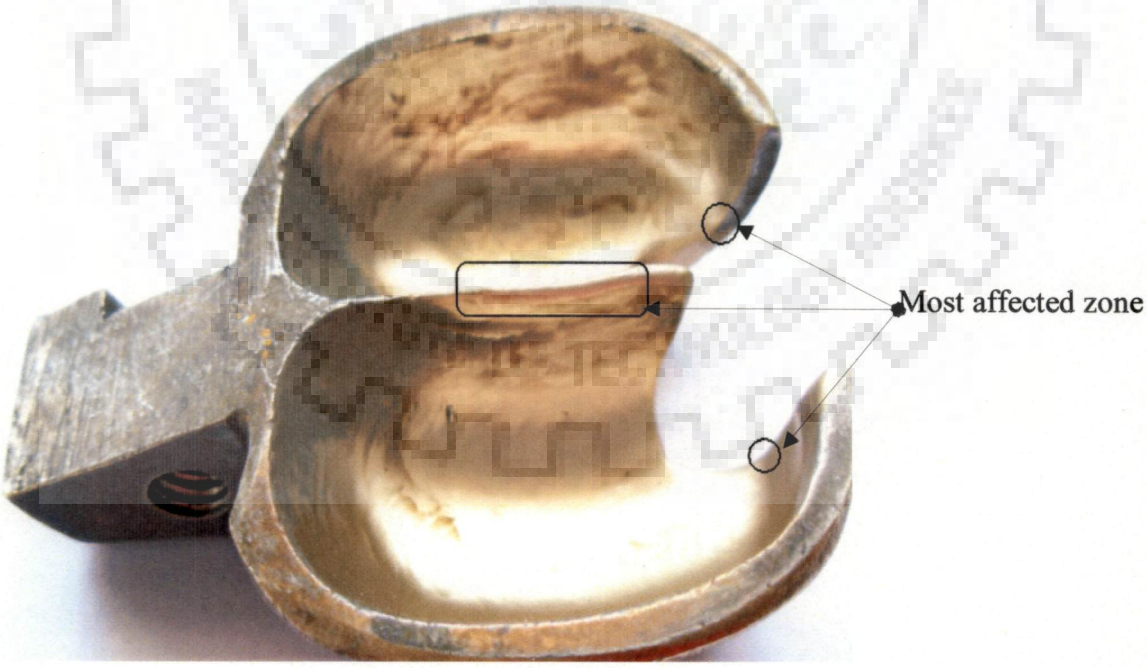

Fig 5.8 (b) Condition of surface of Pelton bucket after experimentation

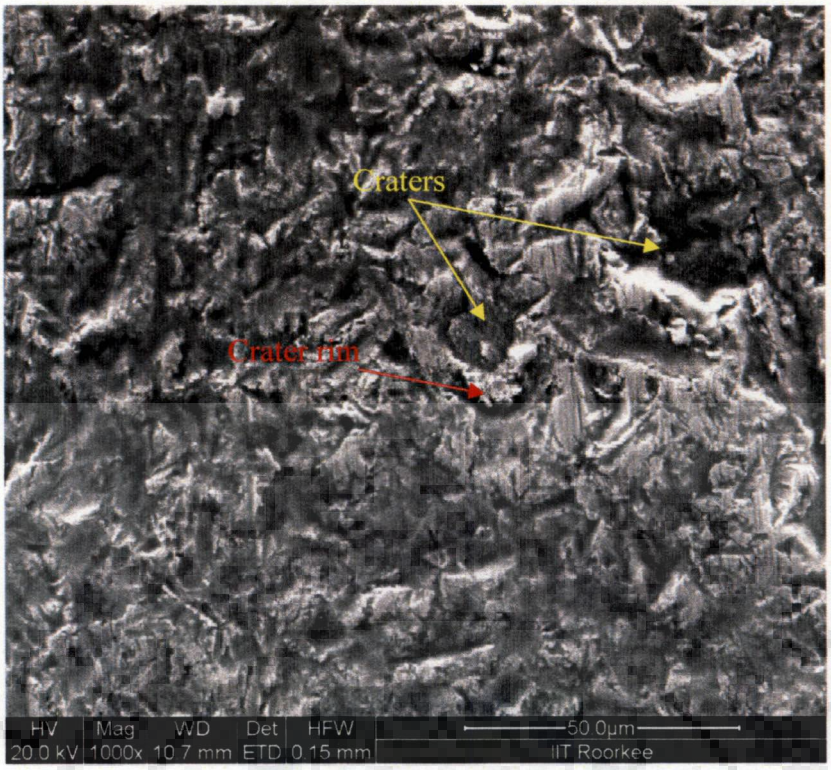

Fig.5.9 Micrograph of splitter tip

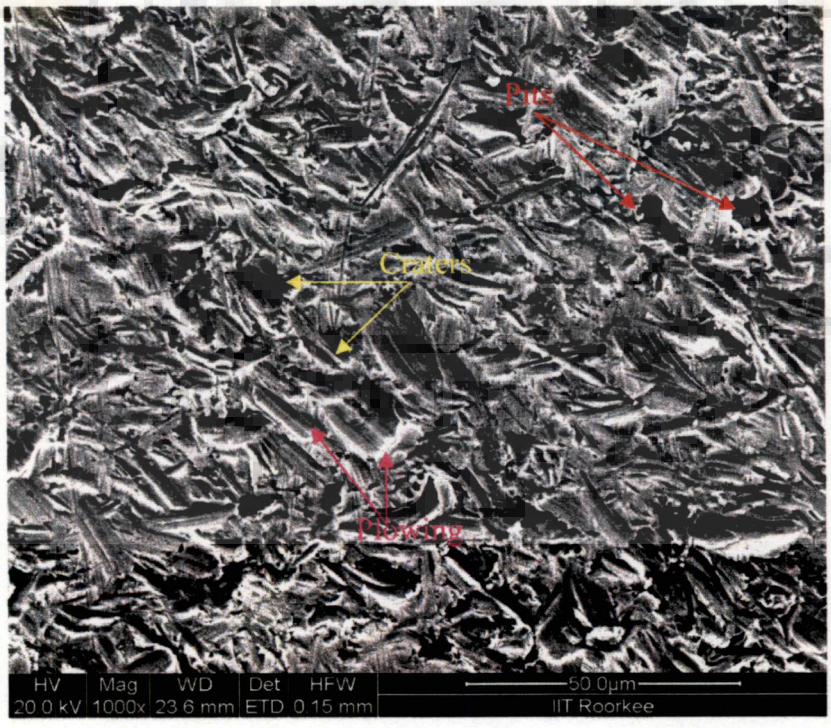

Fig.5.10 Micrograph of the surface along the depth of the bucket

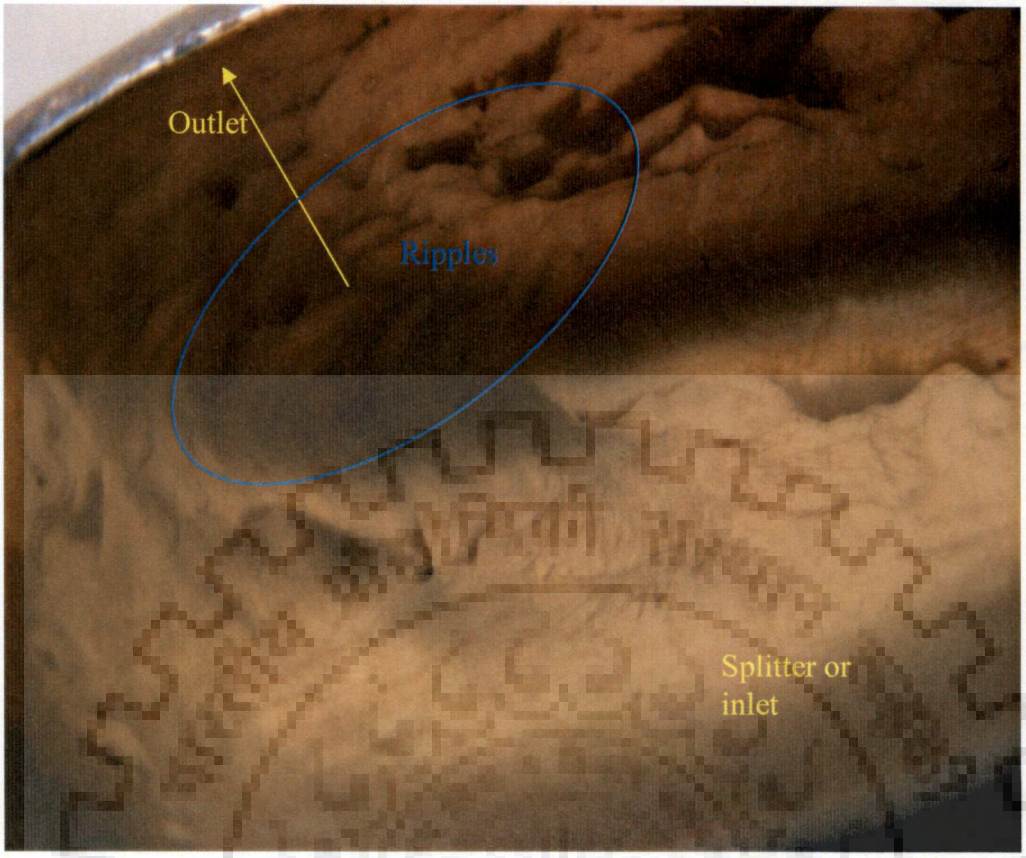

Fig.5.11 Magnified view of the outlet edge of the Pelton turbine bucket

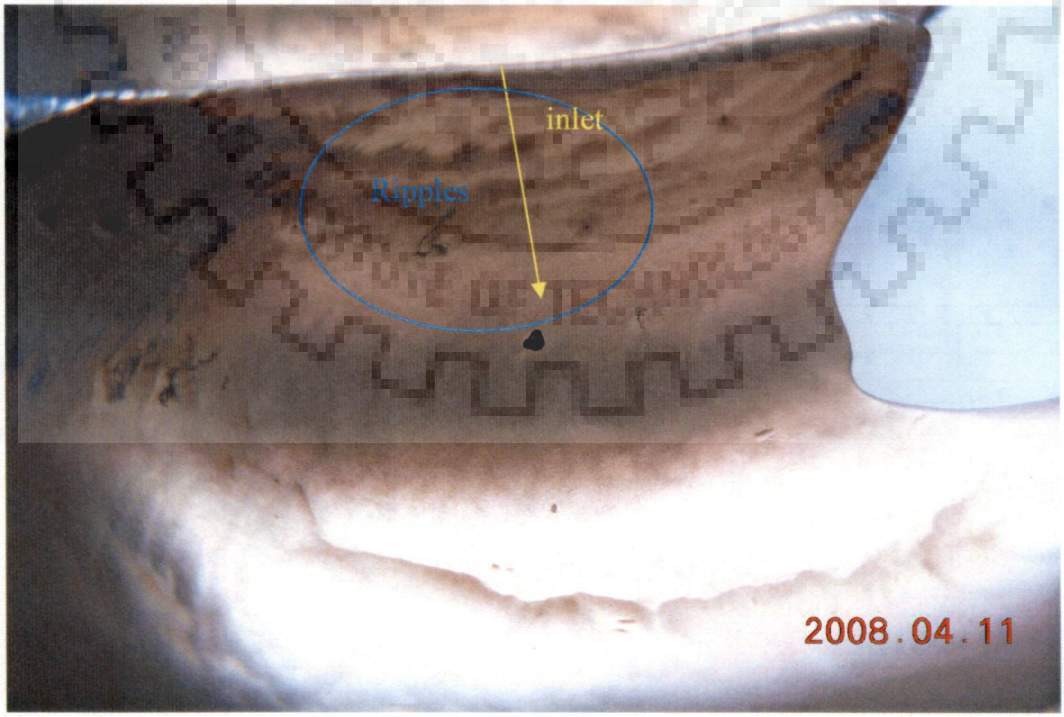

Fig.5.12 Magnified view of the inlet or splitter of the Pelton turbine bucket

Arrow shows the approximate flow direction.

5.4 EFFECT OF SILT AND OPERATING PARAMETERS ON EROSIVE WEAR

The effects of silt and operating parameters on erosive wear of Pelton turbine bucket are discussed under this part of the chapter. As discussed in Chapter-4, mass loss of bucket after every two hour under silt laden water was determined. Each experimental run consisted of eight hours and four sets of readings were taken for each experimental run. Readings for all the sets are obtained by considering the mass loss of each bucket after two hours of operating time. As mentioned earlier, all sixteen buckets are identical in shape and size, it has been observed that the variation in mass loss in all the sixteen bucket is not much. It is therefore, the average values of mass loss for all the sets of experimental run were considered for the analysis. However, attempt has been made to determine the mass loss for individual bucket and mean values of mass loss obtained in sixteen buckets has been considered for analysis.

Figs. 5.13-5.17 show the variation of mass loss of each bucket and the mean values of each set under given conditions. Data for mass loss are plotted for all the sixteen buckets for all experimental runs. One run consisted of four sets of experiments of two hours. As all the buckets are identical, mass loss of each bucket is verified and the maximum absolute deviations of the data are found.

Fig.5.13 shows the plot for bucket mass loss versus bucket number for 45 micron mean size particles and 28.23 m/s jet velocity. Three experimental runs were conducted by varying the concentration from 5000 ppm to10,000 ppm. Four sets of experimental data were recorded from each run and different colours of lines showing for different sets of reading. Mean value of mass loss for a particular set is represented by line having same colour in Fig.5.13.

Similarly, Fig.5.14, Fig.5.15 and Fig.5.16 show the mass loss of all the buckets for different concentration (5000 ppm, 7500 ppm and 10000 ppm) corresponding to silt size of 45 micron,135 micron, 215 micron and 302 micron respectively.

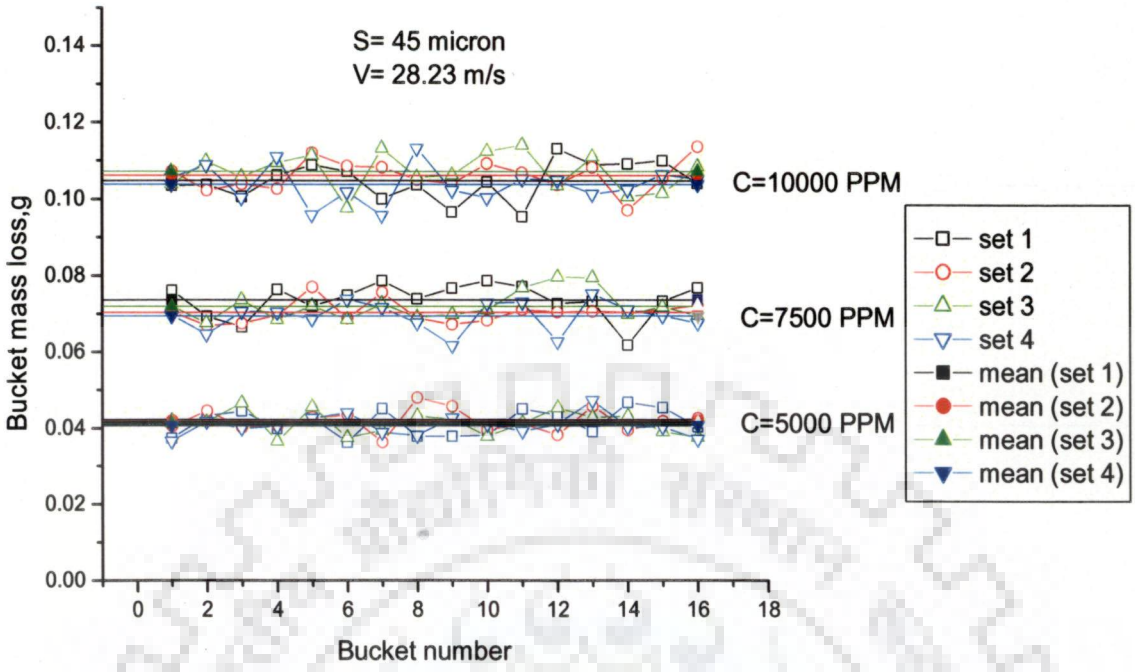

Fig.5.13 Variation in mass loss of different buckets for silt size, S=45micron

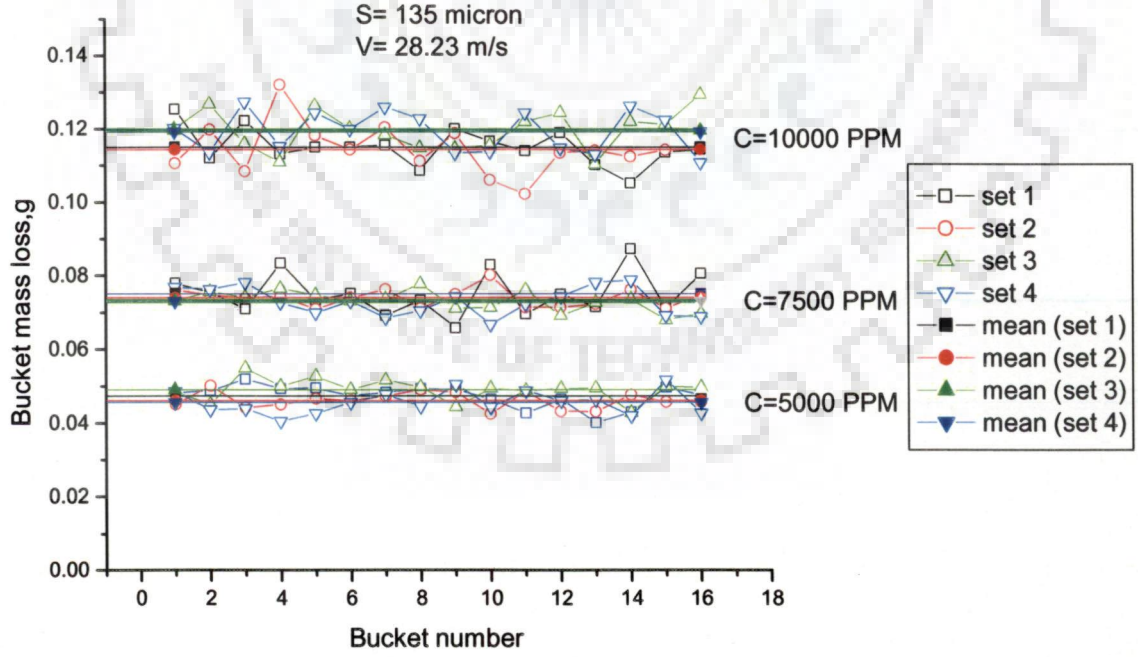

Fig.5.14 Variation in mass loss of different buckets for silt size, S=135 micron

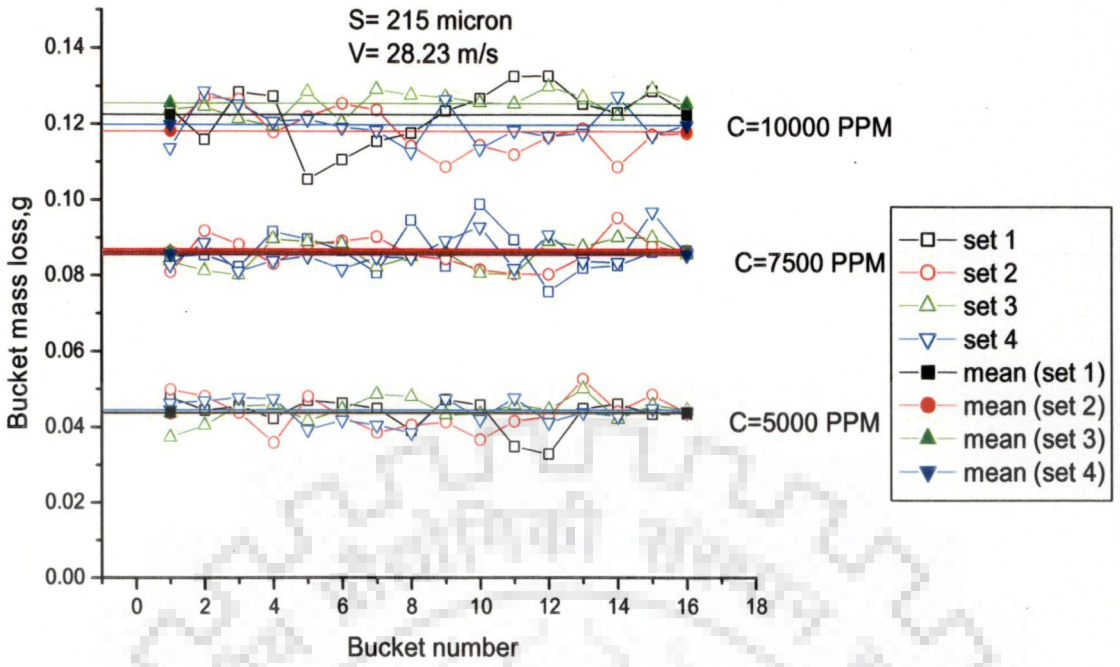

Fig.5.15 Variation in mass loss of different buckets for silt size, S=215 micron

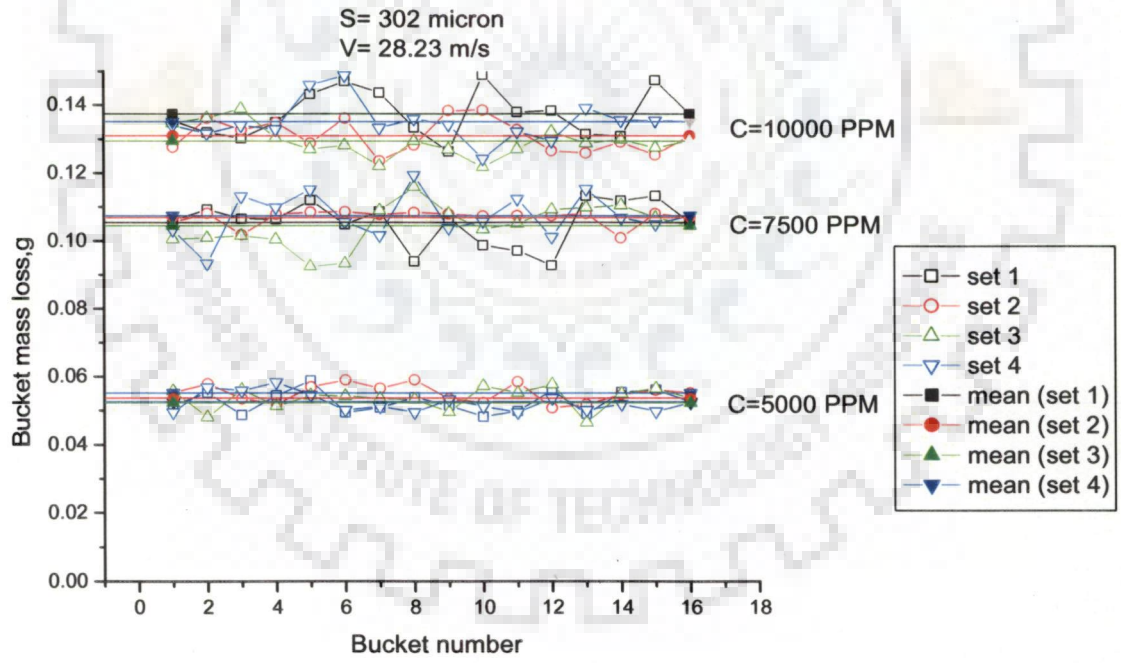

Fig.5.16 Variation in mass loss of different buckets for silt size, S=302 micron

Fig.5.17 shows the variation in mass loss of each bucket for different values of jet velocity. The average absolute percentage deviation in mass loss has been found as 9.56, 8.38, 8.29 and 9.6 correspond to silt size values of 302 micron, 215 micron, 135 micron and 45 micron respectively. The average absolute percentage deviation in case of different jet velocity has been found as 6.4. Based on these findings average value of mass loss in all the sixteen buckets were considered for analysis.

Further, in order to discuss the effect of silt and operating parameters on erosive wear as a function of mass loss of the bucket, erosive wear is converted in the form of normalized wear as a non dimensional parameter. The normalized erosive wear is defined as;

$$\text{Normalized erosive wear, } W = \frac{Mass\ loss\ of\ the\ bucket}{Initial\ mass\ of\ the\ bucket}$$

5.4.1 Effect of Silt Concentration

Silt concentration has been considered as one of the important silt parameter. As discussed above average value of mass loss of all the buckets and then converted into normalized wear has been considered to study the erosion behavior of the Pelton turbine buckets. Based on the experimental data, plots have been prepared to discuss the effect of silt concentration on the normalized wear. Data were generated for different concentration under a fixed value of jet velocity and silt size. Figs.5.18-5.21 show the normalized wear with respect to the operating hours of the turbine. In these figures, each curve corresponds to a particular concentration showing the variation in normalized wear with time.

It can be seen from these figures that the erosive wear increases with operating hours of the turbine. The slopes of these lines indicate the rate of wear with time for different values of silt concentration and silt sizes. These slopes are seen to be increased with increase in silt concentration. It may be concluded that for a given value of silt size, the erosive wear rate increases with silt concentration.

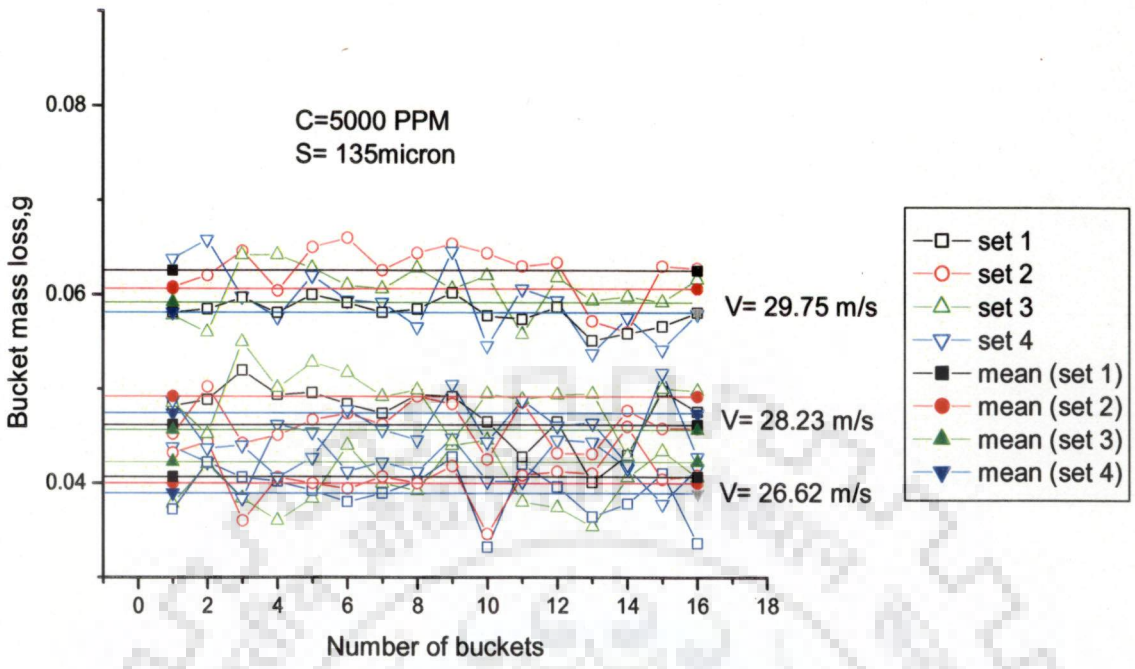

Fig.5.17 Variation in mass loss of different buckets for different jet velocity

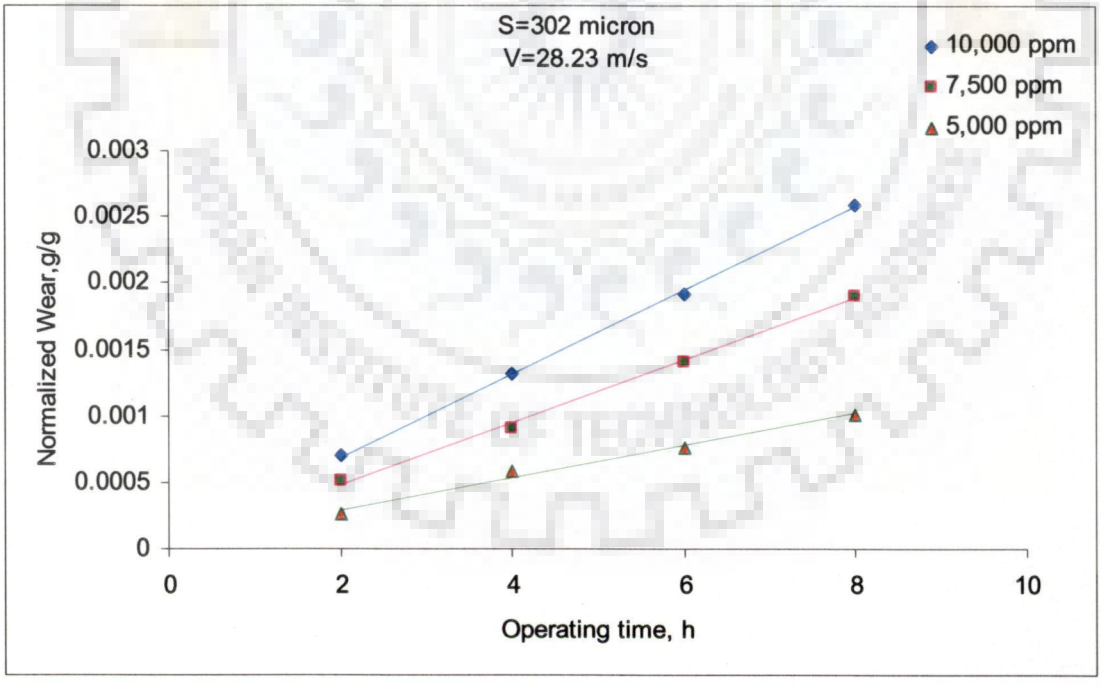

Fig.5.18 Normalized wear versus operating time for different concentration and size range of 250-355μm

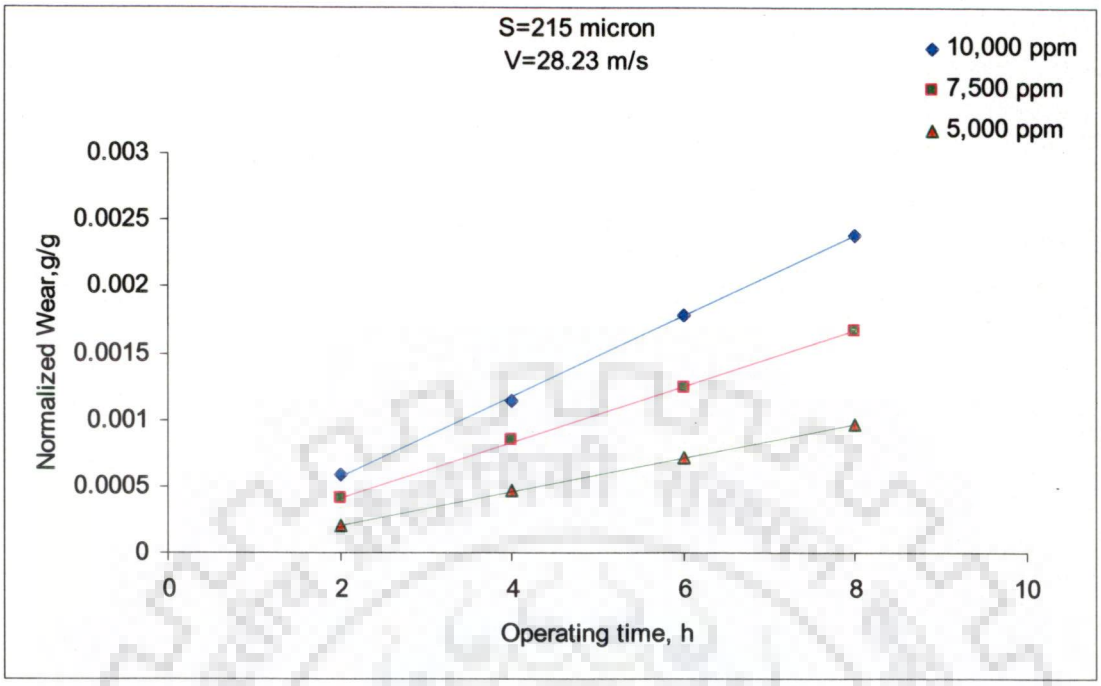

Fig.5.19 Normalized wear versus operating time for different concentration and size range of 180-250μm

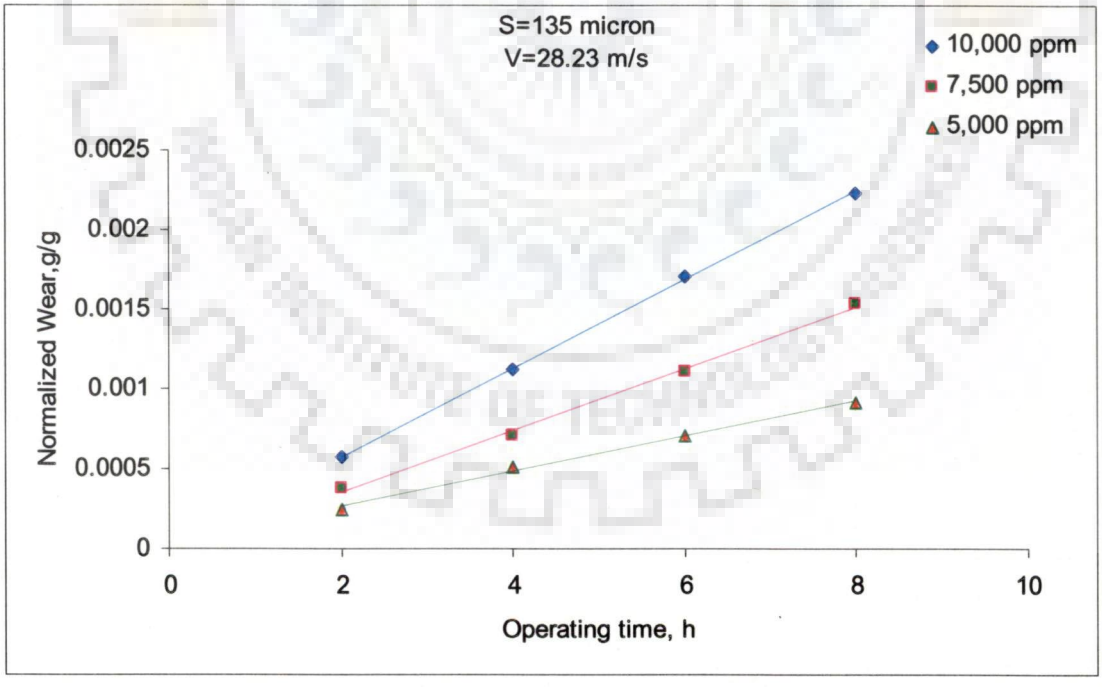

Fig.5.20 Normalized wear versus operating time for different concentration and size range of 90-180μm

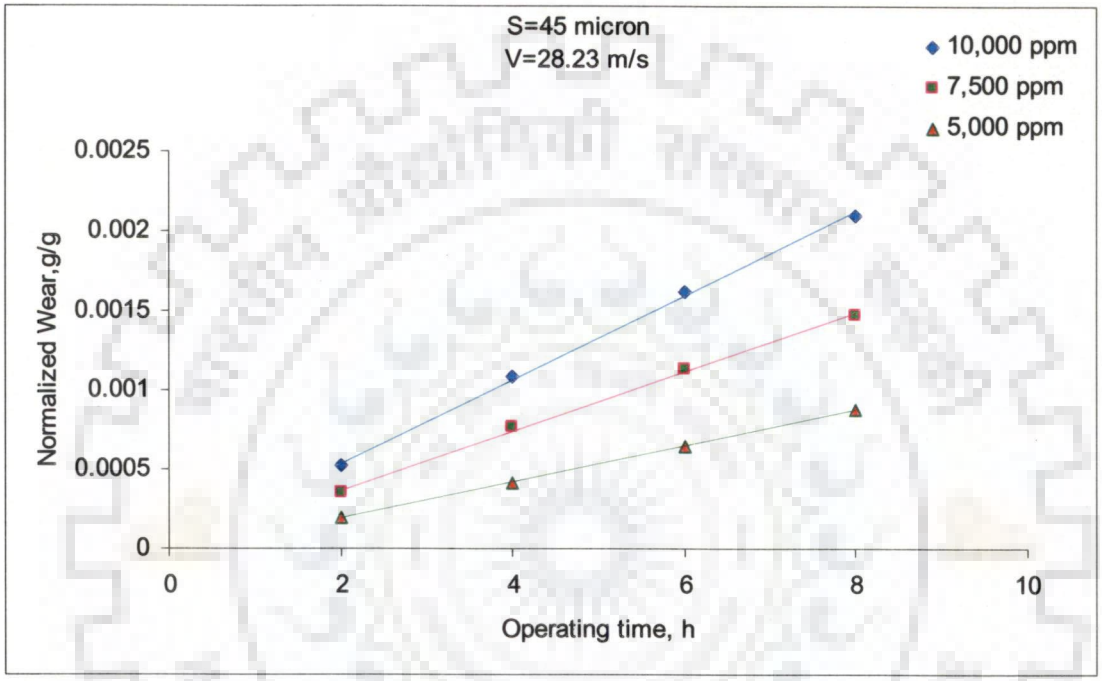

Fig.5.21 Normalized wear versus operating time for different concentration and size range below 90µm

Fig.5.22 shows the effect of silt concentration on normalized wear for different values of silt size of 45 micron, 135 micron, 215 micron and 302 micron and a jet velocity of 28.3 m/s.

It is observed that normalized wear increases with concentration for a given value of silt size and jet velocity. The value of normalized wear has found to be increased from 0.001 to 0.0027 as the concentration increases from 5000 ppm to 10000 ppm, corresponding to the silt size of 302 micron. Trend for the increase of normalized wear with concentration has been found to be similar for all the values of silt size.

5.4.2 Effect of Silt Size

In order to investigate the effect of silt size on the bucket wear, different silt sizes were considered while other parameters i.e., silt concentration, jet velocity and operating hour was kept constant. Under the present investigation, natural silt particles were collected from the site of the existing power house and the ranges of the silt sizes considered were 250-355micron, 180-250 micron, 90-180 micron and below 90 micron. The SEM micrographs of silt samples are shown in Fig.5.23.

For silt particles of different concentrations, the variation of normalized wear with operating time has been shown in Figs.5.24-5.26 for different values of concentration. It is seen from these figures that normalized wear increases with operating time of the turbine for all the values of silt size and concentration as discussed earlier. Initially, the variation in normalized wear has not been found significant with silt size in the higher range of concentration (10,000 ppm). However, in the lower range of concentration (5,000-7,500 ppm), the variation in normalized wear has been found to be significant with silt size.

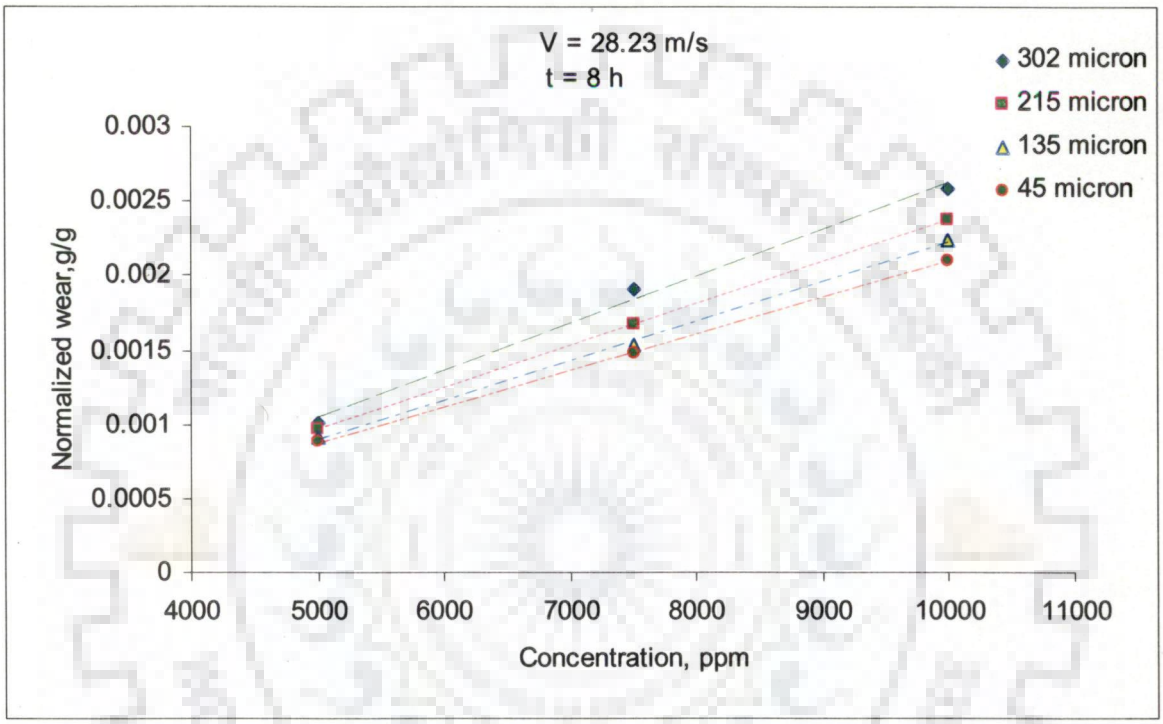

Fig.5.22 Effect of silt concentrations on normalized wear rate for different silt size range

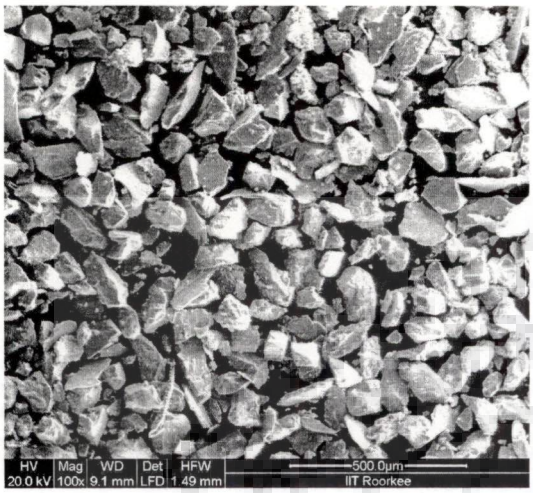

(a) Below 90 micron

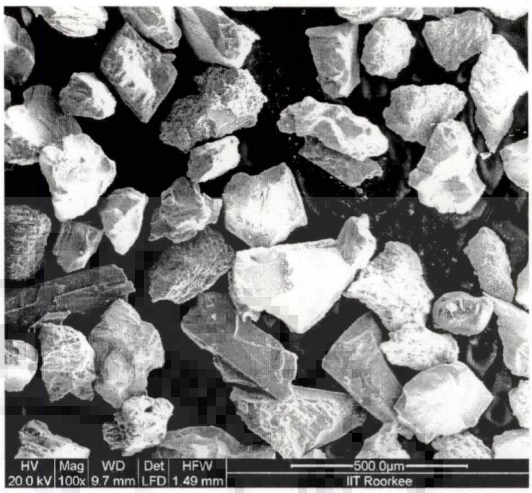

(b) 90-180 micron

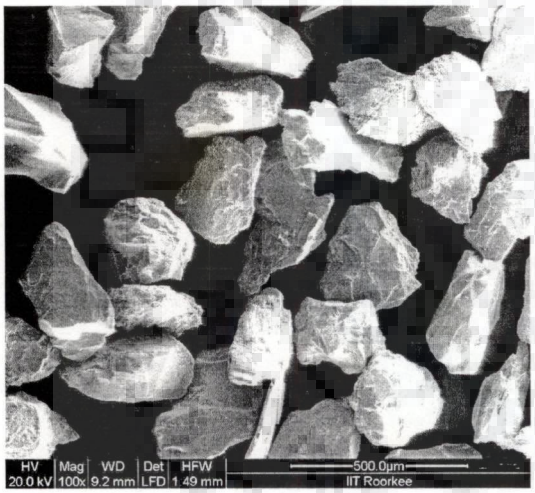

(c) 180-250 micron

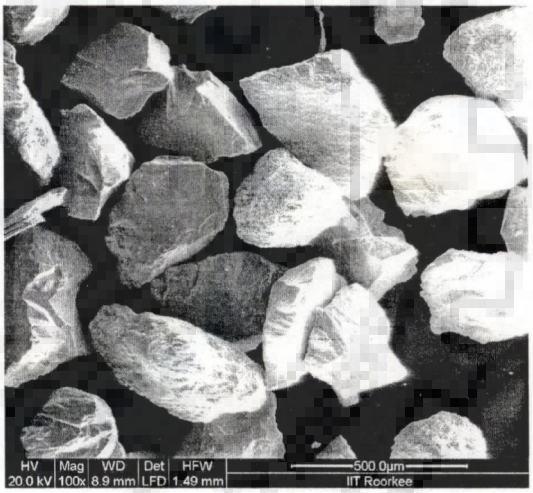

(d) 250-355 micron

Fig.5.23 The SEM photographs of silt samples

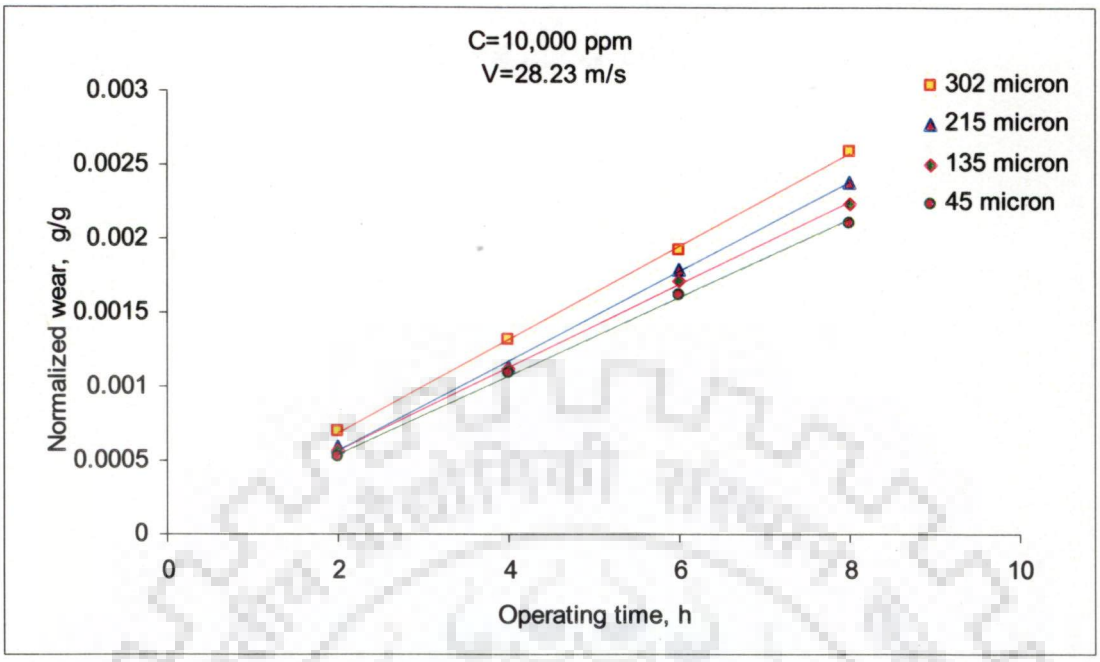

Fig.5.24 Normalized wear versus operating time for different size range and concentration of 10,000 ppm

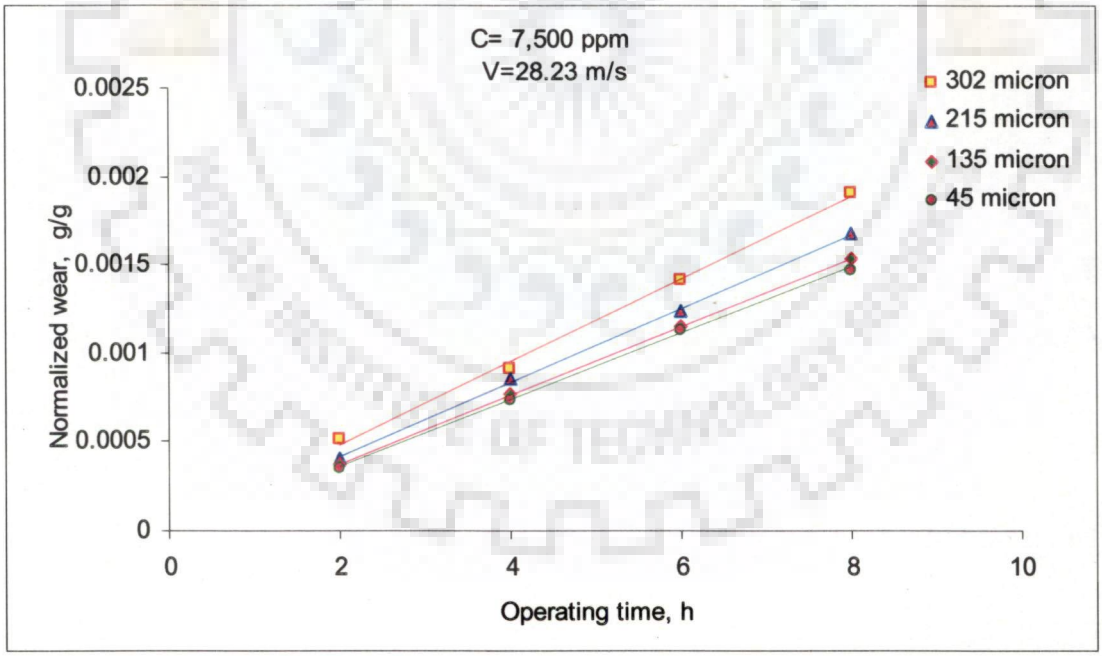

Fig.5.25 Normalized wear versus operating time for different size range and concentration of 7,500 ppm

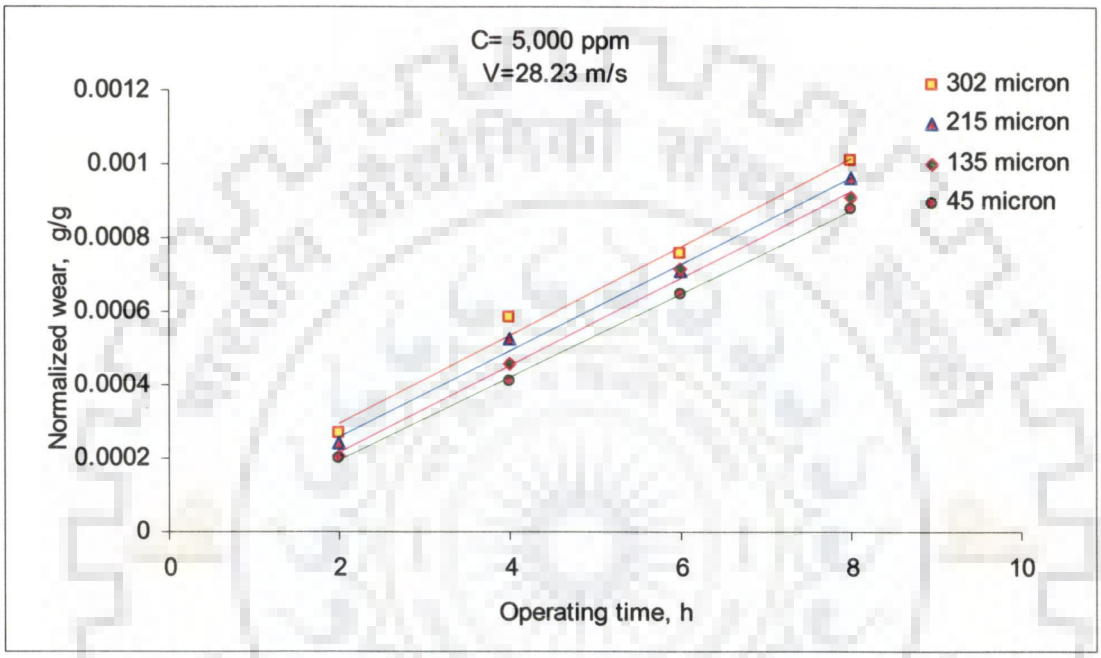

Fig.5.26 Normalized wear versus operating time for different size range and concentration of 5,000 ppm

Fig.5.27 shows the variation of the normalized wear with the particle size (D_{50}) for different values of concentration. It is seen that within the range of the particle size investigated, the erosive wear increases with the increase in the particle size for all the concentrations considered. The increase in the erosive wear rate has been found to be more prominent for the higher values of concentration (10000 ppm). These findings are found in good agreement with the findings of other investigators.

5.4.3 Effect of Jet Velocity

In order to discuss the effect of jet velocity on erosive wear, experiments were conducted at different heads with silt particles range of 90-180 micron and concentration at 5000 ppm. Based on the experimental results, the normalized erosive wear has been analyzed. In order to take care of jet velocity under different head the erosive wear was normalized with corresponding discharge. Fig.5.28 shows effect of the jet velocity on the normalized erosive wear per unit discharge for different values of jet velocity. Four readings were taken for each velocity and average of all data was considered for plotting the plots. Fig.5.28 shows that the wear rate follows the power law with respect to change in velocity (i.e.$W \alpha V^n$). The value of n has been evaluated in the present study as 3.79. The obtained value of n has been found in good agreement with other investigations for Pelton turbine.

5.5 DEVELOPMENT OF CORRELATION FOR NORMALIZED WEAR

Based on experimental data, the effects of silt and operating parameters on normalized wear have been discussed. The effect of silt parameters viz., particle size and concentration and operating parameter viz., jet velocity and operating hours on the erosive wear of buckets has been discussed in the previous part of the Chapter-5. It has been observed that these parameters play critical role in the erosion of turbine buckets. A system designer may require the correlations for erosive wear rate in order to predict the efficiency of Pelton turbine under the actual conditions having silt laden water flow. Correlation of wear rate as a function of the system and the operating parameters is required to be developed from the experimental data.

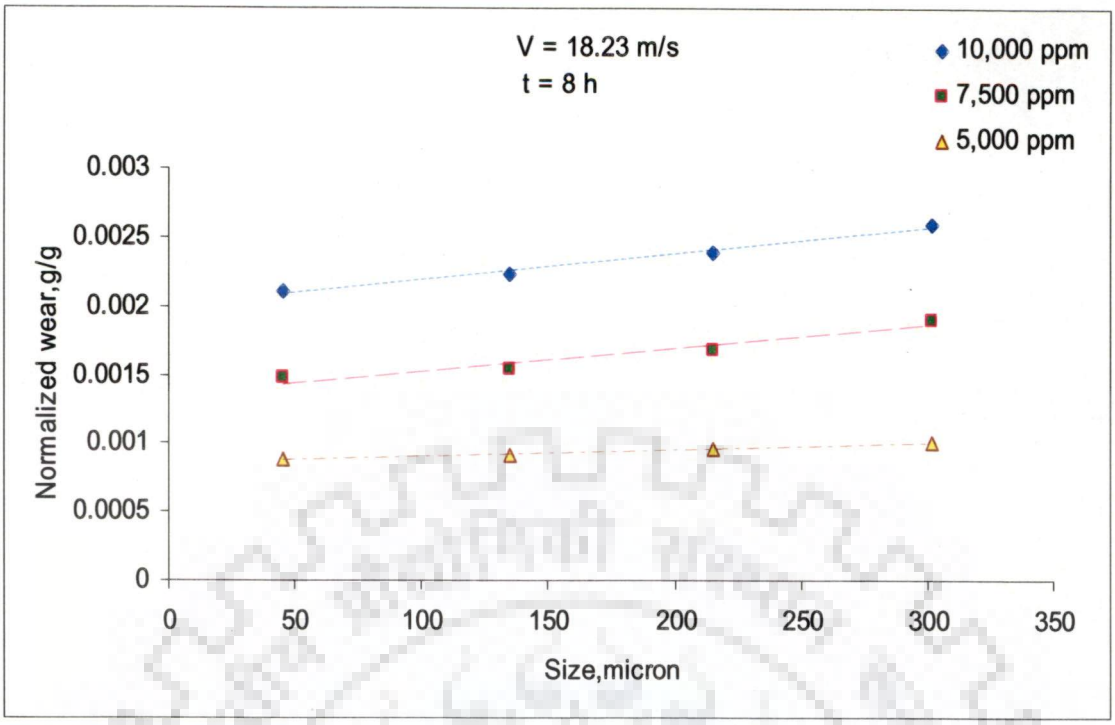

Fig.5.27 Effect of silt size on normalized wear

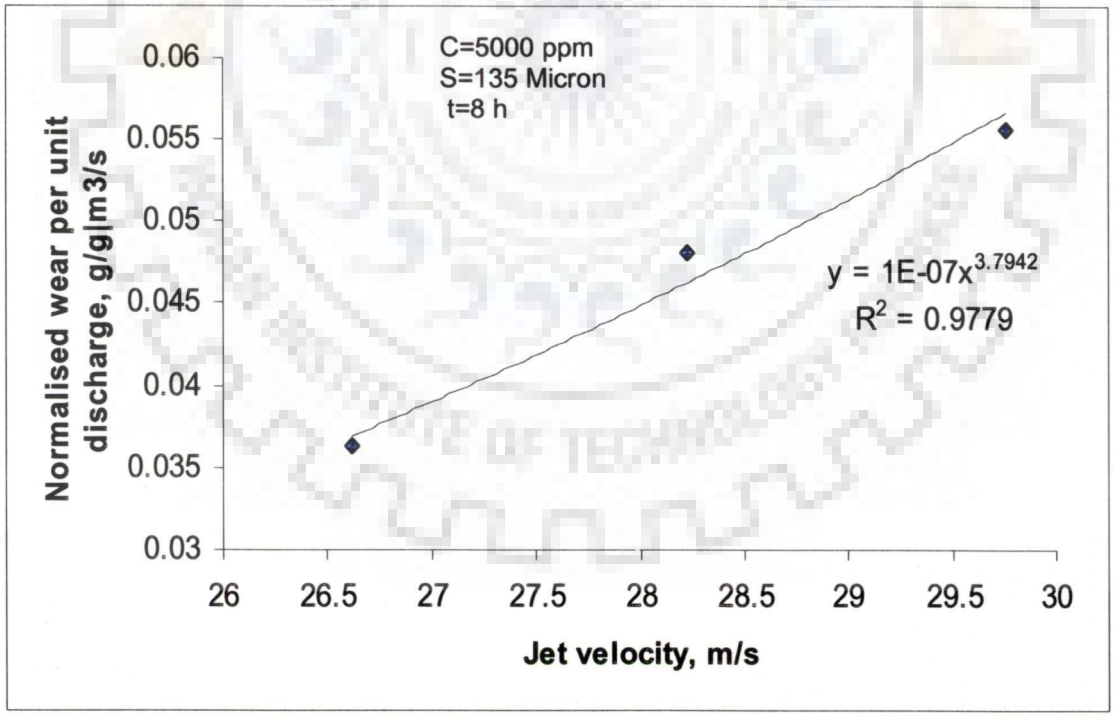

Fig.5.28 Effect of jet velocity on normalized wear

Saini and Saini [158] mentioned that it is feasible to adopt a statistical approach for the development of correlations from experimental data. Under this part of the chapter correlations for normalized wear from the experimental data has been developed by following the procedure given by Saini and Saini [158]. Sigma Plot (version 10.0) software has been employed for carrying out the regression analysis. The different plots are shown on linear scale, however in order to have the best curve fitting, data on log scales have been employed while carrying out the regression analysis.

It has been found that the regression of data deals with first order polynomials. Therefore before presenting the details of developing the correlations, it is necessary to understand the general form of first order equation as has been discussed in the following section.

5.5.1 First Order Equation

The simplest relationship between two variables is when they are equal. The next simplest is when one variable is equal to the other multiplied by a constant. In either case, the relationship is said to be "linear". First order equation for a linear relationship or for a straight line has simple variable with highest power of 1 and can be written as;

$$y = mx + C \tag{5.2}$$

where 'm' is slope of the line and 'C' is intercept of the line on ordinate.

By transforming the x and y data into log form, the first order equation for a straight line can be written as;

$$\log y = m \log x + C_1 \tag{5.3}$$

$$\text{or } \log y = \log \left(x^m \right) + \log \left(\textit{anti}\log C_1 \right) \tag{5.4}$$

$$\text{or } \log\ y = \log\ \left(antilog\ C_1 \times x^m\right) \tag{5.5}$$

By taking antilog on both sides, the above equation can be written as;

$$y = antilog\ C_1\ \left(x^m\right) \tag{5.6}$$

which is the general form of first order equation.

The values of 'C_1' and 'm' can be obtained from the first order regression of the data on plot of '$\log x$' and '$\log y$'. The first order equation can be obtained by putting the values of 'C_1' and 'm' in the Eq. (5.6).

Following the method discussed above, correlation for normalized wear has been established. Experimental data generated for bucket mass loss for a range of system and operating parameters as presented in the previous Chapter-4 have been used to develop normalized wear correlations. It is revealed from the experimental data that the normalized erosive wear is strongly dependent on the silt parameters i.e. silt size (S), silt concentration (C), water jet velocity (V) and operating hours of the turbine (t). Thus the equation for normalized erosive wear can be written as;

$$W = f\ (S, C, V, t) \tag{5.12}$$

The mass loss data obtained from the experimental investigation are normalized with the original bucket mass and unit discharge. The normalized erosive wear is presented as a function of system and operating parameters. Fig.5.29 shows the first order regression of the log scale data of operating time versus normalized erosive wear, which shows the average value of 'm' (average slope of lines) equal to 0.99. Therefore the following first order equation similar to Eq.5.6 can be written to represent the normalized erosive wear correlation as a function of time;

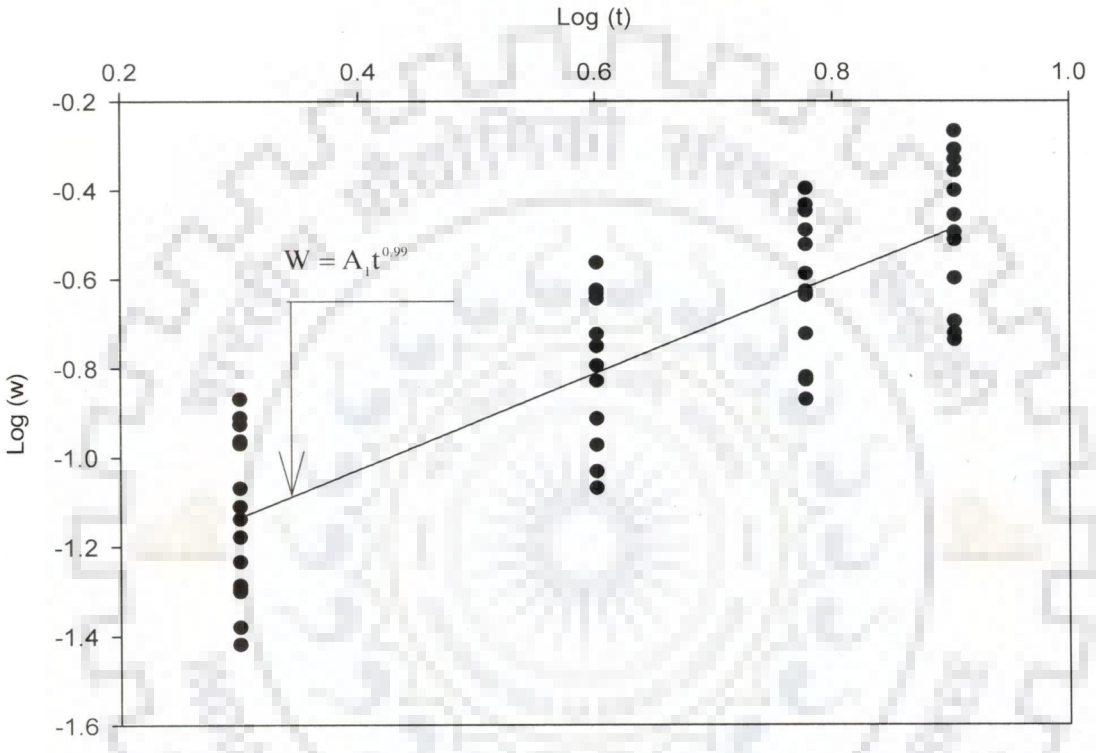

Fig.5.29 Plot for log (W) versus log (t)

$$W = anti\log C_1 t^{0.99} \quad (5.13)$$

or $W = A_1 t^{0.99}$ (5.14)

where $A_1 = antilog\ C_1$. The constant 'A_1' will be a function of the system parameters i.e. silt size, silt concentration and jet velocity.

In order to induce the effect of silt size parameter, the values of $\frac{W}{t^{0.99}}$ are calculated from the data of normalized erosive wear plotted against log value of particle size considered for the experimentation as shown in Fig.5.30. The correlation obtained is presented in the following form;

$$\frac{W}{t^{0.99}} = Anti\log C_2 S^{0.126} \quad (5.15)$$

or, $\frac{W}{t^{0.99}} = A_2 S^{0.126}$ (5.16)

Similarly the effect of silt concentration parameter is induced in the Eq.5.15 by representing coefficient A_2 as a function of silt concentration. These values have been plotted against respective silt concentration values as shown in Fig.5.31. The correlation obtained is presented in the following form;

$$A_2 = Anti\log C_3 C^{1.227} \quad (5.17)$$

or, $\frac{W}{t^{0.99} S^{0.126}} = Anti\log C_3 C^{1.227}$ (5.18)

or, $\frac{W}{t^{0.99} S^{0.126}} = A_3 C^{1.227}$ (5.19)

or, $\frac{W}{t^{0.99} S^{0.126} C^{1.227}} = A_4 V^{3.79}$ (5.20)

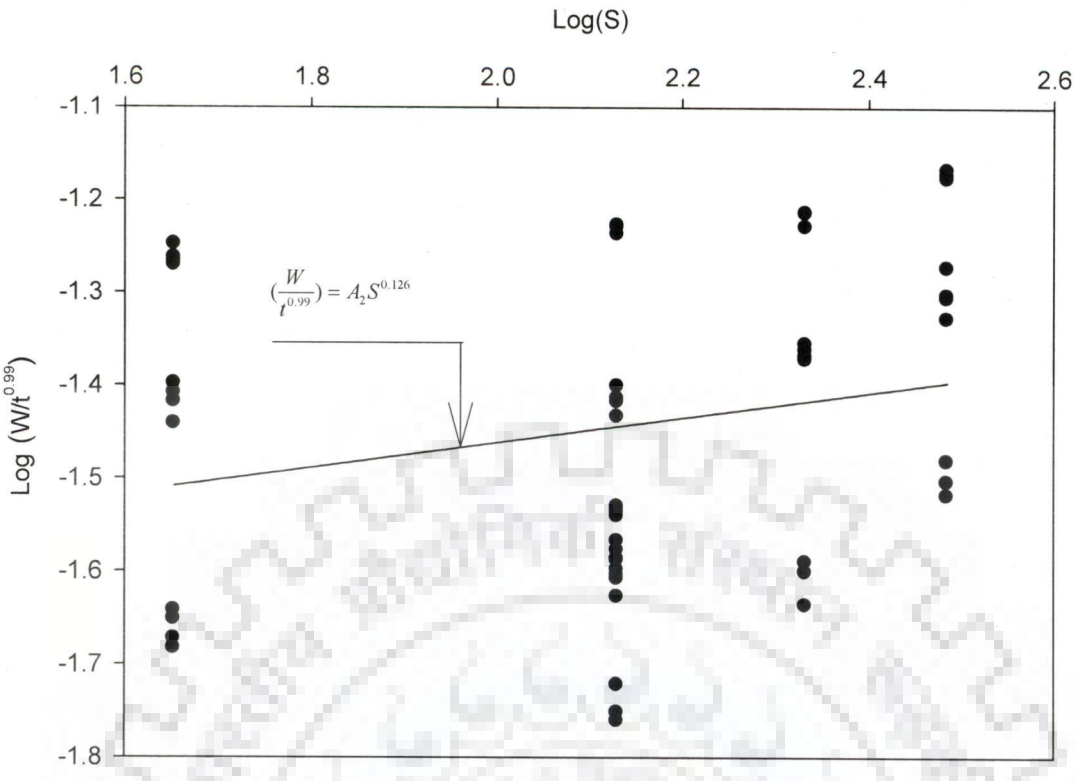

Fig.5.30 Plots for log ($W/t^{0.99}$) versus log (S)

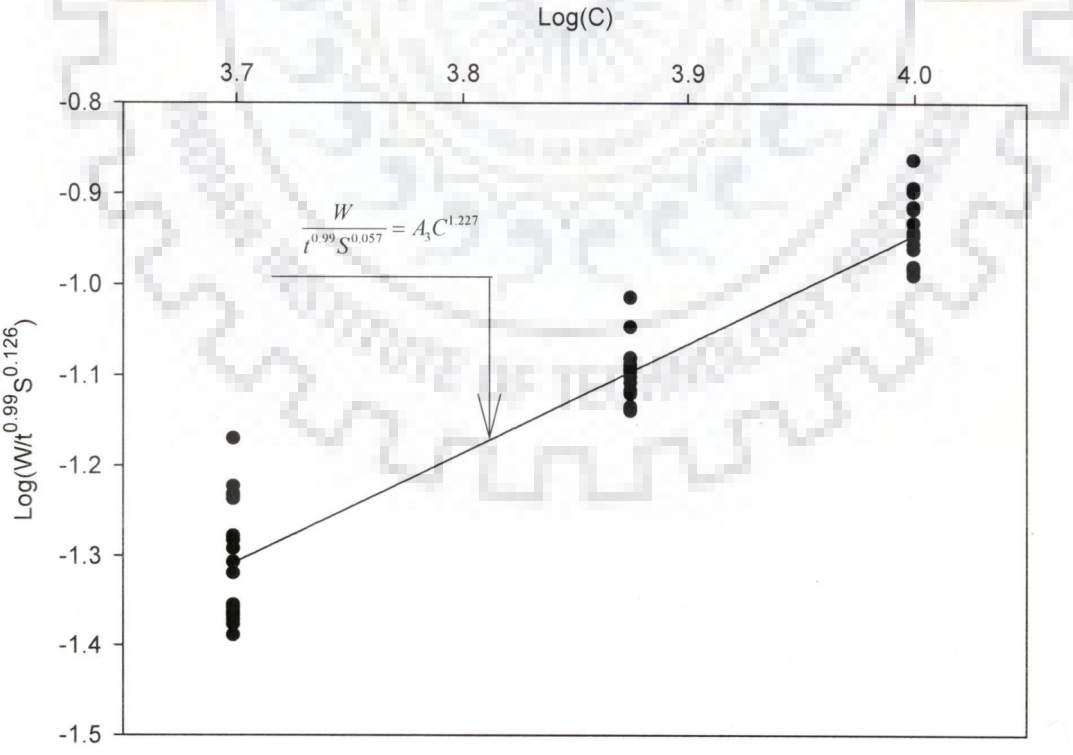

Fig.5.31 Plot for log ($W/t^{0.99}S^{0.126}$) versus log (C)

or, $$W = A_4 V^{3.79} t^{0.99} S^{0.126} C^{1.227} \quad (5.21)$$

In order to induce the effect of velocity parameter in the above equation, the values of correlation for the coefficient A_3 has been developed as a function of jet velocity parameter from the first order regression of the data on log scales. Values of 'C_4' and 'm' are obtained as-11.3473 and 3.79 respectively as shown in Fig.5.32. The correlation obtained is expressed as;

$$\frac{W}{t^{0.99} S^{0.126} C^{1.227}} = Anti\log(C_4) V^{3.79} \quad (5.22)$$

The final form of the correlation for normalized erosive wear rate is obtained as follows:

$$W = 7.91\times10^{-13}(t)^{0.99}(S)^{0.13}(C)^{1.23}(V)^{3.79} \quad (5.23)$$

Fig.5.33 shows the comparison of the experimental data of erosive wear rate and those obtained from the above correlation. A good agreement has been observed. The average absolute percentage deviation between the experimental data and calculated values of erosive wear rate has been found to be within ±6.7%.

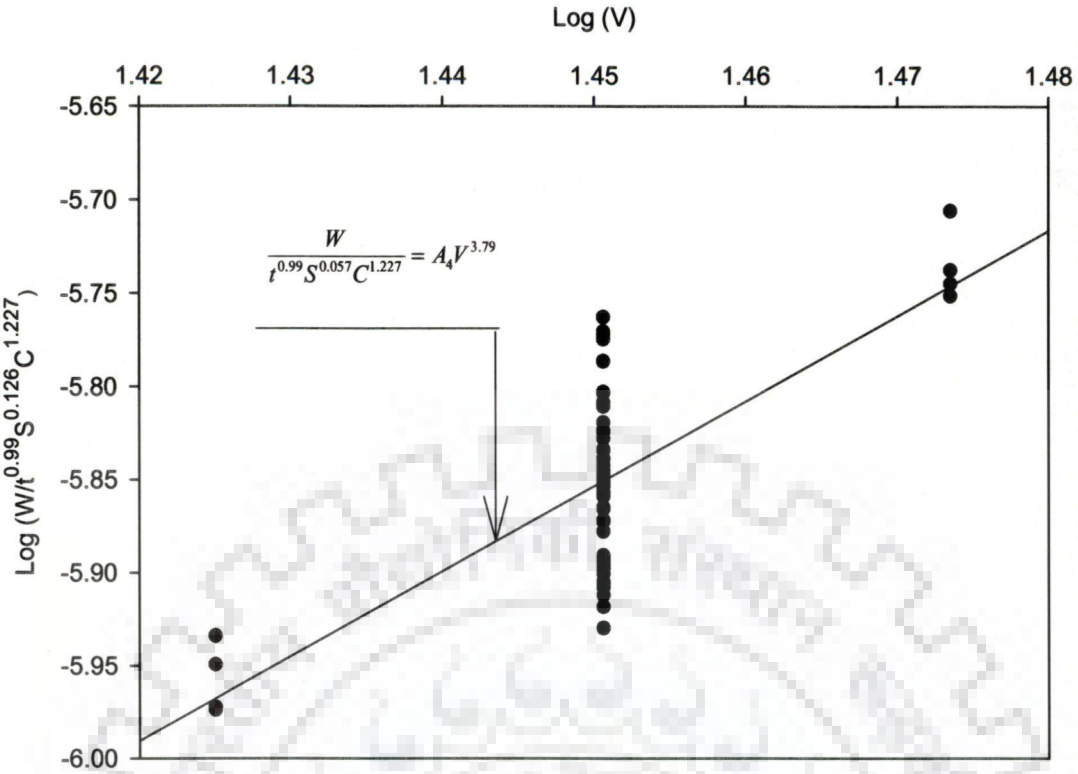

Fig.5.32 Plot for log ($W/t^{0.99}S^{0.126}C^{1.227}$) versus log (V)

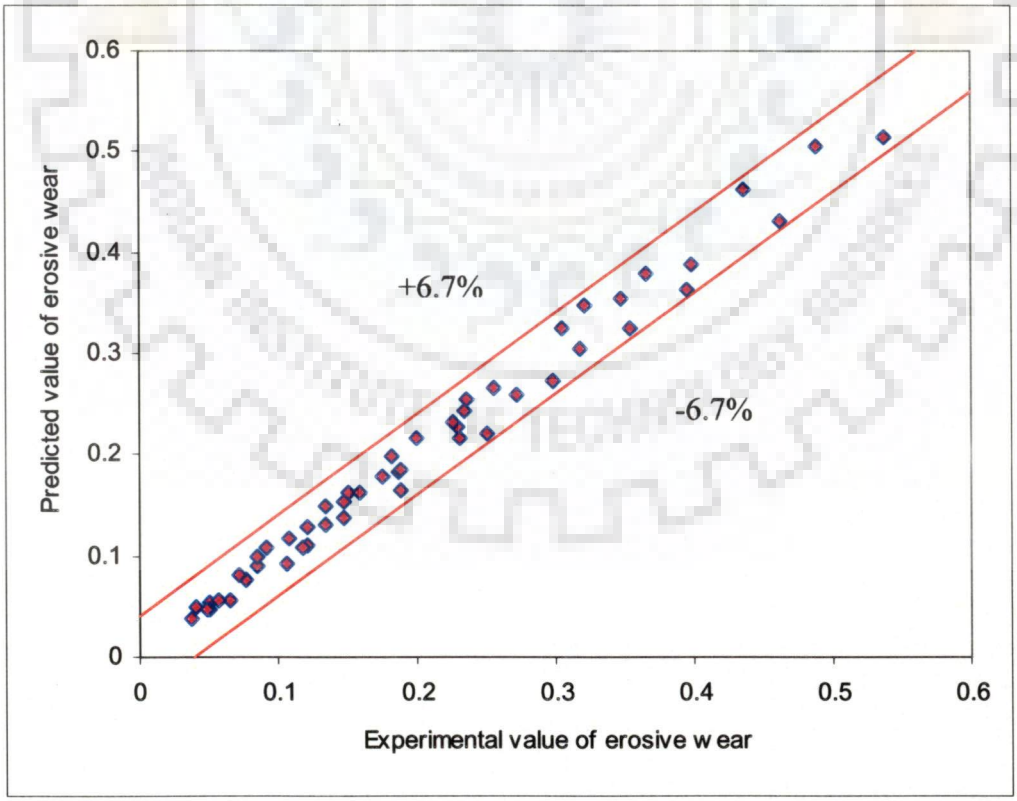

Fig 5.33 Comparison of experimental values and predicted values of erosive wear

CHAPTER-6

INVESTIGATION OF TURBINE PERFORMANCE

6.1 GENERAL

As discussed earlier, the erosion of turbine components causes the decrease in turbine efficiency, increase in the maintenance cost and down time for turbine repair. All these factors contribute to the plant cost and cause the revenue losses. It is therefore, essential to study the amount of efficiency loss owing to the erosion of turbine components due to the silt particles coming in water. Under the present investigation an experimental study has been carried out in order to investigate the effect of silt laden parameters and operating parameters on erosive wear in Pelton turbine buckets. Detail of experimental set up, instrumentations methodology for experimentation and data generated for silt erosion under different conditions are discussed in Chapter-4. Based on the results obtained during experimentation, effect of silt parameters on erosion in turbine buckets are discussed in Chapter-5. The effect of silt laden parameters and operating parameters on the efficiency of Pelton turbine has been discussed under this Chapter-6.

6.2 METHOD OF EFFICIENCY MEASUREMENT

In order to compute the efficiency of Pelton turbine the input to the turbine in terms of head and discharge and out put of the turbine in terms of power generation was recorded continuously for all sets of the experimentation conducted as reported in Chapter-4. A generator was coupled with the runner shaft to generate the electricity and out put of the generator was recorded. The output of the turbine was recorded by considering the efficiency of generator. A control panel was connected to the generator to record the power generation of the generator. The control panel consisted of a Voltmeter, a Wattmeter and electric bulbs as ballast load. The power out put from

the generator was monitored and recorded continuously with the help of Wattmeter having a least count of 10 Watt.

The input to the turbine was maintained constant through out the experiment by keeping the head and discharge as constant to the turbine. The discharge to the turbine for different heads was determined as discussed in Chapter-4. By considering the discharge and head readings, the turbine input was computed. The input to the turbine was calculated from the head and discharge of the turbine by using the following expression;

$$P_i = 9.81 \times H \times Q \qquad (6.1)$$

The efficiency of turbine was calculated as follows.

$$\eta_o = \frac{P_o}{9.81 \times H \times Q \times \eta_g} \times 100 \qquad (6.2)$$

where,

η_o is the efficiency of turbine, %

P_o is the electrical power out put, kW

H is the head to the turbine, m

Q is the discharge through the turbine, m^3/s

η_g is the efficiency of the generator (= 0.98 for the considered generator)

It is observed from the experiments that the power out put is decreasing with the bucket mass loss. Therefore an attempt has been made to establish a correlation for efficiency loss as a function of bucket mass loss for different silt parameters and operating parameters.

Pelton turbine runners are designed either for casting of the disc and buckets in one piece (i.e. monocast) or the disc and the buckets separately. Single piece of

complete runner is the preferred and commonly used method for the Pelton turbines in modern power plants where the turbine units are for high power generation and of bigger sizes. However, in case of defect found in one bucket, the whole runner has to be rejected. Moreover, for manufacturing of runners in disc and buckets separately is of advantageous as in case of defect found in any bucket, the individual bucket is to be discarded. Different methods are adopted for fixing the individual buckets to the disk. The stem of the bucket are suppose to be designed and manufactured of different shapes.

The stem of the bucket is relatively heavier in comparison of the cup (bucket without stem). In order to discuss the output and efficiency loss of turbine with respect to the percentage mass loss of bucket, mass of cup (bucket without stem) is considered. Accordingly, the percentage mass loss of cup has been determined by considering the mass of cup alone. During experimentation presented in Chapter-4, parameters related to input and output of the turbine were measured. The values of these measured parameters were used to find out the efficiency of the turbine under the different conditions considered for this investigation. As discussed above, the output and efficiency of the turbine are determined. The effect of mass loss of buckets on the power output and efficiency of the turbine is discussed.

The basic mass volume method has been adopted to determine the mass of the bucket without the stem. A measuring flask filled with water was used for finding out the mass ratio. The bucket was dipped completely and the volume of water was recorded. Again the stem of the bucket only was dipped in water and the volume of water was recorded. The mass of the bucket without stem was calculated using following relationship;

$$\frac{Mass\ of\ bucket\ without\ stem}{Mass\ of\ bucket\ with\ stem} = \frac{Volume\ of\ bucket\ without\ stem}{Volume\ of\ bucket\ with\ stem} \qquad (6.3)$$

Percentage mass loss has been determined with respect to the total mass of bucket without stem.

6.3 EFFECT OF BUCKET MASS LOSS ON POWER OUTPUT AND EFFICIENCY OF TURBINE

Fig.6.1 shows the power out put verses bucket mass loss. It is found that the power output of the turbine decreases with mass loss of the bucket. It is observed that the rate of power loss initially is more. However the rate of power loss in later stage has been found to be at lower rates and become asymptote. Similar trend has been observed in case of turbine efficiency as shown in Fig.6.2.

As discussed earlier, the presentation of effect of silt parameters on turbine output and efficiency will be more relevant if these are discussed with percentage mass loss of bucket. Accordingly, the effect of silt parameter on percentage efficiency loss has been discussed.

Fig.6.3 shows the percentage efficiency loss of turbine with silt concentration for different values of silt size and a fixed value of jet velocity. Rate of percentage efficiency loss has been found to be significant in this case. However, rate of percentage efficiency loss has been found nominal with silt size as shown in Fig.6.4.

Fig.6.5 shows the percentage efficiency loss of turbine with jet velocity for silt concentration 5000 ppm and for fixed value of mean silt size of 135 micron. Rate of percentage efficiency loss has been found to be significant in this case.

Fig.6.6 shows percentage efficiency loss with percentage mass loss of the bucket. About 8% efficiency loss has been found against a bucket mass loss of 3.5%. An attempt has been made to develop a correlation for efficiency loss of turbine as a function of silt size, silt concentration, jet velocity and operating hours of the turbine.

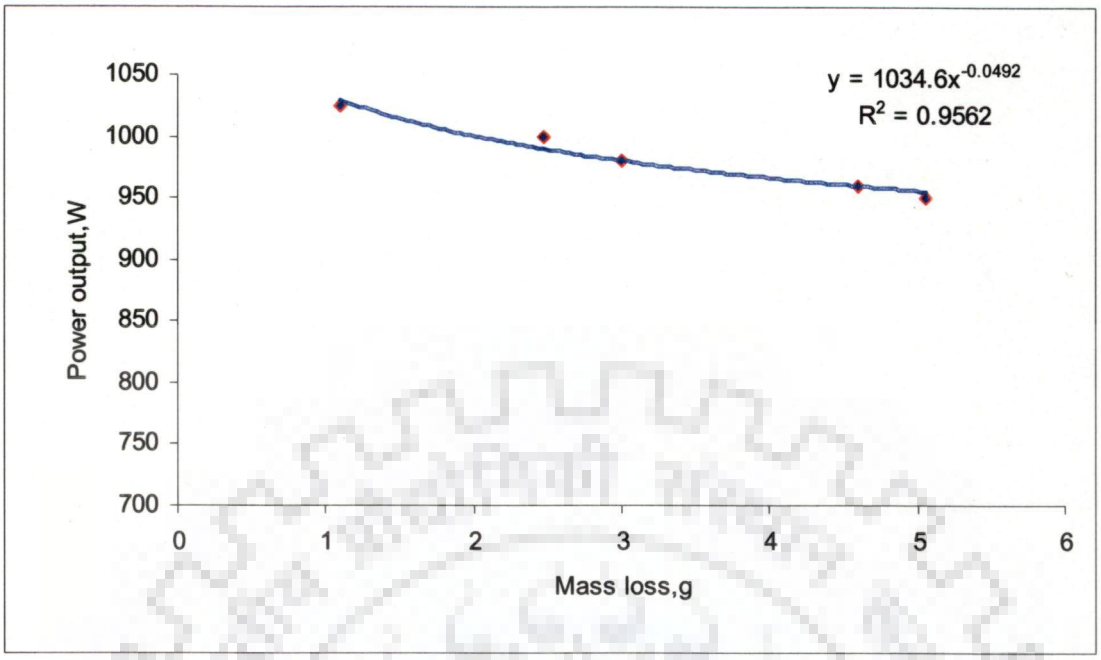

Fig.6.1 Effect of bucket mass loss on turbine power output

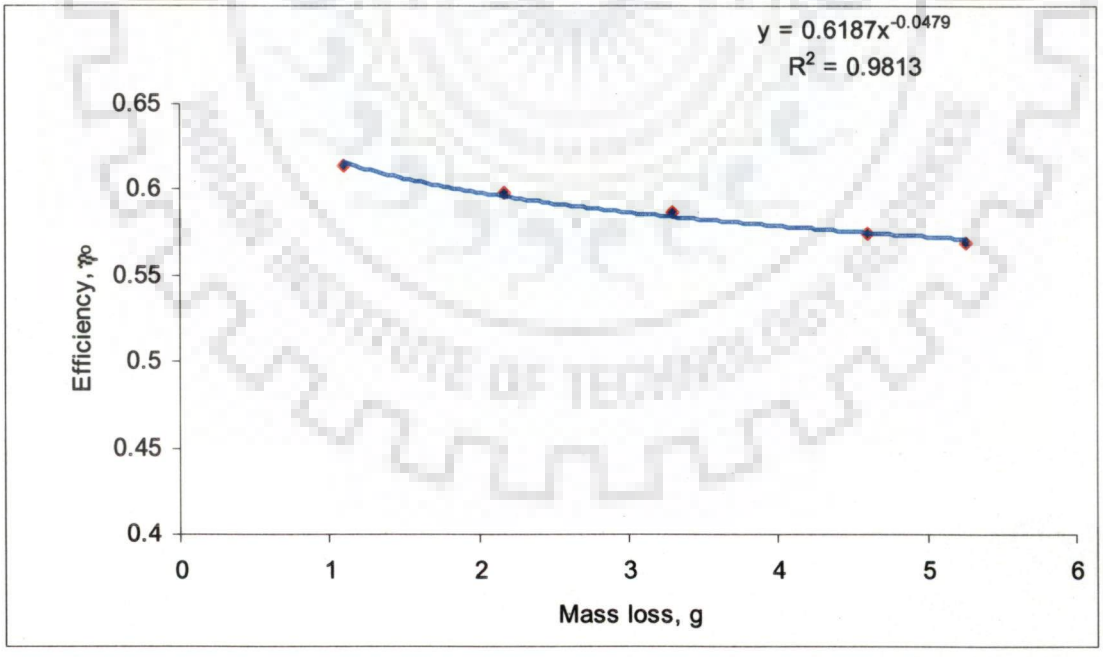

Fig.6.2 Effect of bucket mass loss on turbine efficiency

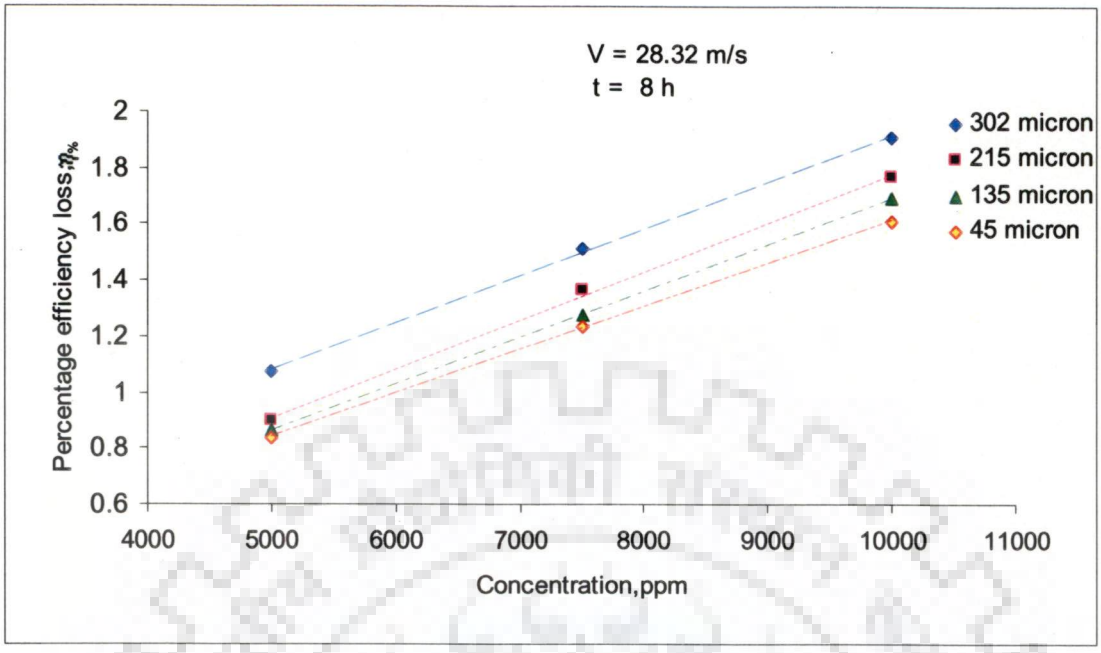

Fig.6.3 Percentage efficiency loss versus silt concentration

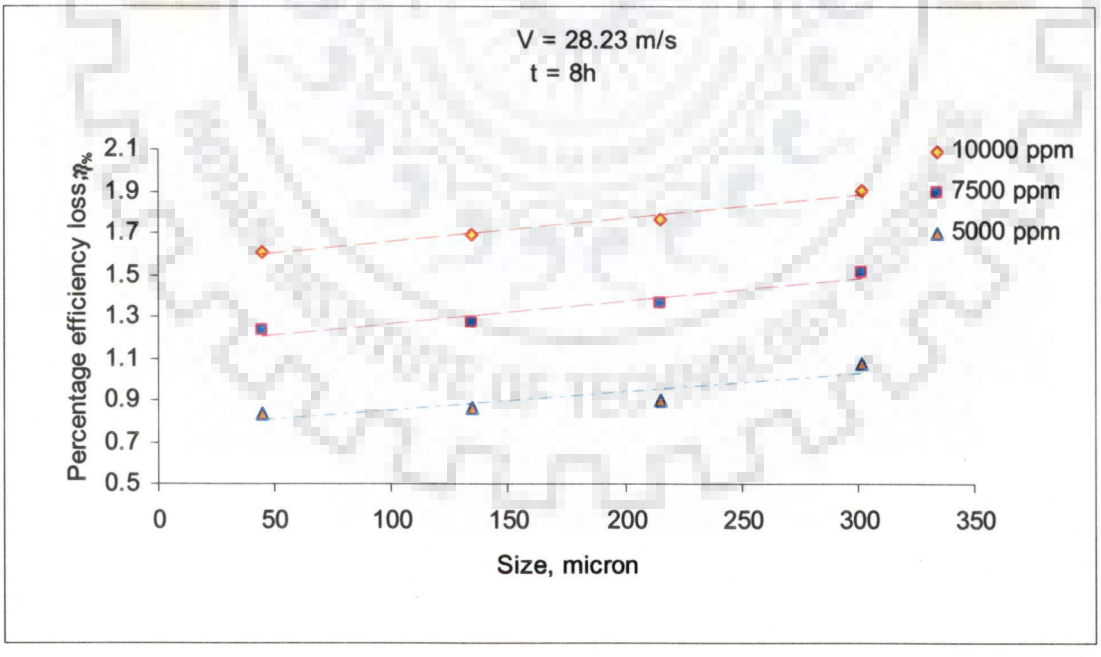

Fig.6.4 Percentage efficiency loss versus silt size

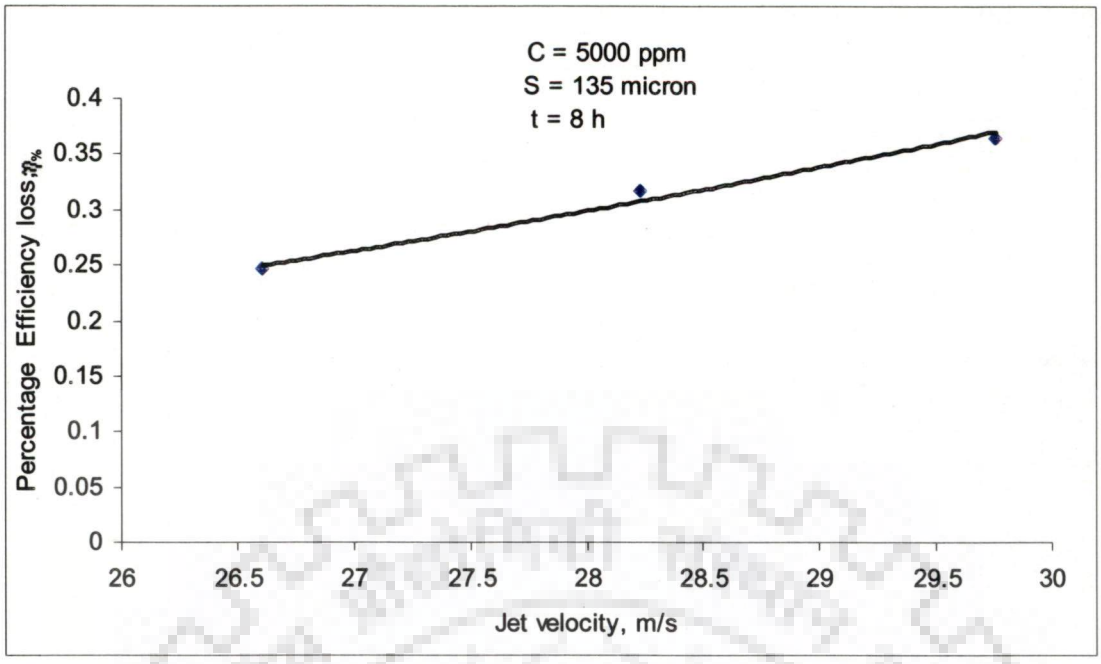

Fig.6.5 Percentage efficiency loss versus jet velocity

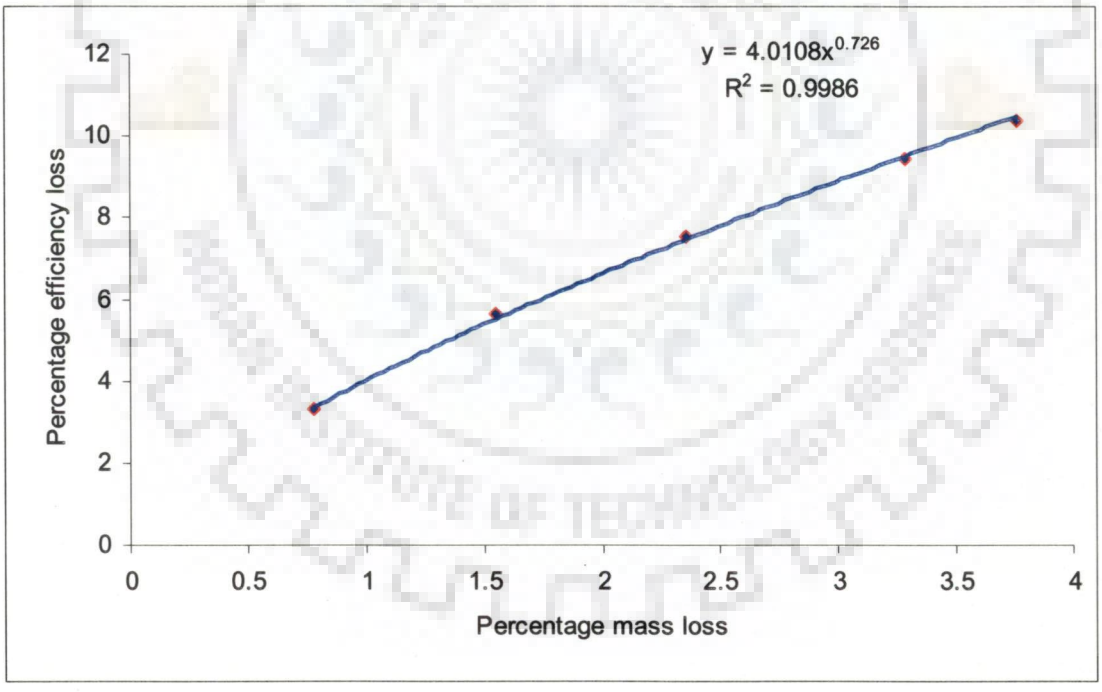

Fig.6.6 Effect of percentage mass loss on percentage efficiency loss of turbine

6.4 DEVELOPMENT OF CORRELATION FOR EFFICIENCY LOSS

The effect of bucket mass loss on the efficiency of Pelton turbine has been discussed in previous part of this chapter. It has been observed that bucket mass loss and alteration of bucket shape play critical role in the Pelton turbine efficiency loss. The system designer may require the correlations for efficiency drop of Pelton turbine under the actual conditions having silt laden water flow. Under the present investigation correlation for efficiency loss as a function of system and operating parameters is required to be developed from the experimental data. As discussed earlier, the efficiency loss is strongly dependent on the silt parameters, silt size(S), silt concentration(C), water jet velocity (V) and operating hours of the turbine (t).

Following the same procedure of development of correlation for normalized wear as discussed in Chapter-5, correlation for turbine efficiency loss is developed and presented as follows;

The percentage efficiency loss is presented as a function of system and operating parameters and can be written as ;

$$\eta = f\,(S, C, V, t) \tag{6.4}$$

Fig.6.7 shows the first order regression of the log scale data of operating time versus efficiency loss, which shows the average value of '*m*' (average slope of lines) equal to 0.75.Therefore efficiency can be written as;

$$\eta_{\%} = anti\log C_1 t^{0.75} \tag{6.5}$$

$$\text{or} \qquad \eta_{\%} = A_1 t^{0.75} \tag{6.6}$$

In order to induce the effect of silt size parameter, the values of $\frac{W}{t^{0.99}}$ are calculated from the data of normalized erosive wear obtained experimentally and plotted against log value of particle size considered for the experimentation as shown in Fig.6.8. The correlation obtained is presented in the following;

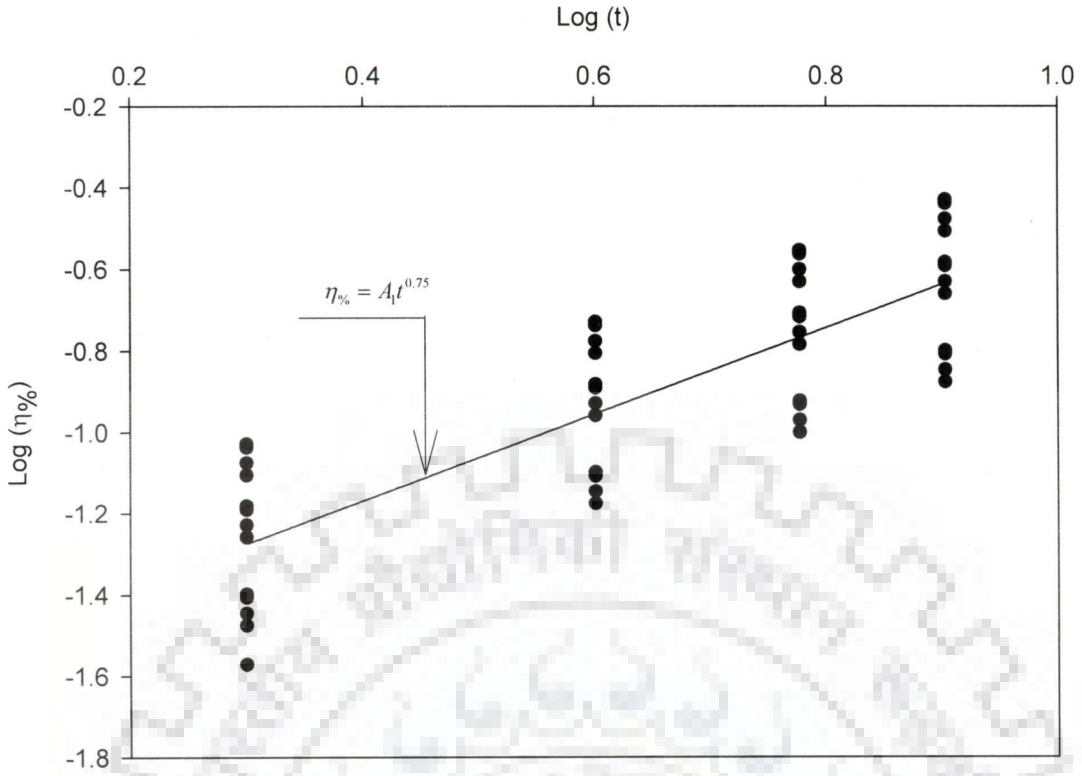

Fig. 6.7 Plot of log ($\eta_{\%}$) versus log (t)

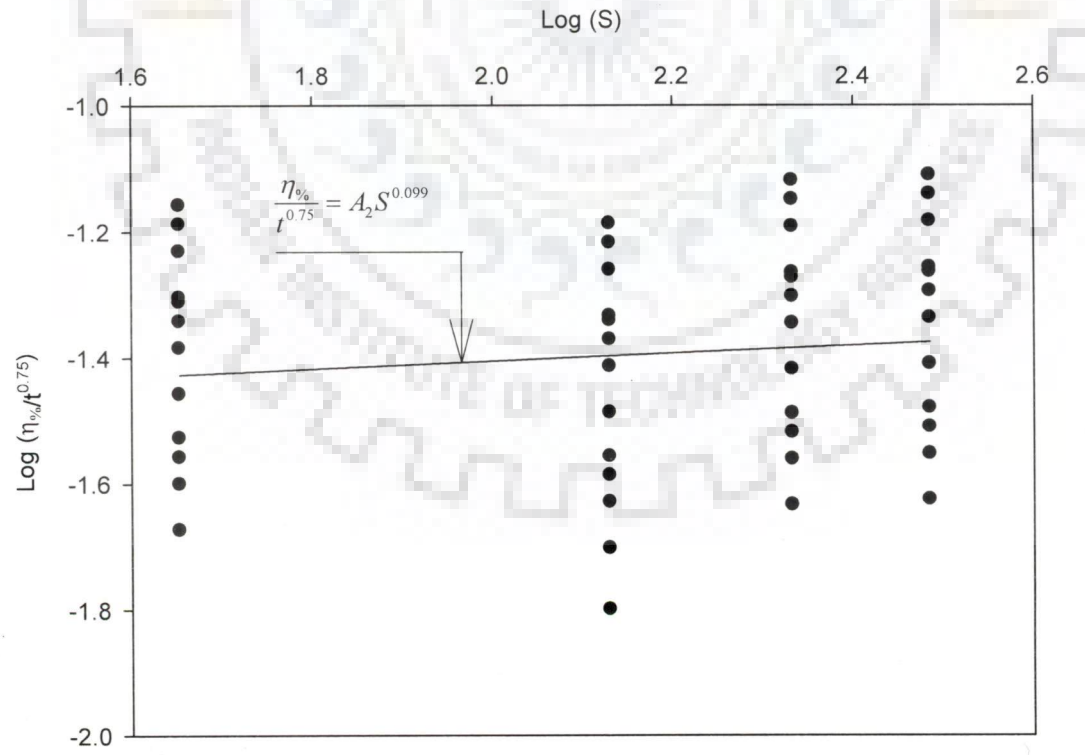

Fig. 6.8 Plot of log ($\eta_{\%}/t^{0.75}$) versus log (S)

$$A_1 = Anti\log C_2 S^{0.099} \tag{6.7}$$

or, $$\frac{\eta_{\%}}{t^{0.75}} = Anti\log C_2 S^{0.099} \tag{6.8}$$

or, $$\frac{\eta_{\%}}{t^{0.75}} = A_2 S^{0.099} \tag{6.9}$$

Similarly, the effect of silt concentration parameter is induced in the Eq.6.9 by representing coefficient A_2 as a function of silt concentration. These values have been plotted against respective silt concentration values as shown in Fig.6.9. The correlation obtained is presented in the following form as in Eq.6.10.

$$A_2 = Anti\log C_3 C^{0.93} \tag{6.10}$$

or, $$\frac{W}{t^{0.75} S^{0.099}} = Anti\log C_3 C^{0.93} \tag{6.11}$$

or, $$\frac{W}{t^{0.75} S^{0.099}} = A_3 C^{0.93} \tag{6.12}$$

In order to induce the effect of velocity parameter in the above equation, the values a correlation for the coefficient, A_3 has been developed as a function of jet velocity from the first order regression of the data on log scales. Values of 'C_4' and 'm' are round to be as -9.6146 and 3.40 respectively. These values have been plotted against the value of jet velocity as shown in Fig.6.10. Finally the correlation obtained is in following form;

$$\frac{W}{t^{0.75} S^{0.099} C^{0.93}} = Anti\log C_4 V^{3.40} \tag{6.15}$$

$$\frac{W}{t^{0.75} S^{0.099} C^{0.93}} = A_4 V^{3.40} \tag{6.16}$$

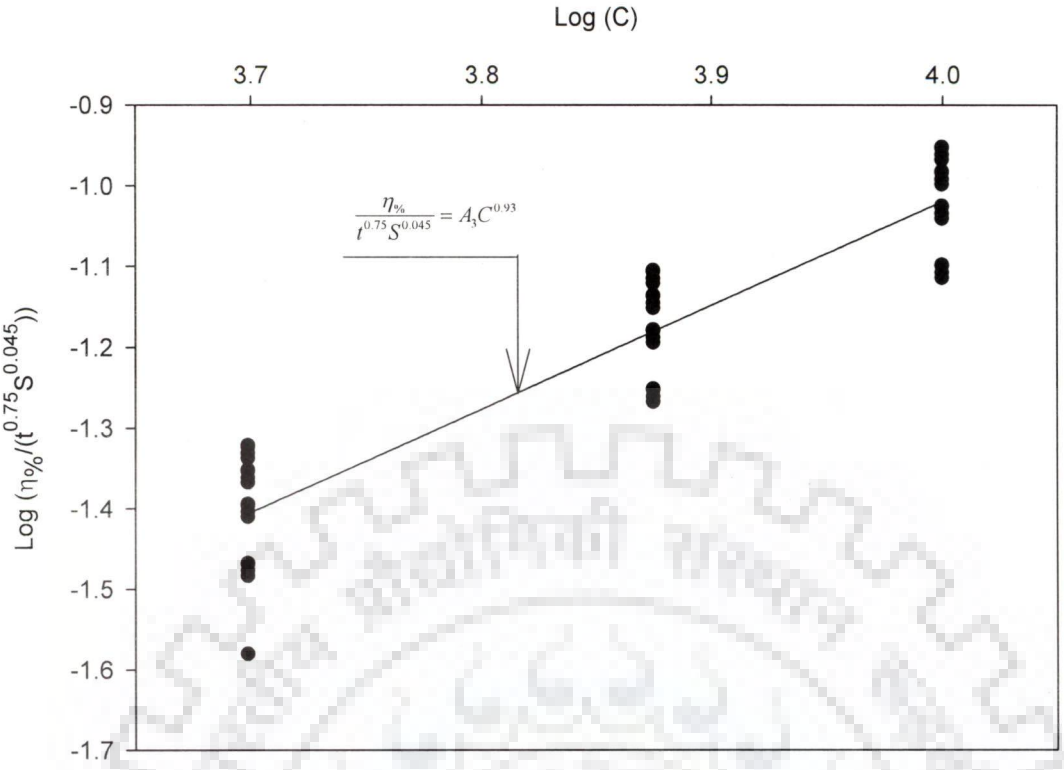

Fig. 6.9 Plot of log ($\eta_{\%}/t^{0.75}S^{0.099}$) versus log (C)

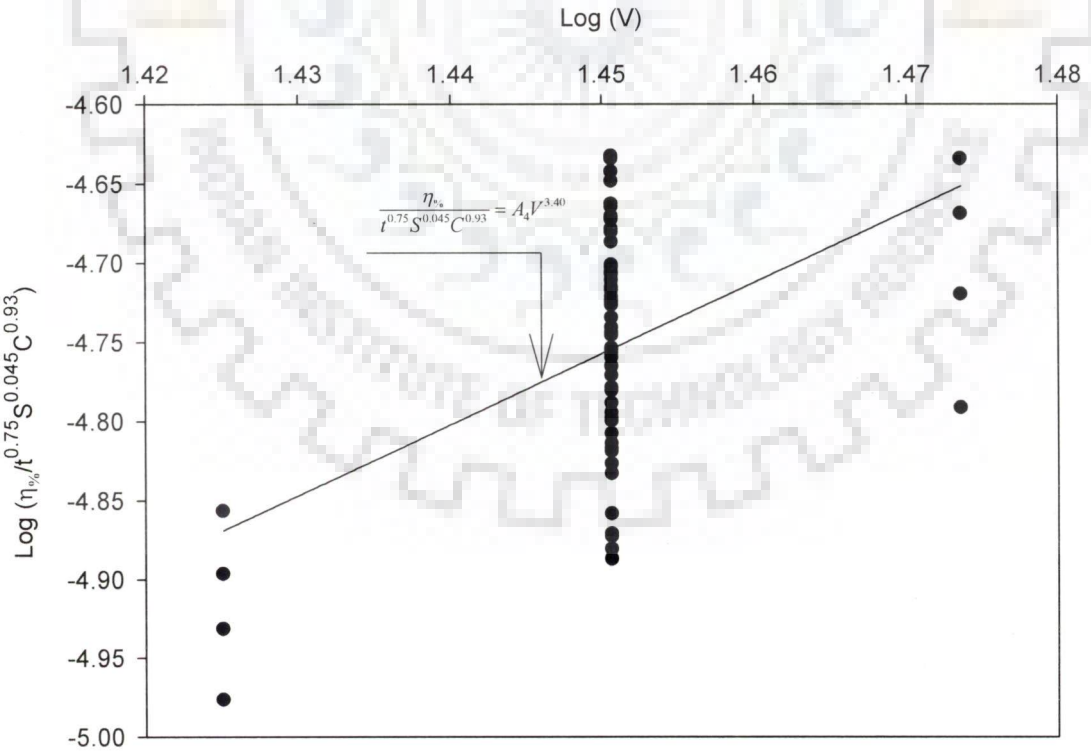

Fig. 6.10 Plot of log ($\eta\%/t^{0.75}S^{0.099}C^{0.93}$) versus log (V)

The final form of the correlation for percentage efficiency loss of rated efficiency is obtained as follows:

$$\eta_{\%} = 2.43\times10^{-10}\,(t)^{0.75}\,(S)^{0.099}\,(C)^{0.93}\,(V)^{3.40} \qquad (6.17)$$

Fig.6.11 shows the comparison between observed value and predicted value of efficiency loss with respect to the mass loss of bucket. A good agreement is observed. The average absolute percentage deviation between the experimental and calculated data for efficiency loss has been found within ±10%.

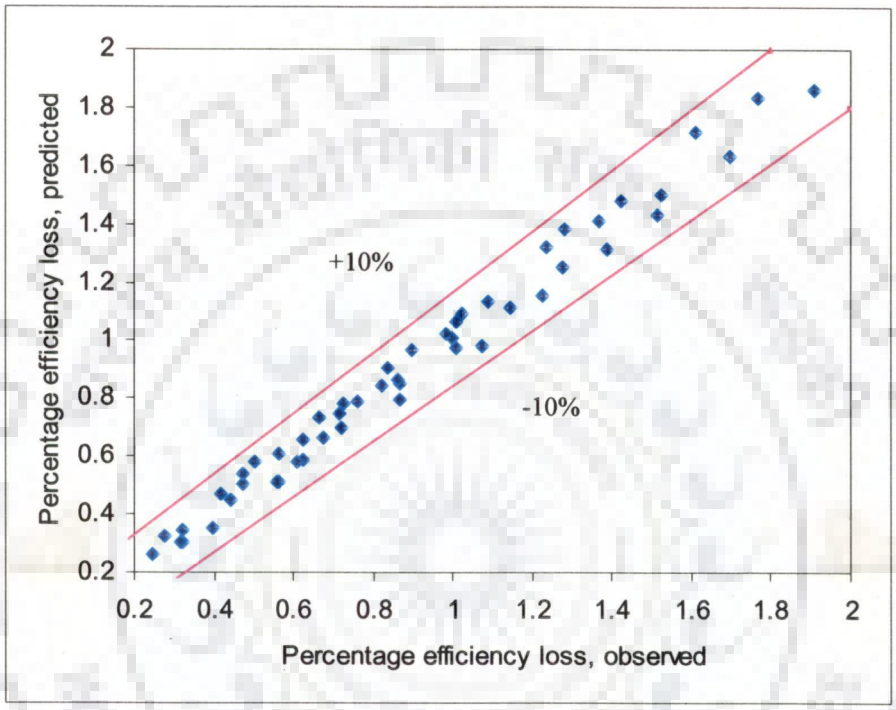

Fig.6.11 Comparison of experimental values with predicted values of efficiency loss

CHAPTER-7

CONCLUSIONS

Sand erosion is a major problem in hydro power plants, especially, under run-of-river schemes. Run-of-river power plants are typically built in rivers and provided with sediment settling basins. Sediment settling basins increase the cost of the hydropower projects significantly, as they are designed for removal of coarser sediment particles. However, smaller particles are allowed to pass through the turbine. During the rainy season, a large amount of sediments remain in water. It becomes difficult and costly to remove all the sediments having particle size less than 0.2mm before passing through the turbine. Severe erosion of turbine components is observed in high head turbines (Pelton and Francis) during monsoon. Pelton turbines are used in hilly areas to generate electricity at low discharge. The performance of the Pelton turbine decreases due to severe silt erosion. The problem of silt erosion is severe in buckets and nozzle of a Pelton turbine.

Literature survey reveals that a very little information is available regarding quantification and prediction of silt erosion in case of Pelton turbine. Keeping this in view an experimental study has been conducted in order to investigate the effect of silt concentration, silt size and jet velocity on erosive wear in Pelton turbine buckets. The mechanism of erosion at different parts such as at inlet, outlet and path along the depth of the bucket has been studied. Based on the results obtained from the experimental investigation and analysis, the following conclusions are drawn;

(i) Under the present study an experimental set up was designed and fabricated for creating actual turbine conditions in order to investigate the effect of the considered parameters on erosive wear. The set up consisted of; (i) Pelton turbine runner, (ii) Water tank, (iii) Stirrer, (iv) Cooling jacket, (v) Service

pump-motor set, (vi) Penstock pipe, (vii) Spear valve and nozzle, (viii) Control valve, (ix) Channel with weir, (x) Generator and a control panel with resistive load and (xi) Instrumentation.

(ii) Experimentations have been carried out in order to generate experimental data for erosive wear of Pelton turbine bucket and efficiency loss due to bucket erosion. Silt was collected from river Bhagirathi (India), near the head works of Maneri Bhali Hydro Electric Project, Phase I, which is one of the most silt affected power house in India. The quartz content in the sand sample were found to be more than 90%.

(iii) Silt related parameters and operating conditions i.e. concentration, size of silt particles, jet velocity and operating hours of the turbine were considered as investigated parameter. Range of the parameters considered for experimental study is as given below:

Table 7.1 Range of parameters

Parameters	**Range**
Concentration	5,000 to 10000 ppm
Silt size	Upto 355 micron
Jet velocity	26.62 m/s to 29.75 m/s
Operating time	8 hrs run for each set

(iv) The total experimental investigation was grouped into two parts. Under the first part of the study wear hot spots were identified inside the Pelton buckets. The mechanism of erosive wear at the hot spots was analyzed by fixing of the thin pieces of soft material as specimens at the hot spots with the help of an adhesive.

(v) The second part of the experiment involved the investigation of the effects of silt parameters (silt concentration and silt size) and operating parameters (jet velocity and operating hour) on erosive wear in Pelton bucket. The efficiency loss of the Pelton turbine due to bucket erosion is also studied.

(vi) Under the first part of the study the inlet or splitter, depth of the bucket and the outlet edges are found to be the prominent parts of bucket erosion. The SEM micrographs of wear specimens fixed at inlet, outlet and at the surface along the depth of the bucket were studied for a silt concentration of 5000 ppm and different silt particles size of 302 micron,215 micron, 135 micron and 45 micron.

(vii) Close examination of the micrographs of the specimens placed at different hot spots of Pelton bucket shows that the bigger particles cause more erosion at the inlet and along the depth of the bucket. Whereas smaller particles are turned to be more responsible for causing erosive wear along the depth of the bucket and at the out let of the turbine bucket.

(viii) Silt particle size of 302 micron and 215 micron posses higher value of kinetic energy and seems to remove material from the inlet surface of Pelton bucket due to plowing and shearing action of silt particles. However, smaller size particles i.e. 135 micron and 45 micron particles pierce into the surface forming lips in front of the travel path of the particles and small indentations are appeared over the surface. The material from the inlet surface was appeared not to be removed in a single impact. The reason may be due to lower kinetic energy possessed by the smaller size particles.

(ix) Close observation of micrographs at out let of turbine bucket indicated that smaller size particles of 135 micron and 45 micron cause more erosion in comparison of bigger particle sizes of 215 and 302 microns. This may be

explained that the bigger size particles travel at a higher relative velocity and loose their kinetic energy before coming to the outer surface. The smaller particles travel along with the water jet with high value of acceleration, strike the outlet surface and caused material removal at a higher rate than the case of bigger particles.

(x) The surface along the depth of the bucket was obtained to be eroded more in comparison of other two hot spots. Craters due to plastic deformation and pits were appeared on the surface in case of particles size of 302 micron. It indicated that the particles might have stroke the surface very close to the normal impact angle. The length of cut increases gradually while the silt size decreases from 302 micron to 45 micron. This may be due to the decreasing kinetic energy as the particles travel a relative distance plowing the surface instead of directly impacting the surface.

(xi) Craters due to plastic deformation and pit are found along the depth of the bucket in case of larger particles while plowing and shearing of specimen surface are observed in case of smaller size particles. In case of larger particles the rate of erosion at the inlet is more than at the outlet but a reverse trend has been observed in case of smaller particle sizes.

(xii) The micrograph of splitter tip indicated that the material loss occurs due to indentation of silt particles. Craters and pits are densely found over the splitter tip which may be due to plastic deformation of erosion. However, the mechanism of material removal of the surface along the depth of the bucket may be due to plastic deformation as well as plowing of surface.

(xiii) A qualitative study was made and it was found that the sharp edge of the splitter became blunt and the depth of the bucket increased. A number of channels or ripples were formed in the flow path of silt laden water jet. These

ripples or dunes are nearly normal to the flow direction. These observations are found to be on similar lines with field observations and experimental studies made by other investigators.

(xiv) Under the second part of the study quantity of mass loss of buckets is obtained by measuring the mass of Pelton buckets before and after the experimentation.

(xv) In order to discuss the effect of silt and operating parameters on erosive wear as a function of mass loss of the bucket, erosive wear is converted in the form of normalized wear as a non dimensional parameter.

(xvi) It is observed that the normalized erosive wear increases with operating hours of the turbine.

(xvii) The normalized wear has been found to be increased with silt concentration for a given value of silt size and jet velocity. Trend for the increase of normalized wear with concentration has been found to be similar for all the values of silt size.

(xviii) The effect of silt size on erosive wear was analyzed and it has been found that within the range of particle size investigated, the erosive wear increases with the increase in the particle size for all the concentrations considered.

(xix) The values of normalized wear for unit discharge were considered for developing correlation as a function of silt and operating parameters.

(xx) The wear rate follows the power law with respect to change in velocity (i.e. $W \alpha V^n$). The value of n has been evaluated in the present study as 3.79. The obtained value of exponent, n has been found to be in good agreement with other investigations for Pelton turbine.

(xxi) Based on experimental data collected for the normalized wear for different silt parameters i.e., particle size and concentration and operating parameter i.e., jet velocity and operating hours of turbine a correlation has been developed for normalized wear of Pelton turbine bucket as a function of the silt and operating parameters. The developed correlation is as given below;

Correlation for normalized wear

$$W = 7.91\times10^{-13}(t)^{0.99}(S)^{0.13}(C)^{1.23}(V)^{3.79} \qquad (7.1)$$

(xxii) A comparison between actual experimental values obtained and the values predicted from the correlation is made and a good agreement has been found.

(xxiii) It is observed from the experiment that the power out put was decreasing with the bucket mass loss. The rate of power loss was initially found at a higher rate, however the rate of power loss has been found to be at lower rates and become asymptote after some operating time of the turbine.

(xxiv) A correlation has been developed as a function of silt and operating parameters. Based on the experimental data obtained under different conditions following correlation for percentage efficiency loss as a function of silt size, concentration, jet velocity and operating hours of the turbine is developed :

Correlation for percentage efficiency loss

$$\eta_{\%} = 2.43\times10^{-10}(t)^{0.75}(S)^{0.099}(C)^{0.93}(V)^{3.40} \qquad (7.2)$$

xxiv) A good agreement is observed among the experimental values and the values predicted from the correlation with average absolute percentage deviation between the experimental and calculated data for efficiency loss has been found within ±10%.

Summarizing, on the basis of experimental investigation it has been concluded that the normalized erosive wear increases with an increase in the silt concentration, silt size and jet velocity. It has been concluded that the silt concentration, silt size, jet velocity and the operating hours of the turbine are strong parameters for erosive wear in Pelton buckets. The developed correlation may be useful for turbine manufacturing industries in order to predict the quantum of erosion in Pelton turbine bucket and efficiency loss at the manufacturing stage of a turbine under a given silt content water a particular site.

APPENDIX-I

A1.1 UNCERTAINTY ANALYSIS

It is very difficult to avoid errors while taking observations from the instruments during experimental work regardless of care taken. When only one parameter is being obtained from an experiment, crude methods of calculations are used to obtain an estimate of the uncertainty of the results. However in many research problems, number of parameters is obtained simultaneously from an equal or greater number of experimental results. In these cases, more formal methods are required to obtain correct estimates of the uncertainty in the parameters. These methods come under the heading of uncertainty analysis.

The uncertainty analysis as proposed by Kline and McClintock was used to calculate the uncertainty associated with experimental results, based on the observations of the scatter in the measured values used in calculating the result.

If a parameter is calculated using certain measured quantities as,

$$y = y\,(x_1, x_2, x_3 \ldots\ldots\ldots x_n) \tag{A1.1}$$

Then uncertainty in measurement of y is given as follows:

$$\delta \frac{\delta y}{y} = \left[\left(\frac{\delta y}{\delta x_1} \delta x_1 \right)^2 + \left(\frac{\delta y}{\delta x_2} \delta x_2 \right)^2 + \left(\frac{\delta y}{\delta x_3} \delta x_3 \right)^2 + \ldots\ldots\ldots\ldots + \left(\frac{\delta y}{\delta x_n} \delta x_n \right)^2 \right] \tag{A1.2}$$

where,

$\delta x_1, \delta x_2, \delta x_3 \ldots\ldots\ldots \delta x_n$, are the possible errors in measurements $x_1, x_2, x_3 \ldots\ldots\ldots x_n$, δy is known as absolute uncertainty and $\delta y/y$ is known as relative uncertainty.

In the present investigation, the important parameters are:

bucket mass loss (M_{bl}) $M_{bl} = M_{bi} - M_{bf}$

i) flow rate (Q) $Q = C_e \times \frac{2}{3} \times \sqrt{2 \times g} \times h_e^{\frac{3}{2}} \times b_e$

ii) jet velocity (V) $V = \sqrt{2 \times g \times H}$

iii) silt size (S) $S=S_1-S_2$

iv) silt concentration (C) $C = \frac{w}{W_w}$,

v) operating hour (t) $t=t_f - t_i$

A1.1.1 Bucket mass loss (M_{bl})

$$M_{bl} = M_{bi} - M_{bf} \tag{A1.3}$$

where,

M_{bl} = Pelton bucket mass loss

M_{bi} = bucket mass before measurement

M_{bf} = bucket mass after measurement

Least count of the balance is 0.1 mg

The maximum mass loss obtained is 200 mg

The minimum mass loss obtained is 10 mg

$$\delta M_{bl} = \left[\left(\frac{\partial M_{bl}}{\partial M_{bf}} \delta M_{bf} \right)^2 + \left(\frac{\partial M_{bl}}{\partial M_{bi}} \delta M_{bi} \right)^2 \right]^{\frac{1}{2}} = \left[\left(\delta M_{bf} \right)^2 + \left(-\delta M_{bi} \right)^2 \right]^{\frac{1}{2}}$$

$$\frac{\delta M_{bl}}{M_{bl}} = \frac{\left[\left(\delta M_{bf} \right)^2 + \left(-\delta M_{bi} \right)^2 \right]^{\frac{1}{2}}}{M_{bl}} \tag{A1.4}$$

For maximum mass loss

$$\frac{\delta M_{bl}}{M_{bl}} = \frac{\left[\left(\pm .1 \right)^2 + \left(\pm .1 \right)^2 \right]^{0.5}}{200} = 0.000707 \tag{A1.5}$$

For minimum mass loss

$$\frac{\delta M_{bl}}{M_{bl}} = \frac{\left[(\pm.1)^2 + (\pm.1)^2\right]^{0.5}}{10} = 0.014142 \qquad \text{(A1.6)}$$

A1.1.2 Flow rate (Q)

$$Q = C_e \times \frac{2}{3} \times \sqrt{2 \times g} \times h_e^{\frac{3}{2}} \times b_e \qquad \text{(A1.7)}$$

$$h_e = h + k_h \qquad \text{(A1.8)}$$

$$b_e = b + k_b \qquad \text{(A1.9)}$$

where,

C_e is the coefficient of discharge,

g is acceleration due to gravity,

b is notch width,

h is the measured head,

k_h is the head correction factor,

k_b is the width correction factor.

δQ = uncertainty in the calculated value of the discharge,

δC_e = uncertainty in the coefficient of discharge is ±1.5 percent,

δb_e= uncertainty in the effective width for a rectangular weir

δh_e = uncertainty in the effective head

h_m= mean of n readings of the head

Discharge measurement made under the following condition:

h=70 mm, p= 100 mm and b=160 mm

Standard deviation based on 10 successive head readings =0.05 mm.

Coefficient of discharge δC_e = 1.5 percent

Head correction δk_h = 0.10 mm

Width correction δk_b = 0.10 mm

Uncertainties estimated are:

Head δh= 0.20 mm

Head-gauge zero δh_o =30 mm

Standard deviation (head) h_m=0.05 mm

Width δb = 0.50 mm

$$\frac{\delta Q}{Q} = \left[\delta C_e^2 + \delta b_e^2 + 1.5^2 \delta h_e^2 \right]^{0.5} \tag{A1.10}$$

$$\frac{\delta \mathrm{Ce}}{\mathrm{Ce}} = 1.5\% \tag{A1.11}$$

$$\frac{\delta \mathrm{b_e}}{\mathrm{b_e}} = \left[\delta b^2 + \delta k_b^2 \right]^{0.5} \tag{A1.12}$$

$$\frac{\delta b_e}{b} = \frac{\left[0.5^2 + 0.1^2 \right]^{0.5}}{160} = 0.0031 \tag{A1.13}$$

$$\frac{\delta h_e}{h} = \frac{\left[\delta h^2 + \delta h_v^2 + \delta k_h^2 + (2 \times Sh_m)^2 \right]^{0.5}}{h}$$

$$\frac{\delta h_e}{h} = \frac{\left[0.20^2 + 0.30^2 + 0.1^2 + (2 \times .05)^2 \right]^{0.5}}{70} = 0.00559 \tag{A1.14}$$

$$\frac{\delta Q}{Q} = \left[0.015^2 + 0.0031^2 + 1.5^2 \times 0.00559^2 \right]^{0.5} = 0.01746 \tag{A1.15}$$

A1.1.3 Jet velocity (V)

$$V = \sqrt{2 \times g \times H} \tag{A1.16}$$

$$H = \frac{P}{\rho g} \tag{A1.17}$$

$$V = \sqrt{2 \times g \times \frac{P}{\rho g}} \quad = \sqrt{2 \times \frac{P}{\rho}} \tag{A1.18}$$

$$\delta V = \left[\left(\frac{\partial V}{\partial P} \delta P \right)^2 + \left(\frac{\partial V}{\partial \rho} \delta \rho \right)^2 \right]^{0.5} \tag{A1.19}$$

$$= \left[\left(\frac{\partial \left(\sqrt{2 \times \frac{P}{\rho}} \right)}{\partial P} \delta P \right)^2 + \left(\frac{\partial \left(\sqrt{2 \times \frac{P}{\rho}} \right)}{\partial \rho} \delta \rho \right)^2 \right]^{0.5}$$

$$= \left[\left(\sqrt{\frac{2}{\rho}} \frac{\partial \left(\sqrt{P} \right)}{\partial P} \delta P \right)^2 + \left(\sqrt{2P} \frac{\partial (\rho)^{-\frac{1}{2}}}{\partial \rho} \delta \rho \right)^2 \right]^{0.5}$$

$$= \left[\left(\sqrt{\frac{2}{\rho}} \times \frac{1}{2} \times \left(P^{-\frac{1}{2}} \right) \delta P \right)^2 + \left(\sqrt{2P} \times \left(-\frac{1}{2} \right) (\rho)^{-\frac{3}{2}} \delta \rho \right)^2 \right]^{0.5}$$

$$= \left[\left(\frac{1}{2} \times \sqrt{\frac{2}{\rho}} \times P^{-\frac{1}{2}} \times \delta P \right)^2 + \left(\left(-\frac{1}{2} \right) \times \sqrt{2P} \times \rho^{-\frac{3}{2}} \delta \rho \right)^2 \right]^{0.5}$$

$$= \left[\left(\frac{1}{\sqrt{2P\rho}} \delta P \right)^2 + \left(\sqrt{\frac{P}{2}} \times \rho^{-\frac{3}{2}} \delta \rho \right)^2 \right]^{0.5}$$

$$\frac{\delta V}{V} = \frac{\left[\left(\frac{1}{\sqrt{2P\rho}} \delta P \right)^2 + \left(\sqrt{\frac{P}{2}} \times \rho^{-\frac{3}{2}} \delta \rho \right)^2 \right]^{0.5}}{\sqrt{2 \times \frac{P}{\rho}}} = \left[\left(\frac{1}{2P} \delta P \right)^2 + \left(\frac{1}{2\rho} \delta \rho \right)^2 \right]^{0.5} \tag{A1.20}$$

Substituting the value of density of water at 30° C as 0.9952 kg/m^3 in the above equation, we get,

$$\frac{\delta V}{V} = \left[\left(\frac{7.375}{2 \times 500} \right)^2 + \left(\frac{0.0048}{2 \times 1} \right)^2 \right]^{0.5} = 0.0077366 \qquad \text{(A1.21)}$$

A1.1.4 Silt size (*S*)

$$S = S_1 - S_2 \qquad \text{(A1.22)}$$

$$\delta S = \left[\left(\frac{\partial S}{\partial S_1} \delta S_1 \right)^2 + \left(\frac{\partial S}{\partial S_2} \delta S_2 \right)^2 \right]^{\frac{1}{2}} = \left[\left(\delta S_1 \right)^2 + \left(-\delta S_2 \right)^2 \right]^{\frac{1}{2}}$$

$$\frac{\delta S}{S} = \frac{\left[\left(\delta S_1 \right)^2 + \left(-\delta S_2 \right)^2 \right]^{\frac{1}{2}}}{S} \qquad \text{(A1.23)}$$

$$= 0.0135$$

A1.1.5 Silt concentration (C)

$$C = \frac{w}{W_W} \qquad \text{(A1.24)}$$

where,

w = weight of silt

W_W = weight of water

$$\delta C = \left[\left(\frac{\partial C}{\partial w} \delta w \right)^2 + \left(\frac{\partial C}{\partial \mathrm{W_W}} \delta \mathrm{W_W} \right)^2 \right]^{\frac{1}{2}} \qquad \text{(A1.25)}$$

$$= \left[\left(\frac{1}{\mathrm{W_W}} \frac{\partial w}{\partial w} \delta w \right)^2 + \left(w \frac{\partial \mathrm{W_W}^{-1}}{\partial \mathrm{W_W}} \delta \mathrm{W_W} \right)^2 \right]^{\frac{1}{2}}$$

$$=\left[\left(\frac{1}{W_W}\delta w\right)^2+\left(w(-1)\left(W_W{}^{-2}\right)\delta W_W\right)^2\right]^{\frac{1}{2}}$$

$$=\left[\left(\frac{1}{W_W}\delta w\right)^2+\left(\frac{w}{W_W{}^2}\delta W_W\right)^2\right]^{\frac{1}{2}}$$

$$\frac{\delta C}{C}=\frac{\left[\left(\frac{1}{W_W}\delta w\right)^2+\left(\frac{w}{W_W{}^2}\delta W_W\right)^2\right]^{\frac{1}{2}}}{\frac{w}{W_W}}=\left[\left(\frac{1}{M}\delta M\right)^2+\left(\frac{1}{W_W}\delta W_W\right)^2\right]^{\frac{1}{2}} \quad \text{(A1.26)}$$

For maximum concentration

$$\frac{\delta C}{C}=\left[\left(\frac{.5}{900}\right)^2+\left(\frac{.5}{900}\right)^2\right]^{\frac{1}{2}}=0.0011 \quad \text{(A1.27)}$$

For minimum concentration

$$\frac{\delta C}{C}=\left[\left(\frac{.5}{250}\right)^2+\left(\frac{.5}{900}\right)^2\right]^{\frac{1}{2}}=0.00207572 \quad \text{(A1.28)}$$

A1.1.6 Operating hour (*t*)

$$t=t_f - t_i \quad \text{(A1.29)}$$

$$\delta t=\left[\left(\frac{\partial t}{\partial t_f}\delta t_f\right)^2+\left(\frac{\partial t}{\partial t_i}\delta t_i\right)^2\right]^{\frac{1}{2}} \quad \text{(A1.30)}$$

$$=\left[\left(\frac{\partial\left(t_f-t_i\right)}{\partial t_f}\delta t_f\right)^2+\left(\frac{\partial\left(t_f-t_i\right)}{\partial t_i}\delta t_i\right)^2\right]^{\frac{1}{2}}=\left[\left(\delta t_f\right)^2+\left(-\delta t_i\right)^2\right]^{\frac{1}{2}}$$

$$\frac{\delta t}{t}=\frac{\left[\left(\delta t_f\right)^2+\left(-\delta t_i\right)^2\right]^{\frac{1}{2}}}{t}=\frac{\left[(30)^2+(-30)^2\right]^{\frac{1}{2}}}{60\times 60}=0.011785 \quad \text{(A1.31)}$$

REFERENCES

1. Moore F. (2006) Report, Earth Policy Institute
2. World Energy Outlook., International Energy Agency 2008
3. Sadananda, S.B. (2006), "World Energy Scenario Focus on Asia Pacific Region.Energy Sources Supply and Demand Scenarios", Workshop on Utilization of Biomass for Renewable Energy (11–15 December, Kathmandu, Nepal).
4. Ministry of New and Renewable Energy-General Review (2008), Government of India, New Delhi, @www.mnre.gov.in,
5. All India Electricity Statistics – General Review, Ministry of Power Government of India, New Delhi, 2008 @ www.cea.nic.in.
6. Elliott, T. C., Chen, K., Swanekamp, R. C. (1998), "Electric power-plants" In: Standard Hand Book of Power Plant Engineering, McGraw-Hill, NY.
7. World Atlas and Industry Guide (2008), International Journal on Hydro Power and Dams
8. "Sectoral Overview Report on Small Hydropower Development in India", (2007), Alternate Hydro Energy Centre, Indian Institute of Technology, Roorkee,.
9. Celso, P., Ingeniero, M. de. (1998), "Layman's Guide Book-How to Develop a Small Hydro Site", European Small Hydropower Association (ESHA), Second Addition.
10. Weerakoon S. B. (2007),"Effect of the Entrance Zone on the Trapping Efficiency of desilting tanks in Run-of- river Hydropower Plants", International Conference on Small Hydropower, Kandy, Sri Lanka, October 22-24, 155-160.
11. Lysne, D.K., Glover, B., Støle, H. and Tesaker, E. (2003), Hydropower Development, Book Series Number 8 - Hydraulic design, NTNU.

12. Levy, A.V. and Chik, P. (1983), "The Effects of Erodent Composition and Shape on the Erosion of Steel", Wear (89), 151–162.

13. Drolon, H., Druaux, F. and Faure, A. (2000), "Particle Shape Analysis and Classification Using Wavelet Transforms", Pattern Recognition Letters (21), 473-482.

14. Winter, R.E. and Hutchings, I.M. (1974), "Solid Particle Erosion Studies Using Single Angular Particles", Wear (29), 181–194.

15. Bahadur, S. and Badruddin, R. (1990), "Erodent Particle Characterization and the Effect of Particle Size and Shape on Erosion", Wear (138), 189–208.

16. Liebhard, M. and Levy, A. (1991), "The Effect of Erodent Particle Characteristics on the Erosion of Metals", Wear (151), 381–390.

17. Kayaba, T. (1984), "The Latest Investigation of Wear by the Microscopic Observations", JSLE Transactions (29), 9-14.

18. Lim, S.C. and Brunton, J.H. (1985), "A Dynamic Wear Test Rig for the Scanning Electron Microscope", Wear (101), 81-91.

19. Moore, M.A. and Douthwaite, R.M. (1978), "Plastic Deformation below Worn Surface", Metallurgical Transections, (7A), 229-243.

20. Challen, J.M. and Oxley, P.L.B. (1979), "An Explanation of the Different Regimes of Friction and Wear Using Asperity Deformation Models", Wear (53), 53-59.

21. Aunemo, H. (1992), "Utprøving av erosjonsbestandige belegg for nål og munnstykke I Mel", (Report in Norwegian)

22. Pande V.K. (1987) "Effect Of Hydraulic Design of PeltonTurbines on Damage Due to Silt Erosion and its Reduction" BHEL Bhopal, INDIA

23. Thapa, B. and Brekke, H. (2004), "Effect of Sand Particle Size and Surface Curvature on Erosion of Hydraulic Turbine", 22nd IAHR Symposium on Hydraulic Machinery and Systems, Stockholm.

24. Grein, H. and Schachenmann, A. (1996), "Abrasion in Hydroelectric Mechinary", Silt Damages to Equipment in Hydro Power Stations and Remedial Measures, CBIP,New Delhi.

25. Krause, M., Grein, H. (1996), "Abrasion Research and Prevention", Silt Damages to Equipment in Hydro Power Stations and Remedial Measures, CBIP, New Delhi.

26. Khera, D.V., Chadhawork RS. (2001), "Silt erosion…Trouble for turbines". International Water Power and Dam Construction(53),22–3.

27. Tong, D. (1981), "Cavitation and wear on hydraulic machines". International Water Power and Dam Construction;(April).

28. Pande, V.K. (1987) "Criteria for developing silt erosion model test facility". Conference of CBIP.

29. Singh, S.C. (1990) "Operational problems and development of a new runner for silty water". International Water Power and Dam Construction (November).

30. Naidu, B.S.K. (2004) "Silting problem in hydro power plant & their possible solutions".India: NPTI.

31. Chaudhary, C.S. (1999) "Impact of high sediment on hydraulic equipment of Marsyangdi hydropower plant". In: Proceedings of the international seminar on sediment handling technique, NHA, Kathmandu..

32. Standard Technology Relating to Wear and Erosion (1998), G 40 Annual Book of ASTM Standards, ASTM.

33. Bhushan, B. (2002), Introduction to Tribology, 1St edition. John Wiley & Sons, New York.

34. Truscott, G. F. (1972), "Literature Survey of Abrasive Wear in Hydraulic Machinery", Wear (20), 29-50.

35. Finnie, I. (1960), "Erosion of Surfaces by Solid Particle", Wear (3), 87-103.

36. Bitter, J. G. A. (1963), "A Study of Erosion Phenomena, Part I and II", Wear (6), 5 - 21 and 169 – 190.

37. Bitter, J. G. A. (1963) "A study of erosion phenomena: part II" Wear (6) 5-21.

38. Neilson, J. and Gilchrist, A. (1968), "Erosion by a Stream of Solid Particles", Wear (11), 111–122.

39. Hutchings, I.M., and Winter, R.E. (1974), "Particle Erosion of Ductile Metals: a Mechanism of Material Removal", Wear (27), 121–128.

40. S.S. Manson, (1996) "Thermal Stress and Low Cycle Fatigue", Mcgraw-Hill, New York, 246–254.

41. Hashish, M. (1987), "Modified model for erosion", Seventh International Conference on Erosion by Liquid and Solid Impact, Cambridge, England, 461–480.

42. Meng, H.C. and Ludema, K.C. (1995), "Wear Models and Predictive Equations: Their Form and Content", Wear (181-183), 443-457.

43. Sheldon, G.L. and Finnie, I. (1966), "The Mechanism of Material Removal in the Erosive Cutting of Brittle Materials", ASME J. Engng. Ind.(88) ,393-400.

44. Goodwin, J.E., Sage, W. and Tilly, G.P. (1969-1970), "Study of Erosion by Solid Particles", Proc. Inst. Mech. Eng., 184 (15), Part 1, 279.

45. Head, W.J. and Harr, M.E. (1970), "The Development of a Model to Predict the Erosion of Material by Natural Contaminants", Wear (15), 1

46. Sheldon, G.L. (1970), "Similarities and Differences in the Erosion Behavior of Materials", .I Basic Eng. (89), 619.

47. Meng, H.C. and Ludema, K.C. (1995), "Wear models and predictive equations: their form and content", Wear (181-183), 443-457.

48. Finnie, I. (1972), "Some Observations on the Erosion of Ductile Metals", Wear (19), 81-90.

49. Sheldon, G.L. and Kanhere, A. (1972), "An Investigation of Impingement Using Single Particles", Wear (21), 195.

50. Tilly, G.P. (1973), "A Two Stage Mechanism of Ductile Erosion", Wear (23), 87.

51. Head, W.J., Lineback, L.D. and Manning, C.R. (1973), "Modification and Extension of a Model for Predicting the Erosion of Ductile Materials", Wear (23), 291.

52. Grant, G. and Tabakoff, W. (1973), "An Experimental Investigation of the Erosion Characteristics of 2024 Aluminum Alloy", Department of Aerospace Engineering Tech. Rep., University of Cincinnati, 73-37.

53. Williams, J.H. and Lau, E.K. (1974), "Solid Particle Erosion of Graphite-Epoxy Composites", Wear (29), 219.

54. Jennings, W.H., Head, W.J. and Manning, C.R. Jr. (1976), "A Mechanistic Model for the Prediction of Ductile Erosion", Wear (40), 93.

55. Hutchings, I.M., Winter, R.E. and Field, J.E. (1976), "Solid Particle Erosion of Metals: the Removal of Surface Material by Spherical Projectiles", Proc. R Sot. Lo&. A, 348, 379-392.

56. Evans, A.G., Gulden, M.E. and Rosenblatt, M.(1978), "Impact Damage in Brittle Materials in the Elastic-Plastic Response" Proc. Royal Society London 343–365

57. Evans, A.G. (1979), "Impact Damage Mechanics: Solid Projectiles", C.M. Preece (ed.), Treatise on Material Science and Technology, Vol. 16, Erosion, Academic, New York, , p.1

58. Ruff, A.W. and Wieherhorn, S.M. (1979), "Erosion by Solid Particle Impact" In: C.M. Preece (ed.), Treatise on Material Science and Technology,Erosion, Academic, New York, (16), 69.

59. Routbort, J.L., Scattergood, R.O. and Turner, A.P.L. (1980), "The Erosion of Reaction-Bonded Sic", Wear (59), 363-375.

60. Routbort, J.L., Scattergood, R.O. and Kay, E.W. (1980), "Erosion of Silicon Single Crystals", J. Am. Cerum. Sot., 63 (11), 635.

61. Hutchings, I.M. (1981), "A Model for the Erosion of Metals by Spherical Particles at Normal Incidence", Wear (70), 269-281.

62. Sundararajan, G. and Shewmon, P.G. (1983), "A New Model for the Erosion of Metals at Normal Incidence", Wear (84), 237-258.

63. Beckmann, G. and Gotzmann, J. (1981), "Analytical Model of the Blast Wear Intensity of Metals Based on a General Arrangement for Abrasive Wear", Wear (73), 325-353.

64. Wiederhorn, S.M. and Hockey, B.J. (1983)," Effect of Material Parameters on the Erosion Resistance of Brittle Materials", J. Mater. Sci. (18), 766-780.

65. Ritter, J.E. (1985), "Erosion Damage in Structural Ceramics", Muter. Sci. Eng. (71), 195-207.

66. Reddy, A.V. and Sundararajan, G. (1986), "Erosion Behavior of Ductile Materials with a Spherical Non-Friable Erodent", Wear (111), 313-323.

67. Johansson, S., Ericson, F. and Schweitz, J. (1987), "Solid Particle Erosion - A Statistical Method for Evaluation of Strength Properties of Semiconducting Materials", Wear (115), 107-120.

68. Lhymn, C. and Wapner, P. (1987), "Slurry Erosion of Polyphenylene Sulfide-Glass Fiber Composites", Wear (119), 1-12.

69. Bardal, E. (1985), "Korrosjon og korrosjonsvern", Tapir, Trondheim (In Norwegian).

70. Bergeron, P. and Dollfus, J. (1958), "The Influence of Nature of the Pumped Mixture and Hydraulic Characteristics on Design and Installation of Liquid/Solid Mixture Pump", Proc. 5th Conf. on Hydraulics, Turbines and Pumps, Hydraulics, 597-605.

71. Schneider, C. and Kachele, T. (1999), "Recent Research Results on Predicting and Preventing Silt Erosion", Proc. of 1st Int. Conf. on Silting Problems in Hydro Power Plants, New Delhi, III-2 – 13.

72. Bain, A.G., Bonnington, S.T. (1970), The Hydraulic Transport of Solids by Pipeline, 1st ed. Oxford: Pergamon Press.

73. Naidu, B.S.K.(1977), "Addressing the Problems of Silt Erosion at Hydro Plants", Hydropower Dams (3), 72–79.

74. Krause, M., Grein, H.(1996), "Abrasion Research and Prevention. Hydropower Dams, (4), 7–20.

75. Takgi, T, Okamura, T, Sato, J. (1988), "Hydraulic Performance of Francis Turbine for Sediment-Laden Flow", Hitachi Review No.-2.

76. Asthana, B.N. (1997), "Determination of Optimal Sediment Size to be Excluded for Run-of-River Project–A Case Study", Seminar on Silting Problems in Hydro Power Stations, WRDTC, Roorkee, India.

77. Mack, R., Drtina, P., Lang, E. (1999), "Numerical Prediction of Erosion on Guide Vanes and in Labyrinth Seals in Hydraulic Turbines", Wear (233–235), 685–691.

78. Date, A., Akbarzadeh, A. (2009)"Design and cost analysis of low head simple reaction hydro turbine for remote area power supply" Renewable Energy (34), 409–415.

79. Doujak, E. (2003) "Practical experiences in preaparing a feasibility study for refurbishing a small hydro power station in Austria"; in: "Hydro Africa 2003", issued by : TANESCO/ICH; International Centre for Hydropower.

80. Doujak E., List B. (2003) "Application of PIV for the Design of Pelton Runners for RO-systems"; in: "Resolutions for Islands, Tourism and Water", issued by: European Renewable Energy Council; European Renewable Energy Council, 533-540.

81. Chaishomphob T., and Kupakrapinyo Chakri, (2003) "Preliminary feasibility study on run-of-river type small hydropower project in Thailand : Case study in Maehongson province", Research and development Journal of the Engineering Institute of Thailand, 14 (4), 34-43,.

82. Keck, H., Dekumbis, R. and Sick, M. (2005), "Sediment Erosion in Hydraulic Turbine and Experiences with Advanced Coating Technologies", India Hydro, International Workshop and Conference.

83. Crowe, C., Sommerfeld, M., Tsuji Y. (1998) "Multiphase Flows with Droplets and Particles" CRC Press, Boca Raton, LISA, 471

84. Majumdar, B. (2000) "Dynamic Stability Analysis of a Remote Hydel Power Station Connected to Infinite Bus Through Long Transmission Line", Indian Journal of Power and River Valley Development, 66-70,.

85. Varun, Bhat I. K. and Prakash, R. (2008) "Life Cycle Analysis of Run-of River Small Hydro Power Plants in India", The Open Renewable Energy Journal, (1), 11-16,.

86. Mehta, R. C., and Soundranayagam S. (1977), "Unstady flow behind axial and mixed flow turbine runners" Proc 7th National Conf. on Fluid Mechanics and Fluid Power , Baroda, B-7.

87. Chattopadhyay, R. (1993), "High Silt Wear of Hydro Turbine Runners", Wear (162–164), 1040–1044.

88. Roman, J.M., Xin, L.Y.and Hui, W.M. (1997), "Reginensi J P, Dealing with Abrasive Erosion in Hydro Turbine", Hydropower Dams (3), 67–71.

89. Mann, B.S. (2000), "High-Energy Particle Impact Wear Resistance of Hard Coatings and their Application in Hydro Turbines", Wear (237), 140–146.

90. Mann, B.S., Arya, V. (2001), "Abrasive and Erosive Wear Characteristics of Plasma Nitriding and HVOF Coatings: Their Application in Hydro Turbines", Wear (249), 354–360.

91. Engelhardt, M., Oechsle, D. (2004), "Smooth Operator", International Water Power Dam Construction, June, 20–22.

92. Desale, G.R., Gandhi, B.K. and Jain, S.C. (2006), "Effect of Erodent Properties on Erosion Wear of Ductile Type Materials", Wear 261 (7-8), 914-921.

93. Tilly, G. P. (1969), "Sand Erosion of Metals and Plastics: A Brief Review", Wear (14:4), 241-248.

94. Tilly, G. P. (1969), "Erosion Caused by Airborne Particles", Wear (14), 63-79.

95. Tilly, G. P. and Sage, W. (1970), "The Interaction of Particle and Material Behaviour in Erosion Processes", Wear 16(6), 447.

96. Tilly, G. P. (1973), "A Two Stage Mechanism of Ductile Erosion" Wear (23:1), 87-96.

97. Liebhard, M. and Levy, A. (1991), "The Effect of Erodent Particle Characteristics on the Erosion of Metals", Wear (151), 381–390.

98. Hutchings, I.M. (1979), "Mechanism of the Erosion of Metals by Solid Particles". W.F. Adler, Editor, Erosion: Prevention and Useful Applications, ASTM, 59–76.

99. Winter, R. E. and Hutchings, I. M. (1975) "The Role Of Adiabatic Shear In Solid Particle Erosion" Wear (34), 141- 14.

100. Stachowiak, G.W. and Batchelor, A. W. (1993), Engineering Tribology, Elesvier, Amesterdam.

101. Sharma, A. and Rajan, T.V. (1994) "Scanning Electron Microscopic Studies of Worn out Leaded Aluminium-Silicon Alloys Surfaces", Wear (174), 217-228.

102. Roy Chowdhury, S. K.and Chakraborti, P. (2008) "Prediction of polymer wear -an analytical model and experimental validation" Tribology Transactions, (51) 798-809.

103. Roy Chowdhury, S. K., Mishra, A., Pradhan, B. and Saha D. (2004) "Wear characteristic and biocompatibility of some polymer composite acetabular cups" Wear (256), 1026-1036.

104. Darling, K. (2006), "Easing Erosion", Inter. Water Power Dam Constr. February, 32–33.

105. Thapa, B., Strestha, R., Dhakal, P. and Thapa, B.S., (2005), "Problems of Nepalese Hydropower Projects due to Suspended Sediments", Aquatic Ecosystem Health Manage, 8(3), 251–257.

106. Pradhan, P.M.S. (2004), "Improving Sediment Handling in the Himalayas", OSH Research, Nepal, October 2004.

107. Singh, A.K., Chandra, S. (1996), "Hydro-Abrasion of Water Turbines in Himalayas", Workshop: Silt Damages To Equipment in Hydro Power Stations And Remedial Measures. CBIP, 1996.

108. Yan, M.Z. (1996), "Protecting Hydro Turbines in Silt-Laden Rivers", Hydropower Dams (4), 22–24.

109. Wood, J. (1998), "An answer to Abrasion", International Water Power Dam Construction, (April), 36–37.

110. Bajracharya,T. R., Joshi, C. B., Saini R. P. and Dahlhaug, O.G. (2006) "Analysis of Sand Particles Led Damages of Pelton Turbines in Nepal" 14th International Seminar on Hydropower and Plants, Viena, Austria, Nov.22-24.

111. Bajracharya,T. R., Sapkota, D., Thapa, R., Poudel, S. P., Joshi, C. B., Saini R. "P. and Dahlhaug, O.G., (2006) " Comparative Study of Erosion of Pelton Turbines with Sand Led Erosion test and Numerical Flow Analysis" Journal of Institute of Engineering, 6(1),114-123.

112. Fenandez E., Saini R.P. and Devadas V. (2003) "Economic Factors: Effect on Energy Consumption Pattern in Rural Hilly Areas" Nigerian Journal of Renewable Energy, Sokoto, Nigeria, (1 & 2), 124-131.

113. Fenandez E., Saini R.P. and Devadas V. (2005),"Relative Inequality in Energy Resource Consumption: A case of Kanvashram Village, Pauri Garhwal District, Uttaranchal (India)" International Journal of Renewable Energy (30), 763-772.

114. Nand Kishor, Saini R.P. and Singh, S.P. (2005) "Small hydro power plant identification using NNARX structure", Journal of Neural Computing and Applications, Published by Springer Verlag London Limited, 14(3), 212-222.

115. Singal S.K. and Saini, R.P. (2007) "Cost effective technology for low head small hydro power schemes", Indian Journal The Environ Monitor, 7(6), 4-10.

116. Nand Kishor, Saini, R.P. and Singh, S.P. (2007) "A review of hydropower plant models and control", International Journal of Renewable & Sustainable Energy Reviews, 11(5), 776-796.

117. Singal, S.K., Saini, R.P. and Raghuvanshi, C.S. (2007) "Estimation of cost for low head small hydropower installations", Indian Journal of Power & River Valley Development, July-August ,179-183,.

118. Singal S.K. and Saini, R.P. (2008) "Analysis for Quick Estimation of Canal Based Small Hydropower Schemes", Renewable Energy (IEEMA) Journal, (September)76-80.

119. Saini R.P. and Pash, O. (1997)"The development of Traditional Himalayan water mills for sustainable village scale micro-hydro power" Ist International Conference on Renewable Energy, Hydrabad, February 3-7,.

120. Saini R.P. (1999), "SHP turbines and their selection", Proc. of International Short Term Course on Small Hydro Power, BUET, Dhaka, Bangladesh, pp. 193-203, May 6-9,.

121. Saini R.P.(2002), "New Design Concepts of Micro Hydro Power Plants." National Symposium on Recent Advances in Renewable Energy Technologies, Shivaji University, Kolhapur, (August)13-15.

122. Saini R.P., (2003) "Cost Effective Approach for the Development of Micro Hydropower" National Conference on Emerging Energy Technologies (NCEET) Mechanical Engineering Department, National Institute of Technology, Hamirpur (H.P.), March 28-29.

123. Singal, S.K. and Saini, R.P. (2004) "Cost Effective Development of Canal Based Hydropower Scheme-A Case Study" First International Conference on Renewable Energy, Central Board of Irrigation and Power, New Delhi, October 6-8.

124. Singal, S.K. and Saini, R.P. (2004) " Small Hydro Power –A promising Source of Renewable Energy", National Seminar on Renewable energy Technologies, Innovations and Market Penetration, Solar Energy Society of India, Kolkata October 8-9.

125. Akella, A.K., Saini, R.P.and Sharma, M.P.(2004)"An aspects of small/mini/micro/pico/nano-hydro power for developing countries", International Conference on Systematics, Cybernetics and Informatics, PENTAGRAM, Hyderabad, pp. 33-38,.

126. Nand Kishor, Saini R.P. and Singh, S.P. (2005)"The identification of nonlinear dynamics of hydropower plant using ARX structure", National Conference of Control and Dynamical Systems, Indian Institute of Technology, Bombay, January 27-28.

127. Saini R.P. and Arun Kumar, (2006)"Development of Standard Water Mills", International Himalayan Small Hydropower Summit, Dehradun, Oct. 12-13, 282-293.

128. Saini, R.P. and Arun Kumar, (2007) "Water Mills for Multipurpose Applications", International Conference on Small Hydropower "Hydro Sri Lanka", Kandy, Sri Lanka, Oct. 22-24, 207-214.

129. Singal, S.K. and Saini, R.P. (2007) "Analytical Approach for Cost Estimation of Low Head Small Hydro Power Scheme", International Conference on Small Hydropower "Hydro Sri Lanka", Kandy, Sri Lanka, Oct. 22-24, 513-518.

130. Anurag Kumar, Saini, R.P. and Singal, S.K. (2008) "Design of Small Hydropower Plants with Bulb Turbines-A Review", Proceeding of National

Conference on Trends in Mechanical Engineering 'TIME-2008', Chandigarh Engineering College Landran, Mohali, Feb.8-9, 336-346.

131. Duan, C.G. and Karelin, V.Y., Abrasive Erosion and Corrosion of Hydraulic Machinery, Imperial College Press, London.

132. Bajracharya, T.R. , Acharya, B. , Joshi, C.B. , Saini, R.P. , Dahlhaug, O.G. (2008), "Sand Erosion of Pelton Turbine Nozzles and Buckets: A Case Study of Chilime Hydropower Plant", Wear (264), 177–184.

133. Bajracharya,T. R., Joshi, C. B. and Dahlhaug, O.G. (2004) "Experiences on Sand Erosion Led Efficiency Losses in Micro and Small Hydro Power Turbines in Nepal" International Seminar on Hydropower and Plants,Viena, Austia, Nov.24-26.

134. Bajracharya,T. R., Joshi, C. B., Saini R. P. and Dahlhaug, O.G. (2004) "Efficiency Improvement of Hydro Turbines through Erosion Resistant Design Approach" International Conference on Power Systems, Kathmandu, Nepal, Nov 3-5. Nov.24-26.

135. Bajracharya,T. R., Acharya, B., Karki, B., Lohia, L., Joshi, C. B., Saini R. P. and Dahlhaug, O.G. (2005), "Sand Particle Led Pelton Needle Analysis :Case Study of Chilime Hydropower Plant" Journal of Institute of Engineering, Vol 5(1), 89-98.

136. Bajracharya,T. R., Joshi, C. B., Sapkota, D., Thapa, R., Poudel, S. P., Saini R. P., Nakarmi, K., and Dahlhaug, O.G. (2006), "Correlation Study of Sand Led Erosion of Buckets and Efficiency Losses" 1st International Conference on Renewable Energy Technology for Rural Development(RETRUD-06), Kathmandu, Nepal, Oct.12-14.

137. Bajracharya,T. R., Joshi, C. B., Saini R. P. and Dahlhaug, O.G.(2007), "Correlation between Sand led Erosion of Pelton Buckets and Efficiency Losses in High Head Hydropower Schemes" Workshop on NUFU Supported Doctoral Research, Institute of Engineering, TU, Kathmandu, Nepal.

138. Brekke, H. (1978), "Discussion of Pelton Turbine versus Francis Turbines for High Head Turbines", IAHR, Colorado.

139. Brekke H. (2002), "Design of Hydraulic Machinery Working in Sand Laden Water", In: Duan C.G. And Karelin V.Y. (Eds), Abrasive Erosion and Corrosion Of Hydraulic Machinery, Imperial College Press, London.

140. Indian Standard, IS:9108–1979, (Reaffirmed 1997) "Liquid Flow Measurement In Open Channels Using Thin Plate Weirs".

141. Eisenring, M. "Harnessing Water Power in a Small Scale Micro Pelton turbines", MHPG Series, (9), 5.

142. Kline. S.J. and Mc clintock, F.A. (1953) "Describing Uncertainties In Single Sample Experiments". Mech. Eng.(75), 3–8.

143. Hutchings, I.M. (1992) "Friction and wear of Engineering Materials", Tribology Inc. CRC Press, 171-197.

144. Schumacher, W. J., Miller, J. E. and Schmidt, F. E. (1987) "Slurry Erosion: Uses, Applications, and Test Methods" ASTM Spec. Tech. Publ. (964) 5-18.

145. Thapa, B.(2004), "Damage of Hydraulic Machinery due to Sand Erosion" Norwegian University of Science and Technology. Ph. D. Thesis.

146. Harry, H. T., Graeme, R. A., Edward, P. B. (2007) "A New Impact Erosion Testing Setup Approach" Wear (263), 289–294.

147. Finnie, J., Wolak, Y. Kabel, (1967), "Erosion of Metals by Solid Particles" J. Mater. (2), 682–700.

148. Verspui, M.A. (1998), "Modeling Abrasive Processes of Glass", PhD Thesis, Technische Universitieit Eindhoven.

149. M. Buijs, J. M. M. Pasmans, (1995) "Erosion of Glass by Alumina Particles: Transitions and Exponents" Wear (184), 61–65.

150. Slikkerveer, P. J., Bouten, P.C.P., in't Veld, F.H. Scholten, H. (1998) "Erosion and Damage by Sharp Particles" Wear (217), 237–250.

151. Arnold, J.C. and Hutchings, I.M. (1989), "Flux Rate Effects in the Erosive Wear of Elastomers", J. of Material Science (24), 833-839.

152. Karimi A. and Schmid R.K. (1992) "Ripple formation in solid-liquid erosion", Wear (156), 33-47.

153. Abrahamson, G. R. (1961)"Permanent Periodic Surface Deformations Due to a. Traveling Jet" J. Appl. Mech. (28), 519-528.

154. Cousens, A. K., Hutchings, I. M., Field, J. E. and Comey feds., N. S. (1983), Proc. 6th Znt. Conf. on Erosion by liquid and Solid impact, Cavendish Laboratory, Cambridge, Cambridgeshire, Paper 41.

155. Carter, G., Nobes, M. J. and Arshak, K. I. (1980) "The mechanism of ripple generation on sandblasted ductile solids" Wear (65), 151-174.

156. Stringer J., Wright, I. G., Field J. E. and Dear J. P. (1987), Proc. 7th In &. Conf: on Erosion by Liquid and Solid Impact, Cavendish Laboratory, Cambridge, Cambridgeshire, Paper 47.

157. Hunt, J. N. (1968) "Wave formation in explosive welding". Philos. Mag.(17), 669-680.

158. Saini, R.P. and Saini, J.S. (1997), "Heat Transfer and Friction Factor Correlations for Artificially Roughened Ducts with Expanded Metal Mesh as Roughness Element." Int. J. of Heat and Mass Transfer, 40(4), 973-986.

PUBLICATIONS FROM THIS WORK

Publication in Journals

1 Mamata Kumari Padhy, R.P. Saini (2008) "A Review on Silt erosion in Hydro turbines" published in Renewable and Sustainable Energy Reviews, (12), 1974–1987.

2 M. K. Padhy, R.P. Saini (2009) "Effect of size and concentration of silt particles on erosion of Pelton turbine buckets" article in press, Energy (34), 1477-1483.

Publication in Conferences

3 Mamata Kumari Padhy & R.P.Saini November (2006) "Silt Erosion in Hydro Turbines – A Review" published in IInd National Conference on Recent Development in Mechanical Engineering at Thapar Institute of Engineering and Technology, Patiala

4 M.K. Padhy, R.P. Saini (2008) "Effect of Buckets Erosion due to Silt Laden Flow on Pelton Turbine Efficiency" REA-2008, IITD,New Delhi,11-13 Dec. 2008.

5 M.K. Padhy, R.P. Saini (2009) "Effect of Lower Concentration on Erosive Wear of Pelton Turbine Bucket" 33rd IAHR Congress, Vancouver, B.C. Canada 9-14 Aug. 2009.